MINISTRY OF HIGHER EDUCATION,
SCIENCE AND INNOVATION
OF THE REPUBLIC OF UZBEKISTAN

FERGANA STATE TECHNICAL UNIVERSITY

DEVELOPMENT OF THE DESIGN AND SUBSTANTIATION OF THE PARAMETERS OF A DRUM SCREENING DEVICE

MONOGRAPH

B.N. DAVIDBAYEV, V.M. TURDALIYEV, KH.SH. RUZALIYEV

DOI: https://doi.org/10.37547/gbps-46

ISBN: 978-1-957653-67-9

FERGANA – 2026

B.N. DAVIDBAYEV, V.M. TURDALIYEV, KH.SH. RUZALIYEV

DEVELOPMENT OF THE DESIGN AND SUBSTANTIATION OF THE PARAMETERS OF A DRUM SCREENING DEVICE

(MONOGRAPH)

DOI: https://doi.org/10.37547/gbps-46 **ISBN: 978-1-957653-67-9**

FERGANA – 202

UDK:621.01

B.N. Davidbayev, V.M. Turdaliyev, Kh.SH. Ruzaliyev.

“Development of the design and substantiation of the parameters of a drum screening device”/Monograph/ Fergana – 2026/ 98 p.

Reviewers:

Doctor of technical sciences, Professor A.D. Djurayev

Doctor of technical sciences, Professor T.S. Nabiyev

The monograph presents the results of research on the development of a bulk material screening device equipped with a shaft with elastic blades. The results of theoretical studies of the device are described, and optimal operating modes for its working components are substantiated.

Based on the selection of optimal parameters of the oscillating drum, the screening efficiency of the device is determined. In addition, experimental results and comparative data obtained under industrial conditions are presented.

The monograph is intended for researchers, specialists, and doctoral students engaged in the development and investigation of bulk material screening machine designs.

The monograph was recommended for publication by the Scientific Council of Fergana State Technical University under Resolution № 9 dated May 2, 2026 y.

CONTENTS

INTRODUCTION

Currently, at the global level, the rapid development of industrial production requires the improvement of processes for supplying industries with raw materials and processing them. In particular, achieving high efficiency in the screening of bulk materials, improving product quality, and reducing energy consumption are among the key scientific and technical challenges. From this perspective, research aimed at developing new types of screening devices, designing their structural solutions, and scientifically substantiating their main parameters is of great importance.

In recent years, drum-type screening devices have been widely used in the processing of bulk materials and are distinguished by their high productivity and screening quality. However, existing devices are characterized by high energy consumption, structural complexity, and certain technological shortcomings, which necessitate further improvement. Therefore, developing new designs of drum screening devices with low energy consumption, simple structure, and high efficiency, as well as creating their calculation methods, is an important task.

Extensive scientific research is being conducted in leading research centers and higher education institutions around the world on studying the operating processes of drum-type screening devices, improving their efficiency, developing modern calculation methods, and creating next-generation technological machines. Particular attention is paid to improving the energy efficiency of the screening process, determining optimal operating modes based on the physical and mechanical properties of materials, and enhancing the operational performance of the equipment.

In our country as well, large-scale reforms are being implemented aimed at industrial development, the introduction of energy-efficient technologies, and increasing production efficiency. In particular, the Development Strategy of New Uzbekistan for 2022–2026 sets priority tasks

such as increasing industrial production volumes, improving labor productivity, efficient use of resources, and reducing losses. In implementing these tasks, the development of new, highly efficient, resource-saving designs of devices for screening bulk materials is of great importance.

This monograph considers the development of the design of a drum screening device and the scientific justification of its main parameters. In addition, the operating processes of the device are analyzed, and structural and kinematic solutions aimed at improving its efficiency are proposed. As a result, the developed device makes it possible to improve screening quality and productivity, reduce energy consumption, and enhance overall production efficiency.

CHAPTER I. STATE AND FORMULATION OF THE RESEARCH

1.1. Analysis of research conducted on the screening of bulk materials

The main purpose of studying the process of screening bulk materials is to determine the dependence of the kinematic and structural parameters of screening machines on the physical and mechanical properties of the material being screened.

In the search for effective methods of screening bulk materials, considerable attention is paid to the use of centrifugal screeners. This is because, during the screening process, the bulk material is subjected to inertial forces that exceed the force of gravity. When the bulk material is within the influence of centrifugal force, the screening process intensifies. This ensures continuous interaction of the bulk material particles with the screening surface and increases the probability of passing through the screen apertures, while the high velocity of the bulk material contributes to an increase in the efficiency of the screener [1, 2].

A.N. Konoplin [1], V.P. Goryachkin [3], B.M. Drinch [4], Y.S. Goncharov [5], B.B. Gortinskiy [6], A.V. Zilbernagel [7], I.Y. Kojukhovskiy [8], B.T. Tarasov [9, 10], B.D. Papina [11], S.V. Lekanov [12], N.O. Kurinnaya [13], A. Akase [15], C. Harris [16], R.A. Zverkov [17], A.P. Slepov [18] and others have been engaged in studying the designs of screeners, the course of the process, and the types of particle motion.

The general structure and operating principles of flat screeners have been extensively studied in many respects. Based on these studies, schemes for the arrangement of screens in working units have been developed and classifications have been compiled. The general scheme of existing centrifugal screeners can be presented as follows (Fig. 1.1) [19; pp. 12–14].

Any centrifugal screener is considered a technical system consisting of interconnected parts and assemblies. In screeners, the preparation platform can be considered as a common element. On this platform, the material to be screened is layered, and the initial velocity and direction are imparted precisely at this point.

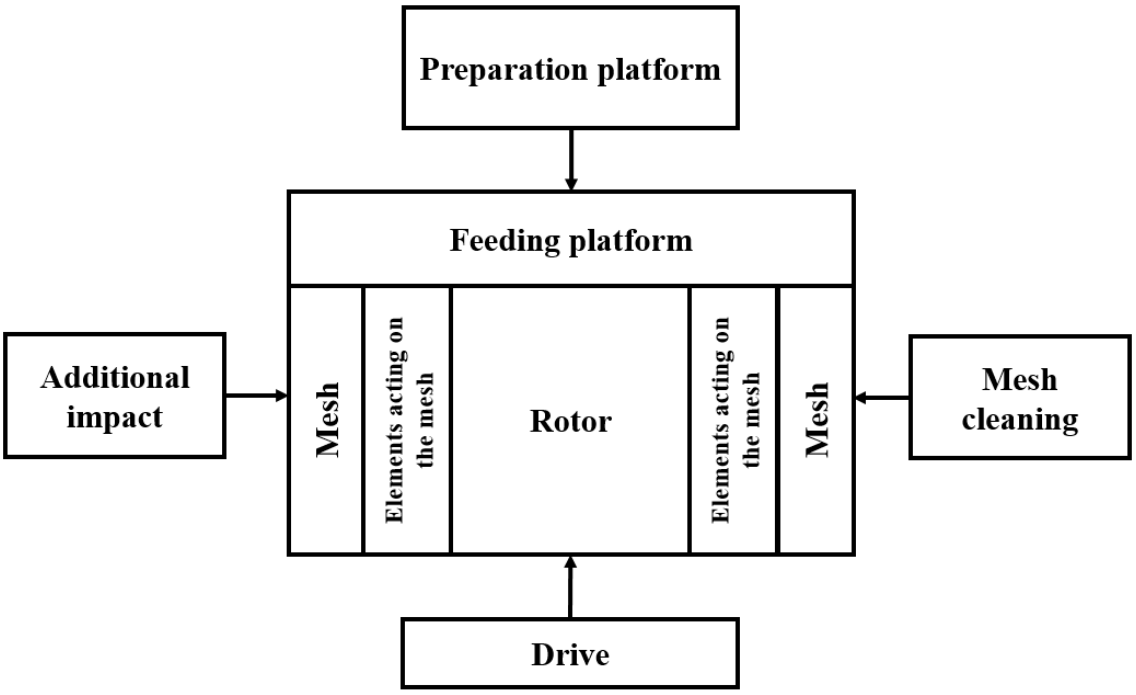

Fig. 1.1. Classification scheme of a centrifugal screener with a mesh surface

Next, a feeding platform is installed, which may be either stationary or rotating and consists of mechanisms for distributing the material uniformly across the width or surface area.

The main working element of screening machines is a mesh of various shapes (cylindrical, conical, and parabolic), which directly separates bulk materials into fractions. Based on the size and shape of the mesh openings, bulk materials are divided into fractions from the total mass.

An additional mechanism that promotes the agitation of bulk material may be installed inside the rotor in various forms (cylinder, plate drum, screw, spiral, etc.). In mesh-type centrifugal screeners, the mesh and rotor form a unified structure through various technical solutions.

The motion of the mesh-type centrifugal screener and its working elements is provided by an electric motor and various transmission mechanisms.

To improve the efficiency of the mesh cleaning process, additional devices may be used, such as vibration generators (vibro-drives), air flow devices (blowers), and others. Particles of bulk material adhering to or clogging the mesh openings can also be removed using brushes.

According to the studies of S.V. Tarasevich, during the screening process, bulk material moves in a layer of certain thickness along the mesh surface. During this movement, particles smaller than the mesh openings fall through it, while larger particles move along the mesh and are discharged from it. It should be noted that the law of particle movement along the mesh is not determined solely by the motion law of the mesh itself, since the interaction between the mesh and bulk material is a kinematically non-rigid dynamic connection. In addition, inertial and impulse forces from neighboring particles act on the particles of the material. The interaction between the mesh and particles occurs through friction forces that vary in direction and magnitude [20; pp. 8–9].

In vibrating meshes, the completeness of screening depends on the number of complete vibrations (from the initial position to an equal opposite horizontal direction and back to the initial position), as well as on the length of the zigzag trajectories of the bulk material particles along the mesh (Fig. 1.2).

The parameters of the relative motion of bulk material particles along the mesh significantly affect the quality of the screening process. Based on his research, M.N. Letoshnev concluded that "…the completeness of screening depends on the velocity of material movement along the mesh and the total path traveled by the particle" [21].

N.G. Gladkov concluded that "…the degree of completeness of screening on a flat mesh depends on the number of successive displacements of each particle during its residence on the mesh" [22].

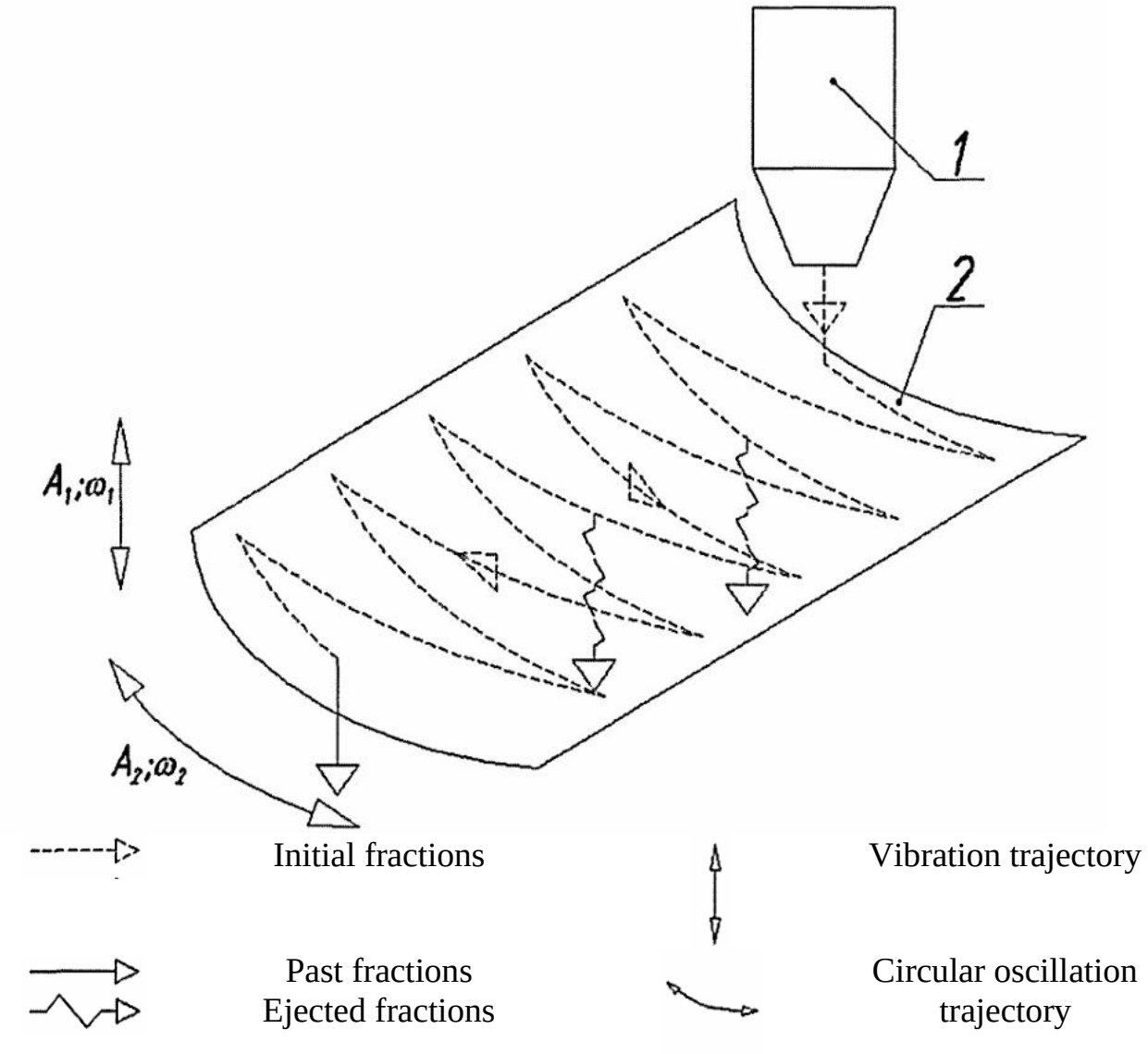

1-feeder; 2-mesh

Fig. 1.2. Schematic diagram for determining the parameters of the movement of bulk material on a vibrating mesh

The optimal regime of the screening process can be achieved under the following conditions:

The bulk material must move along the mesh in such a way that it mixes along the mesh surface, while at the same time fine fractions have sufficient time to pass through the openings.

The resultant force acting on a particle of bulk material should be as close as possible to the vertical direction, i.e., normal to the mesh surface.

The bulk material must be uniformly distributed along the mesh surface.

1.2. Analysis of the operating processes of mesh drums

The operating processes of mesh drums have been studied by R.A. Zverkov [17], N.Y. Avdeyev [23], V.I. Belyaev [24], N.I. Ivanov [26], S.V. Lekanov, N.I. Strikunov, S.A. Cherkashin [27], A.A. Sukhoparov [28], V.V. Tkachev [29], A.A. Khizhnikov [30], A.V. Chernyakov [31] and others.

The results of studies on mesh drums show that hollow drums operate in the first type of kinematic motion regimes. This regime is characterized by the fact that the screened material is located in the lower part of the drum (in the I and IV quadrants), performs oscillatory motion, and the maximum lifting angle does not exceed 90°. In this case, the screened material inside the drum forms a moving layer along the arc αp in the IV and I quadrants (Fig. 1.3a). Approximately 1/4–1/6 of the mesh surface is used in the working process. This leads to inefficient utilization of the mesh area and a reduction in specific load on the mesh.

The study of particle motion within the layer shows that particles located on the drum surface move at a velocity close to the surface velocity but do not reach it. Particles located on the upper open surface of the layer move in the opposite direction at approximately the same speed. Particles located in the center of the layer gradually move along the drum axis and practically do not participate in the rotational motion of the layer [32; pp. 25–27].

In drums equipped with internal transporting devices, the screened material is intensively mixed by spirals or blades, creating conditions for fine particles to approach the surface. However, these mesh drums, like hollow drums, are effective only under first-type low-speed motion conditions. Attempts to increase efficiency by increasing the rotation frequency of such

mesh drums lead to the formation of an annular layer and disruption of the operating regime of the drum [33].

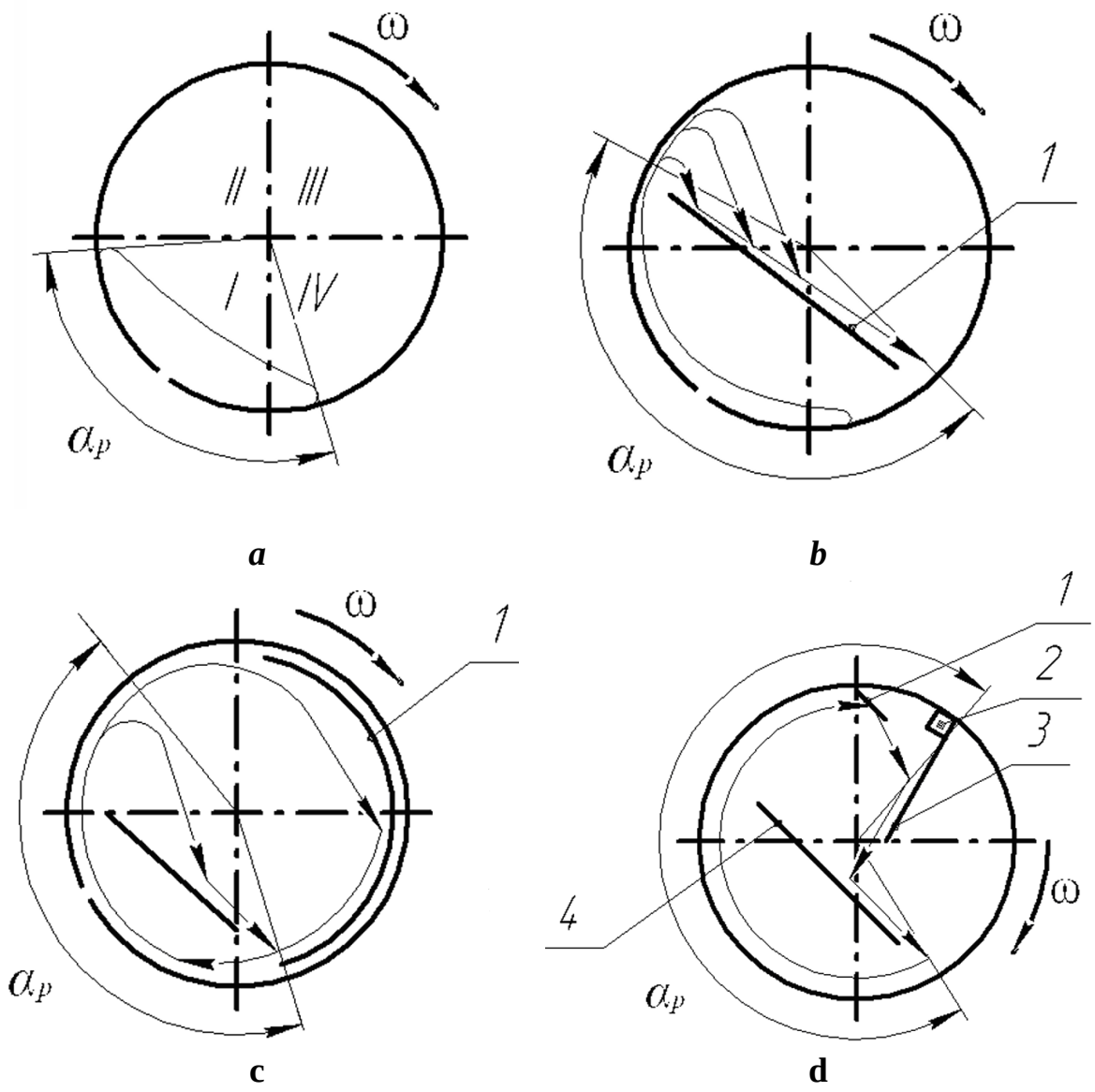

Fig. 1.3. Operating processes of mesh drums

By installing a fixed inclined plate (1) inside the drum, it becomes possible to slightly increase the rotation frequency of the drum without disrupting the operating process (Fig. 1.3b). The screened material lifted along the drum surface into the II quadrant falls onto the inclined plate and is redirected back to the IV quadrant of the surface. In order to transfer the screened material onto the surface, a certain angle is selected, which ensures process continuity when increasing the drum speed. In this case, the second type of motion regime is used, where the screened material is lifted up to the

II quadrant, detached at an angle of 90°…180°, and moves freely inside the drum along a parabolic trajectory until it falls onto the inner surface. According to experimental data by B.G. Turbin, the efficiency of a mesh drum with an inclined plate is not significantly higher than that of a simple low-speed drum, while the structure of the screener becomes more complex and its stability decreases.

The second type of operating regime is also used in drums equipped with an inclined plate and a semi-cylindrical baffle (Fig. 1.3c). This regime is characterized by the fact that the screened material is lifted up to the II quadrant, detached at an angle of 90°…180°, and moves freely inside the drum along a parabolic trajectory until it reaches the inner surface. The baffle receives particles leaving the drum surface in the II quadrant and redirects them again to the lower part of the drum, the IV quadrant. The installation angle of the baffle is selected in such a way that the lifting of the screened material up to the II quadrant is ensured. This makes it possible to increase both the rotation frequency of the drum and its productivity. According to [34; pp. 30–48], the productivity of baffle-equipped mesh drums is 2…2,5 times higher than that of simple drums.

Mesh drums equipped with a cleaner (1), brush (2), return baffle (3), and inclined plate (4) are used in cases where the screened material does not detach from the mesh surface (Fig. 1.3d). The material flowing from the inclined plate falls into the IV quadrant of the drum. The mesh induces the material to perform rotational motion and lifts it up to the III quadrant. In this process, the material is directed from the cleaner and brush to the return baffle and inclined plate. The disadvantage of this design is the accelerated wear of working elements at high drum speeds [32; p. 28].

A number of researchers have studied the motion of bulk materials inside rotating mesh drums. Among them are the works of Y.L. Ding, R. Forster, J.P. Seville, and D.J. Parker from the University of Birmingham, England [35; pp. 635–663]. In their study, a mathematical model describing

the motion of bulk material in a rotating drum was developed based on the Eulerian approach (Fig. 1.4).

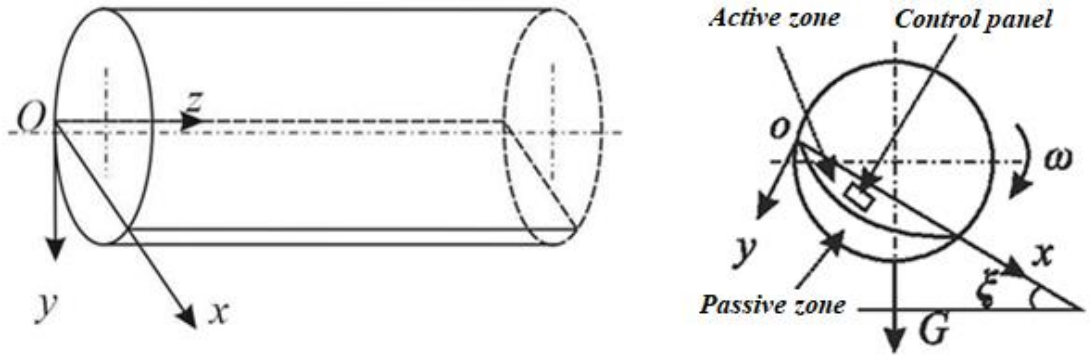

Fig. 1.4. Schematic diagram and model of a rotating drum

Based on the studies, integro-differential mass and momentum equations were obtained, namely:

$$\begin{aligned} &\frac{d}{dx}\int_0^{\delta} u dy = \omega\left[(L-x)-(h+\delta)\frac{d\delta}{dx}\right] \\ &\frac{d}{dx}\int_0^{\delta} u^2 dy = \omega^2(h+\delta)\left[(h+\delta)\frac{d\delta}{dx}-(L-x)\right]+g\cos\xi(tg\xi-tg\beta)\delta \end{aligned}, \quad (1.1)$$

Here, L is the half-chord length, m; h is the shortest distance between the drum center and the layer surface, m; ω is the angular velocity of the drum, rad/s; δ is the depth of the active layer, m; ξ is the angle of dynamic deviation, degrees; β is the angle of internal friction, degrees.

By solving equation (1.1) and using the schematic shown in Fig. 1.5, an equation describing the velocities of moving particles of bulk material has been derived

$$u = \frac{\omega(h+\delta)}{1-\Delta^2}\left[\Delta^2 - \left(\frac{y}{\delta}\right)^2\right], \quad (1.2)$$

Here, Δ is a parameter characterizing the rheological properties of granular materials, rad/m.

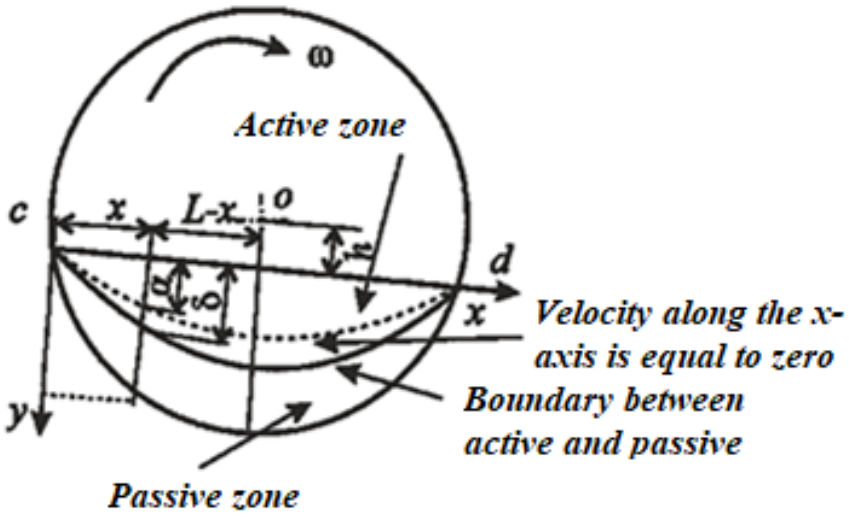

Fig. 1.5. Schematic of the material layer in a rotating drum

Researchers from China have studied the motion of bulk materials in three types of horizontal drums with different geometries, rotating at a constant angular velocity, using the finite element method. The studies were carried out in two circular and one elliptical drum, with angular velocities ranging from 0,01 rad/s to 21,9 rad/s. By varying the angular velocity, four flow regimes were identified (Fig. 1.6) [36].

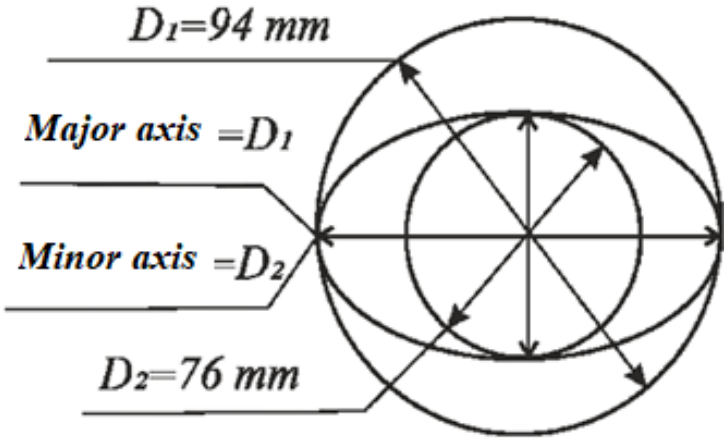

Fig. 1.6. Two circular and one elliptical drum shapes

In [37], the motion of material inside a drum was theoretically investigated, and differential equations describing the motion of a body along the surface of a rotating drum were derived, together with corresponding

computational schemes (Fig. 1.7). The differential equations of displacement and sliding motion of the body relative to the drum are expressed as follows:

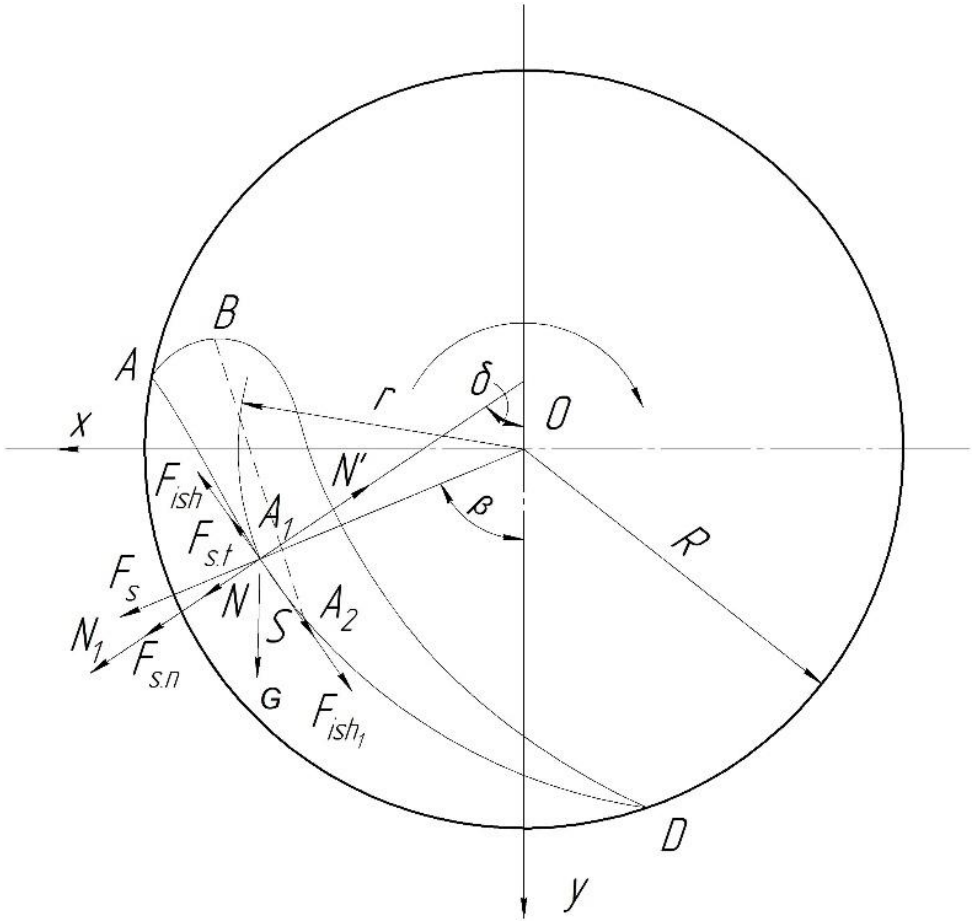

Fig. 1.7. Schematic for determining the sliding surface

$$\frac{d\omega_0}{d\beta} - \mu_0\omega_0 - \frac{g\left(\mu_0\cos\beta - \sin\beta\right) + \mu_0\omega^2 R}{\omega_0 R} = -2\mu_0\omega$$
$$\frac{d\omega_0}{d\beta} + \mu_0\omega_0 + \frac{g\left(\mu_0\cos\beta - \sin\beta\right) + \mu_0\omega^2 R}{\omega_0 R} = 2\mu_0\omega \quad , \qquad (1.3)$$

Here, ω is the angular velocity of the drum, rad/s; ω_0 is the angular velocity of the body sliding relative to the drum, rad/s; β is the angle of the body position measured from the vertical diameter, rad; μ_0 is the coefficient of friction during sliding; R is the inner radius of the drum, m.

The analysis of the operating processes of mesh drums shows that, in the screening of bulk materials, the geometric dimensions of the drums, rotation frequency, inclination angle relative to the horizontal plane, type of motion, and friction angles are of key importance. Therefore, in their design

and calculation, it is possible to develop energy- and resource-saving structures by taking the above parameters into account.

1.3. Meshes and the screening processes on them

The screening of bulk materials using meshes is considered one of the most complex and widely used technological processes [38, 39].

In the screening of bulk materials, the use of wire meshes with a circular cross-section is considered effective (Fig. 1.8). This is because, in wire meshes with a circular cross-section, particles of bulk material are in an unstable position on the wires, which facilitates their passage through the openings. Analyses have shown that the use of this type of mesh reduces screening time and increases specific productivity by up to 85% compared to flat wire meshes. Wire meshes have a sufficiently high open area coefficient μ. The value of this coefficient is determined as the ratio of the total area of all openings in the mesh S_0 to the total surface area of the mesh S_{tot} [32; pp. 17–19].

$$\mu = \frac{S_0}{S_{tot}}. \qquad (1.4)$$

When the wire diameter in wire meshes is (0.8…1.0) mm, the open area coefficient μ is in the range of 0,68…0,70. In such cases, the maximum screening capacity reaches 3,5 kg/(s·m^2) [40; p. 15, 41; pp. 3–9].

The main disadvantage of wire meshes is the low strength of the interconnected joints (Fig. 1.8a). When bulk material is subjected to inertial forces and the gravitational load of the upper layers, particles may become jammed at the joints, which in turn leads to a reduction in the effective working area of the openings. In addition, the tension forces in the wires are relatively high, ranging from (150…300) N [32; p. 17].

Profiled wire meshes differ in that the steel wires are arranged in two parallel planes in the transverse direction (Fig. 1.8b). The specific feature of such meshes is that particles falling onto the upper row of joints first change their initial direction and then fall onto the joints of the lower row, becoming

unstable and subsequently passing through the openings. According to A.I. Klimk's studies, the time required for particles of bulk material to pass through the openings in such meshes is 2,0…2,5 times higher than in ordinary wire meshes and 4,0…4,5 times higher than in flat meshes. In this case, the optimal specific productivity of profiled wire meshes is in the range of (1,6…1,8) kg/(s·m^2) [40; pp. 10–15].

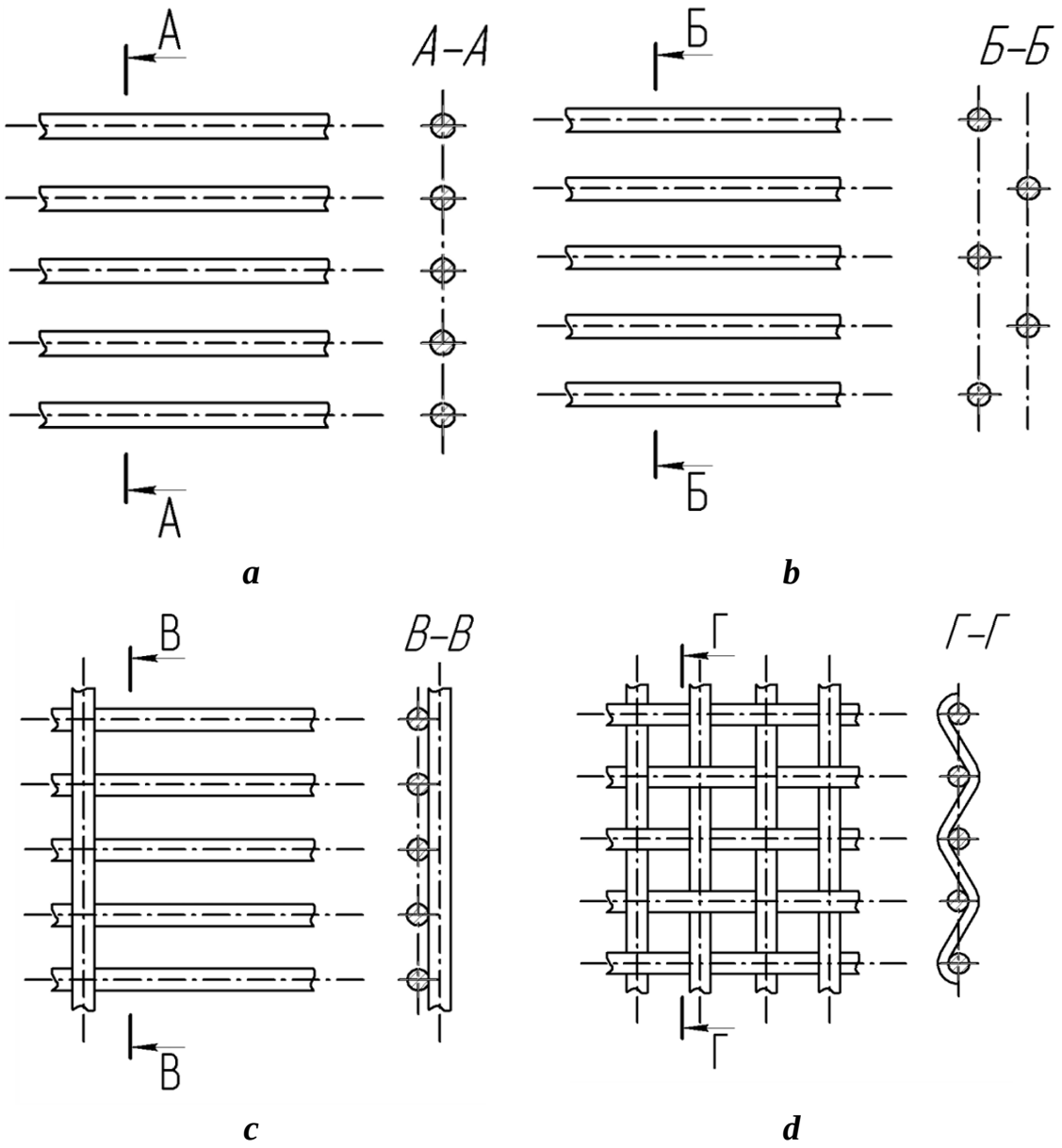

a ***b*** ***c*** ***d***

a – wire mesh; b – profiled wire mesh; c – welded wire mesh; d – woven wire mesh

Fig. 1.8. Wire meshes with circular cross-section

The main advantage of welded wire meshes is their sufficient strength and the stability of the opening working area (Fig. 1.8c) [42, 43]. The invariability of the parameters is ensured by the rigid connection between the longitudinal and transverse joints. Due to the circular cross-sectional shape of the wires, the efficiency is high as a result of the unstable positioning of bulk material particles on them. Their main disadvantage is the perpendicular arrangement of the transverse wires relative to the longitudinal wires.

Fig. 1.8d shows a woven wire mesh. In such meshes, square openings are formed by weaving wires together. These meshes operate intensively due to a larger open area compared to other types. However, the accuracy of the mesh openings is low, which may further reduce the quality of screening during operation. At the same time, in woven wire meshes, the diagonals of the square openings are 1,4 times larger than the sides, which increases the probability of particles passing through the openings [44].

The performance of meshes is usually evaluated by the screening efficiency coefficient or the discharge coefficient η of passing fractions. The discharge coefficient η is defined as the ratio of the mass m_1 of fractions that pass through the mesh to the total mass m_0 of all passing fractions and is determined as follows [19; p. 31]:

$$\eta = \frac{m_1}{m_0}. \qquad (1.5)$$

According to a large number of researchers, the main parameter affecting the screening quality and the productivity of screening machines is the relative velocity of bulk material particles [45; pp. 548–554, 46; pp. 205–213, 47; pp. 139–141, 48; pp. 39–43, 49; pp. 49–54, 50, 52, 55; pp. 13–14, 56; pp. 11–12].

The relative velocity of bulk material particles depends on so many factors that it is not possible to take all of them into account when mathematically modeling the process. Therefore, in modeling the screening process, particles are usually replaced with simplified models whose physical

and mechanical properties are close to those of the real material being screened [57; pp. 10–13, 58; pp. 33–36].

The conditions for particle passage through mesh openings during screening, as well as the dependence of kinematic and structural parameters on relative velocity, have been considered in detail in studies [59, 60].

M.N. Letoshnev, taking into account the forces acting on bulk material particles, derived the following differential equation describing the relative motion of particles [21]

$$\begin{cases} \frac{1}{\delta}\frac{d^2x_B}{dt^2} = \omega^2 r\cos\omega t - g\frac{\sin(\gamma+\alpha)}{\cos(\sigma+\alpha+\gamma)} \\ \frac{1}{\lambda}\frac{d^2x_H}{dt^2} = \omega^2 r\cos\omega t - g\frac{\sin(\gamma-\alpha)}{\cos(\sigma+\alpha-\gamma)} \end{cases}, \qquad (1.6)$$

here, ω is the angular velocity of the drive shaft, rad/s; r is the vibration amplitude of the mesh, m; α is the inclination angle of the mesh relative to the horizontal plane, degrees; σ is the angle of the vibration direction, degrees; γ is the angle of friction, degrees.

$$\delta = \frac{\cos(\alpha+\varepsilon+\gamma)}{\cos\gamma},\ \lambda = \frac{\cos(\alpha+\varepsilon-\gamma)}{\cos\gamma}$$

$\frac{d^2x_B}{dt^2}, \frac{d^2x_H}{dt^2}$ - the acceleration of particles moving upward and downward along the mesh, m/s^2.

By integrating equation (1.6), expressions were obtained that make it possible to determine the distances traveled by particles during upward (x_B) and downward (x_H) motion.

$$x_B = \delta r\left[\cos\psi_1 - \cos\psi_2 - (\psi_2-\psi_1)\sin\psi_1 - 0{,}5(\psi_2-\psi_1)^2\cos\psi_0\right],$$

(1.7)

$$x_H = \sigma r\left[\cos\theta_1 - \cos\theta_2 - (\theta_2-\theta_1)\sin\theta_1 - 0{,}5(\theta_2-\theta_1)^2\cos\theta_0\right],$$

(1.8)

here, ψ_1 and ψ_2 are the initial and final phases of the upward displacement; θ_1 and θ_2 are the initial and final phases of the downward displacement; ψ_0 and θ_0 are the phases corresponding to the maximum relative velocities in the upward and downward motions, respectively.

The relative velocities of bulk material particles moving upward and downward on the mesh can be determined respectively as follows:

$$\frac{1}{\delta}\frac{dx_B}{dt} = \omega r\left(\sin\omega t - \sin\omega t_1\right) - g\left(t - t_1\right)\frac{\sin\left(\gamma + \alpha\right)}{\cos\left(\sigma + \alpha + \gamma\right)}, \qquad (1.9)$$

$$\frac{1}{\lambda}\frac{dx_H}{dt} = \omega r\left(\sin\omega t - \sin\omega t_1\right) - g\left(t - t_1\right)\frac{\sin\left(\alpha - \gamma\right)}{\cos\left(\sigma + \alpha - \gamma\right)}, \qquad (1.10)$$

here, t and t_1 are the initial and final times of the particle's relative motion along the mesh, s.

The final equation describing the particle velocity is as follows:

$$V = \frac{x_H + x_B}{T} = \frac{x_H + x_B}{2\pi}\omega, \qquad (1.11)$$

here, T is the full vibration period, s.

From the above equations, it can be seen that the relative motion of bulk material particles is influenced by friction, as well as the amplitude and frequency of vibration.

In the screening of bulk materials, the limiting velocity of particles is also an important parameter (Fig. 1.9).

X.A. Ksifilinov derived an expression that makes it possible to determine the limiting velocity of a spherical particle on a mesh inclined at an angle to the horizontal plane, namely [14].

$$V_{\lim} = \left(D\cos\alpha - r\right)\sqrt{\frac{g}{2\left(r \pm D\sin\alpha\right)}}, \qquad (1.12)$$

here, D is the diameter of the mesh opening, m; r is the radius of the spherical particle, m; g is the acceleration due to gravity, m/s^2; α is the inclination angle of the mesh relative to the horizontal plane, degrees.

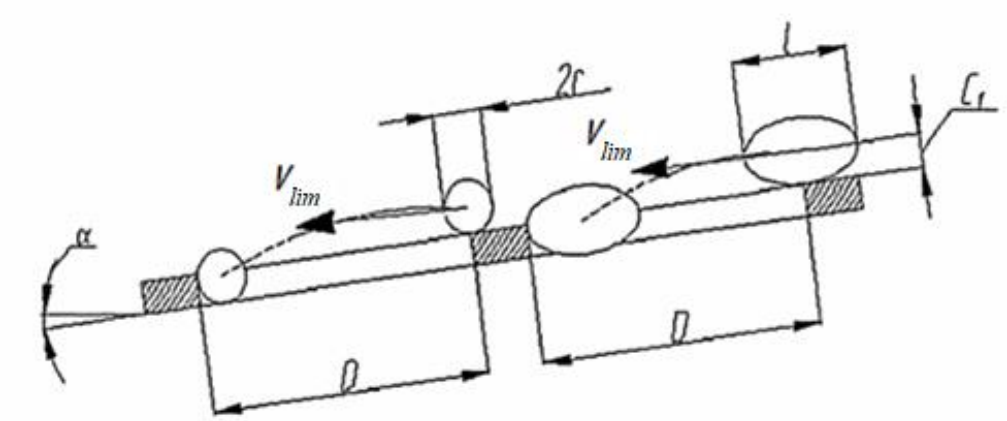

Fig. 1.9. Computational scheme for determining the limiting velocity of particle motion along the mesh

N.G. Gladkov derived an expression that makes it possible to determine the limiting velocity of an ellipsoidal particle on a mesh inclined at an angle to the horizontal plane, namely [22; p. 15].

$$V_{\lim} = \left(D\cos\alpha - \frac{c_1}{2} \right) \sqrt{\frac{g}{c_1 + 2D\sin\alpha}}, \qquad (1.13)$$

here, c_{11} is the distance from the center of gravity to the edge of the opening, m.

In [63; p. 80], a design method for determining rational values of the structural and kinematic parameters of screening machines for bulk materials was proposed. In this approach, the vibrational displacement theory was used to develop a mathematical model of the motion of bulk material on the mesh and the passage of particles through mesh openings [64; pp. 35–36], as well as the individual motion of spherical particles within the openings [65].

The following assumptions were made in constructing the model: fine fractions with spherical particles were replaced by equivalent diameters; both the particle and the mesh were considered absolutely rigid bodies; the mesh openings were assumed to be identical in size and shape; and the collisions of particles with the edges of the openings were considered elastic. In the studies, the particle and the mesh were considered in a fixed *XOY* coordinate system (Fig. 1.10).

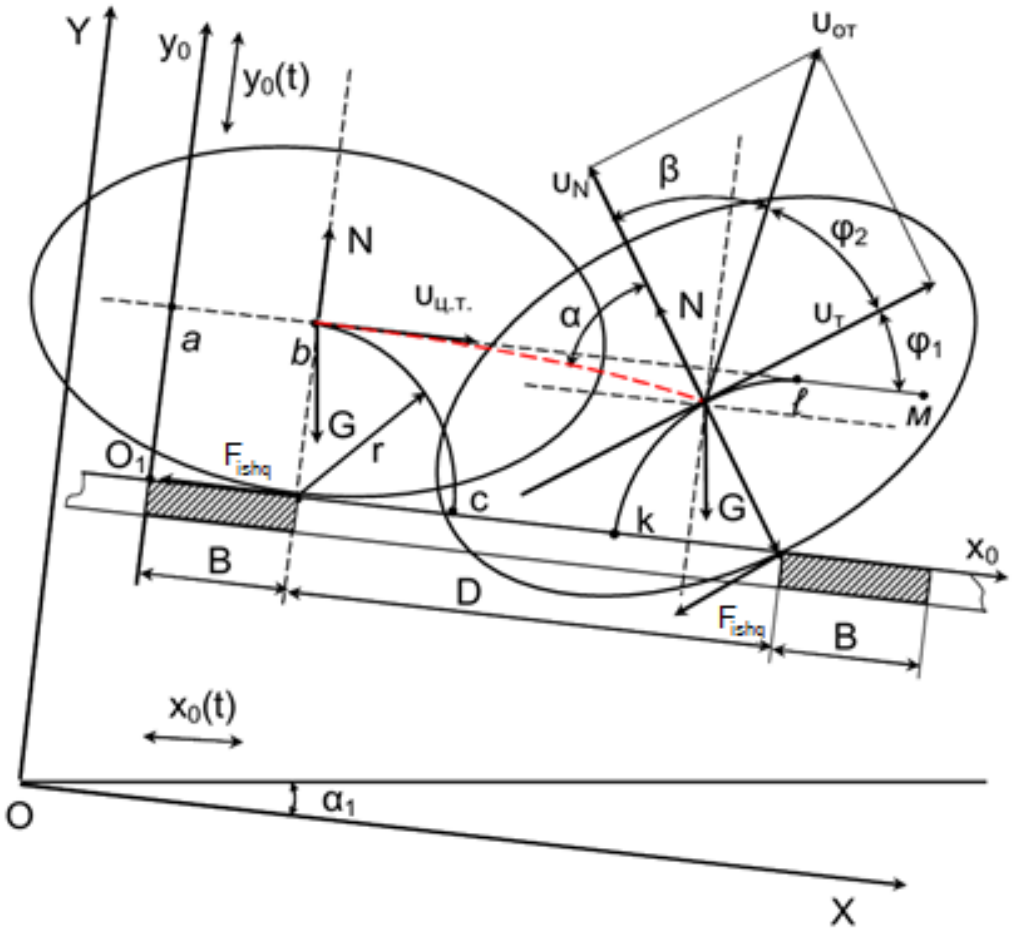

Fig. 1.10. Computational scheme of the motion of bulk material on the mesh and the passage of spherical particles through mesh openings

The majority of studies on the operating processes of meshes are mainly devoted to increasing the screening capacity of the mesh, since the efficiency of the screening process and the specific productivity of the working elements are determined by this factor. The analysis of the conducted studies shows that the kinematic operating regime has a significant influence on the screening capacity of the mesh [66; p. 25, 67; pp. 28–32]. The passage or non-passage of particles through a mesh opening depends on the magnitude and vector direction of their velocity relative to the mesh. The duration of the passage process through the mesh also significantly depends on this velocity. Therefore, in calculating the screening capacity of a mesh, it is necessary to know the velocities at different cross-sections along its length [68; p. 73].

A.V. Fominikh and V.G. Chumakov, based on their studies of screening processes and devices, presented the following schematic

representation of the screening system on meshes (Fig. 1.11) [69; p. 77].

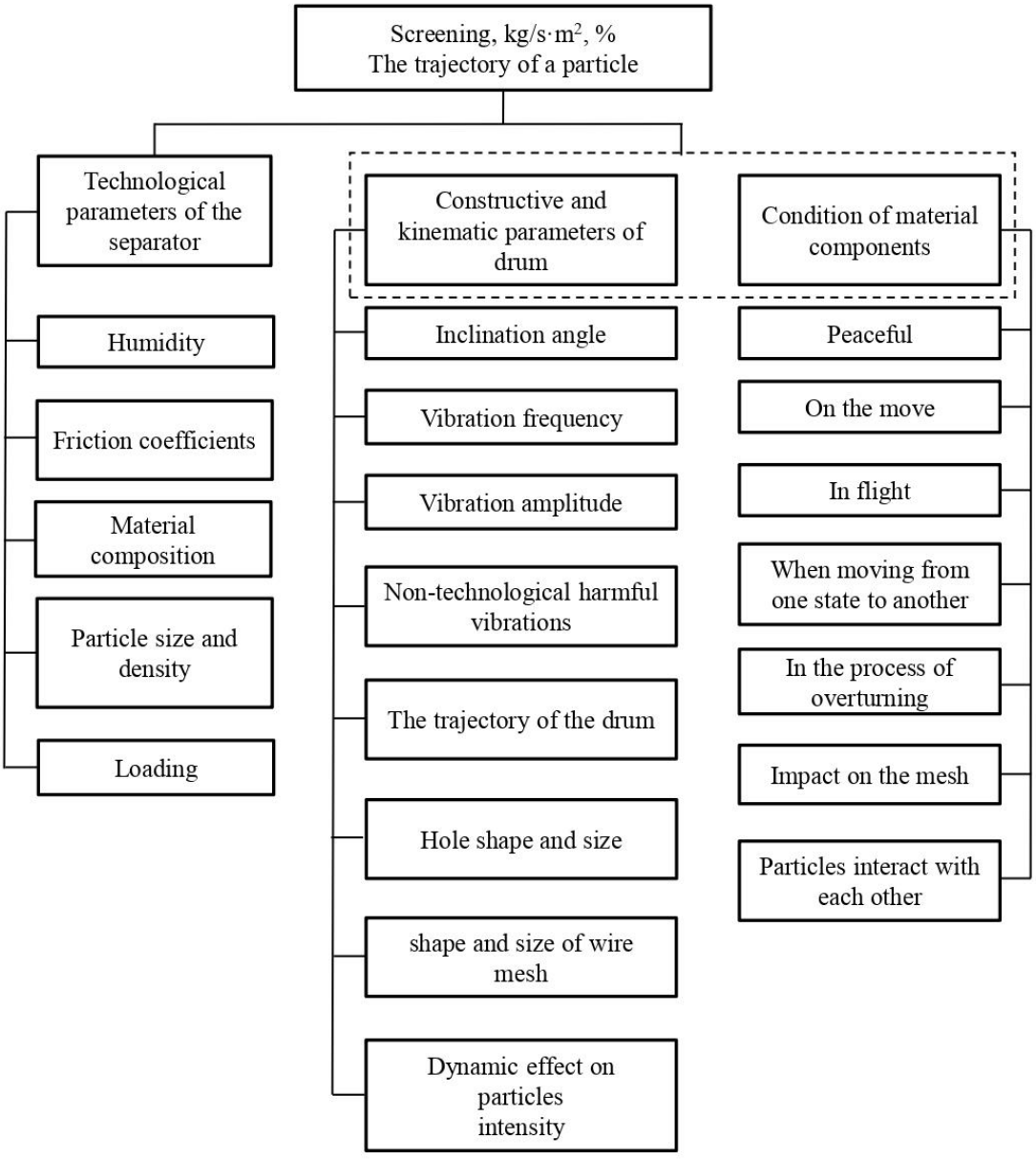

Fig. 1.11. Screening system in meshes

Based on many years of operational observations of screening machines, it has been determined that the intensity of the discharge of fractions passing through mesh openings depends on the following factors [19; p. 31]:

- the type of mesh motion (reciprocating, vibrating-reciprocating, rotational);
- the design of the mesh;

- the kinematic parameters of the mesh (amplitude and frequency of vibrations, inclination angle relative to the horizontal plane);
- the mesh cleaning device for removing clogged particles;
- the length of the mesh;
- the composition of the screened material and the loading of the mesh.

Based on the above, the technological process of screening bulk materials can be represented schematically as follows (Fig. 1.12).

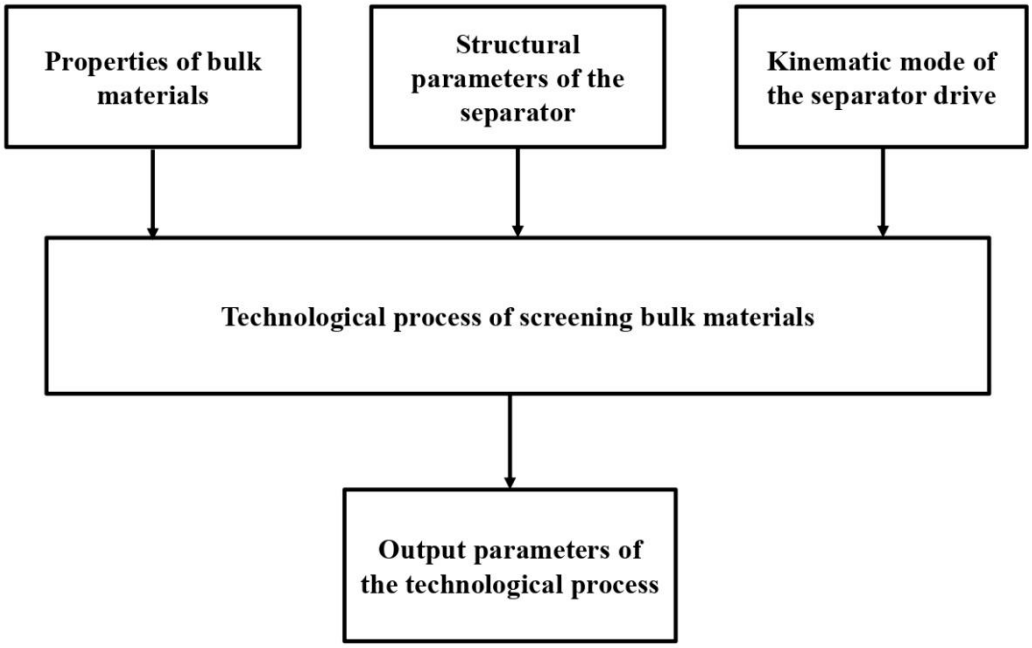

Fig. 1.12. Schematic of the technological process of screening bulk materials

Conclusions to Chapter I

1. It is advisable to use centrifugal rotating mesh drums in order to increase the intensity of the screening process, ensuring that bulk material is subjected to inertial forces greater than gravitational force.

2. In the screening of bulk materials, the geometric dimensions of drums, rotation frequency, inclination angle relative to the horizontal plane, type of motion, and friction angles are of key importance. Therefore, in their

design and calculation, it is possible to develop energy- and resource-saving structures by taking the above parameters into account.

3. In developing an efficient design of a mesh drum, the use of wire meshes with circular cross-sections to ensure the instability of bulk material particles, as well as the study of additional vibration excitation methods, has a positive effect on screening efficiency.

CHAPTER II. DEVELOPMENT OF THE DESIGN OF A DRUM SCREENING DEVICE AND ITS THEORETICAL INVESTIGATION

2.1. Development of the design of a drum screening device

Based on the analysis of the literature, an improved design of a drum screening device was proposed (Fig. 2.1).

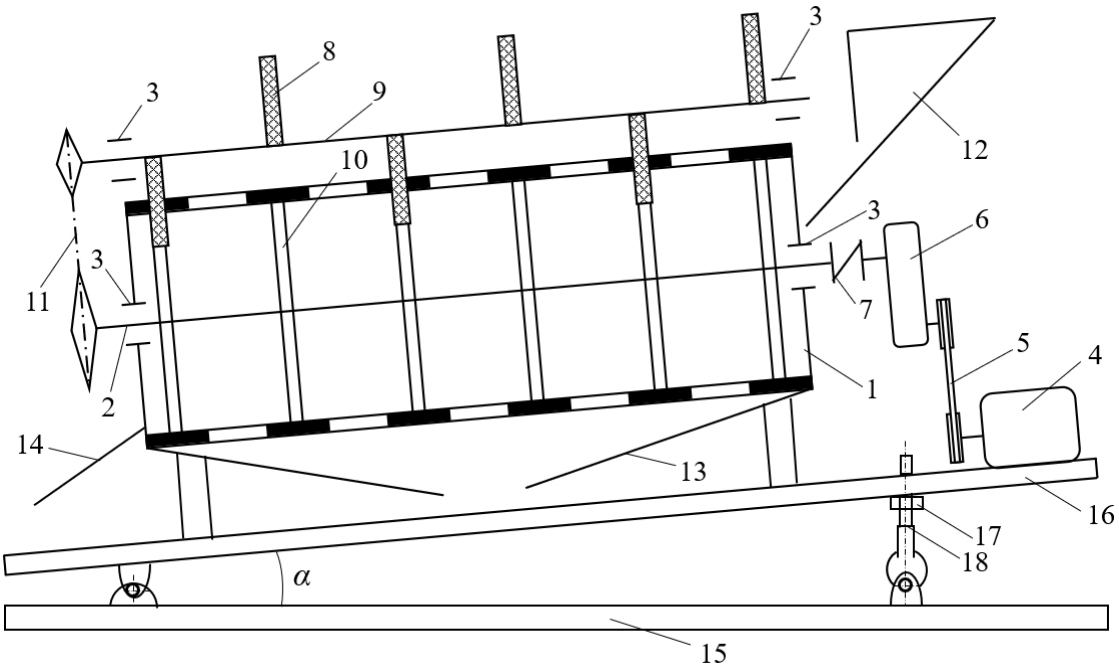

Figure 2.1. Improved design of a device for screening bulk materials

This device consists of the following components: a mesh cylinder 1 and its shaft 2, which ensures its rotational motion, mounted on bearings 3. The rotational motion is transmitted from the electric motor 4 through a V-belt drive 5 to the reducer 6, and from there through a coupling 7 to the mesh cylinder 1. To intensify the screening process of bulk materials, a blade shaft 9 equipped with elastic blades 8 that exert periodic impact forces is mounted in bearings 3 in the upper part of the mesh cylinder 1. In this case, ribs 10 are provided on the mesh cylinder 1 to receive the impact forces. The rotational motion of the blade shaft 9 is transmitted from the mesh cylinder 1 through a chain drive 11. A feed hopper 12 is installed to supply bulk material into the mesh cylinder 1, a chute 13 is provided for discharging separated fine

fractions, and a chute 14 is used for discharging coarse fractions. To adjust the inclination angle α of the device relative to the foundation 15, the frame 16 is equipped with an adjusting screw 18 with a rotating nut 17.

The drum screening device operates as follows: During operation, bulk material is fed through the hopper 12 into the rotating mesh cylinder 1. The rotational motion is transmitted in the following sequence: from the electric motor 4 through the V-belt drive 5 to the reducer 6, and then from the output shaft of the reducer 6 through the coupling 7 directly to the shaft 2 of the mesh cylinder 1. In this way, the mesh cylinder 1 rotates with a constant angular velocity. Since the device is installed at an inclination angle α relative to the foundation 15, the material being screened moves both rotationally and axially along with the mesh cylinder 1 during operation.

Fractions of bulk material smaller than the mesh openings of the mesh cylinder 1 pass through the openings sequentially and are collected in the chute 13 for fine fractions. To increase the efficiency of separating fine fractions passing through the mesh openings, the blade shaft 9 receives rotational motion from the mesh cylinder 1 via the chain drive 11, and its elastic blades 8 periodically apply impact forces to the ribs 10, causing additional vibration of the mesh cylinder 1. This intensifies the screening process. Coarse fractions, which are larger than the mesh openings, are discharged from the process through the chute 14. The inclination angle α of the device relative to the foundation 15 is adjusted by moving the frame 16 using the adjusting screw 18 by rotating the nut 17.

The proposed bulk material screening device ensures an increase in screening efficiency and productivity.

2.2. Determination of the impact point of the elastic blade acting on the mesh drum

In the force analysis of mechanical systems, the following aspects are mainly considered: based on the given law of motion of the driving link and the applied forces, the inertial forces, reaction forces in kinematic pairs, and

the balancing force or moment in the driving link are determined. In this case, the given forces include driving forces, technological resistance, and the weight of the link. In force calculations, the inertial force to be determined is reduced for each link to the resultant vector and the resultant moment of inertia forces, namely [1; pp. 78–79].

$$P_i = -ma_s, \qquad (2.1)$$

$$M_i = -J_s\varepsilon, \qquad (2.2)$$

Here, m is the mass of the link, kg; a_s is the acceleration of the center of mass of the link, m/s^2; ε is the angular acceleration of the link, rad/s^2; J_s is the moment of inertia of the link about an axis passing through its center of mass and perpendicular to the plane of motion, kg·m^2.

The inertia force P_i and the moment of the force couple M_i can be reduced to a single force P_i (Fig. 2.2a and b), but not applied at the center of mass; instead, it is applied at a certain lever arm h. If, as shown in Fig. 2.2c, three forces act on the link, then when selecting the lever arm h, it is necessary to satisfy the condition $P_i \cdot h = M_i$. In this case, two equal and oppositely directed forces P_i can be eliminated, and the force P_i and moment M_i acting on the link can be replaced by a single force P_i applied at a distance h from the center of mass, namely

$$h = \frac{M_i}{P_i} = \frac{J_s\varepsilon}{ma_s}. \qquad (2.3)$$

The resultant force is transferred to point S in such a way that the moment taken about the center of mass is directed opposite to the angular acceleration ε. At the same time, the force and moment can be replaced by two forces of equal magnitude applied at points A and B (Fig. 2.2d).

$$P = \frac{M_i}{l_{AB}} = \frac{J_s\varepsilon}{l_{AB}}. \qquad (2.4)$$

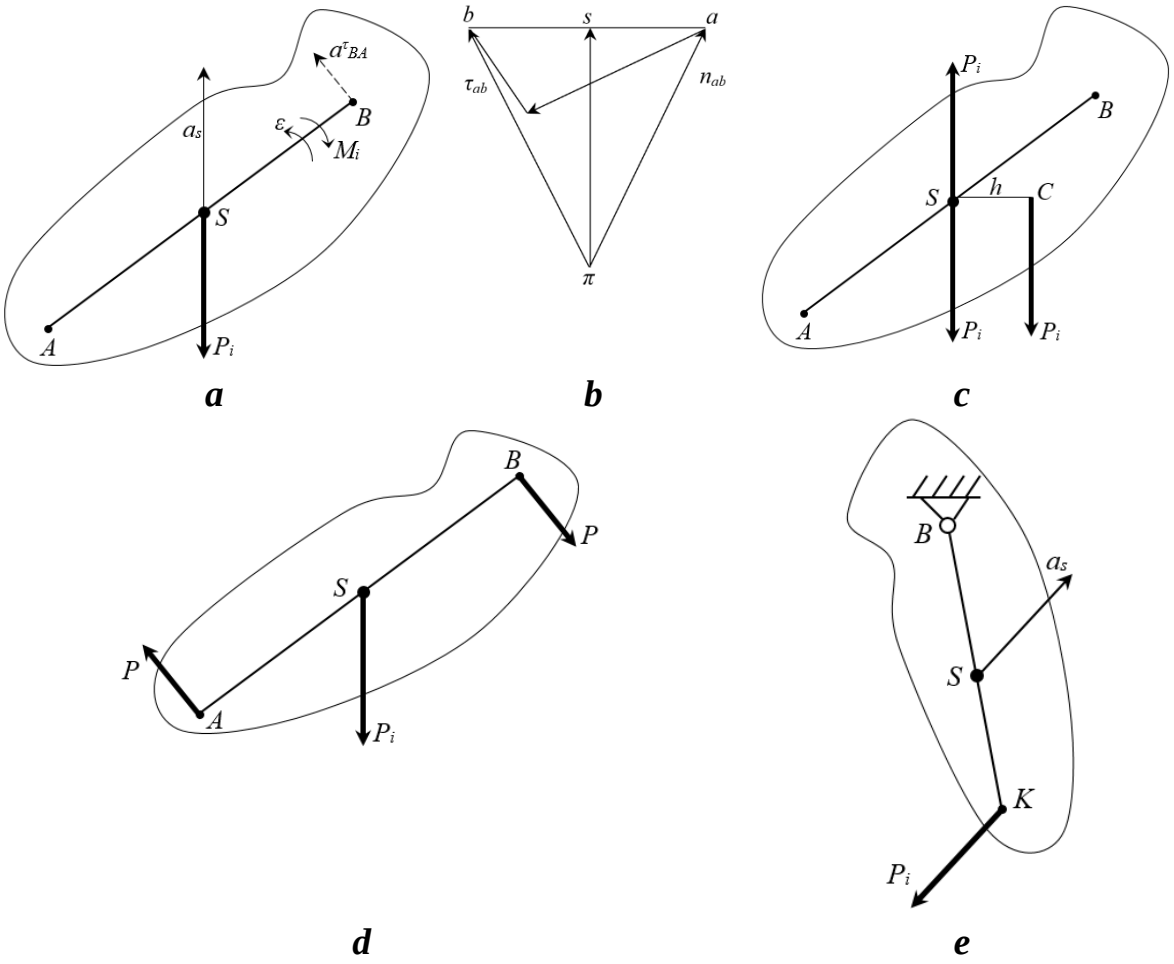

Fig. 2.2. Scheme for the force analysis of a lever

If the link performs rotational motion about a fixed center, then the resultant inertia force must be applied at the center of percussion (Fig. 2.2e). The distance between the center of rotation and the center of percussion is determined from the following expression known from the course of theoretical mechanics

$$l_{BK} = \frac{J_B}{ml_{BS}} = l_{BS} + \frac{J_s}{ml_{BS}}, \qquad (2.5)$$

Here, J_B is the moment of inertia of the link about the rotation center B, kg·m^2; l_{BS} is the distance from the rotation center B to the center of mass S, m.

Taking the above into account, theoretical studies are carried out to determine the impact point on the elastic blade. In a drum-type bulk material screening device, during the screening process, elastic blades periodically exert impact forces on the mesh drum in order to increase its operational efficiency. In this case, the occurrence of impact forces, while improving the

performance of the device, also has a negative effect on the working elements. For example, when the elastic blades interact with the mesh drum, stresses arise at the supports where the blades are fixed to the shaft. Therefore, determining the point of interaction between the working elements is of significant importance.

In the conducted studies, the elastic blade is considered as a lever rotating with a constant angular velocity about its support, with its center of mass located at point S and with mass uniformly distributed along its length, while the mesh drum is considered as a curved surface (Fig. 2.3).

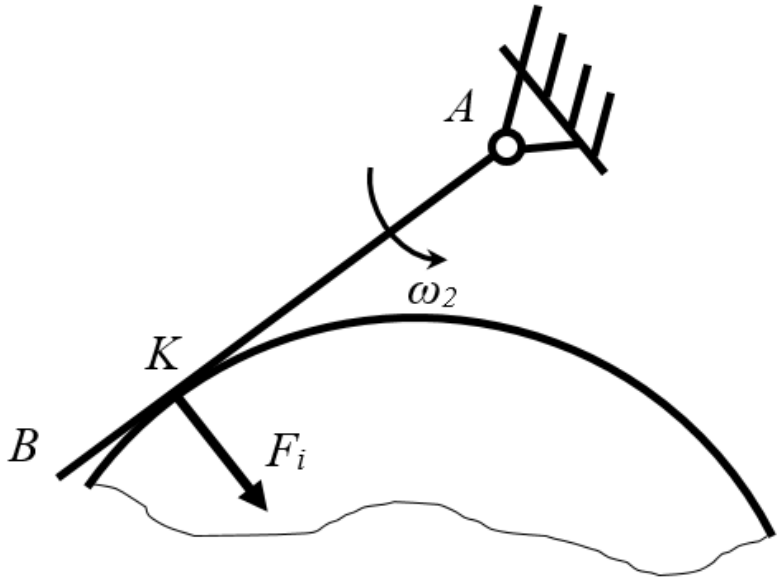

Fig. 2.3. Lever with uniform cross-section rotating with constant angular velocity and mesh drum

In order to reduce the reaction forces at point *A* of the elastic blade and ensure its reliable operation, the impact point is determined, and the inertia force is applied at this point. This is because determining the impact point and transferring the point of application of the force to this location is important in oscillating mechanical systems. Using Fig. 2.4, the impact point of the elastic blade is determined.

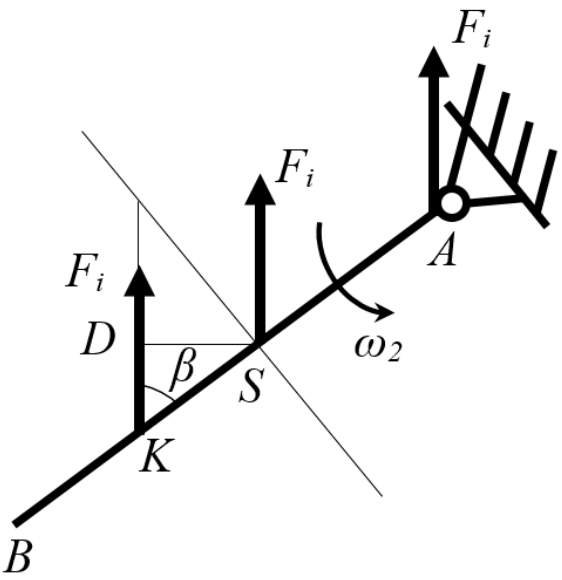

Fig. 2.4. Schematic for determining the impact point of the elastic blade

According to [71; p. 296], the impact point is the point at which the resultant of all inertia forces acting on a link performing rotational motion is applied. The center of mass of the elastic blade is located at its midpoint, namely

$$AS = SB = \frac{AB}{2}, \qquad (2.6)$$

here, AB is the length of the elastic blade, m..

To determine the impact point, first the moment of inertia of the elastic blade about point A is determined.

$$J_A = J_s + m_p \left(AS\right)^2, \qquad (2.7)$$

or

$$J_A = m_p AK \cdot AS, \qquad (2.8)$$

Here, m_p is the mass of the elastic blade, kg.

The moment of inertia of the blade about an axis passing through its center of mass and perpendicular to the plane of motion is expressed as follows

$$J_s = \frac{m_p \left(AB\right)^2}{12}. \qquad (2.9)$$

By equating expressions (2.7) and (2.8), and taking into account relations (2.9) and (2.6), the following expression is obtained

$$AK = \frac{4}{3} \cdot AS = \frac{2}{3} \cdot AB. \qquad (2.10)$$

Thus, the impact point of the blade is located at a distance equal to two-thirds of its length from the axis of rotation.

2.3. Investigation of the force exerted by the elastic blade on the ribs of the mesh drum

As stated above, during the screening process, elastic blades periodically exert impact forces on the mesh drum in order to increase its operational efficiency. This, in turn, causes additional movement of the screened material. Figure 2.5 presents a schematic diagram for determining the effect of the elastic blade on the ribs of the mesh drum.

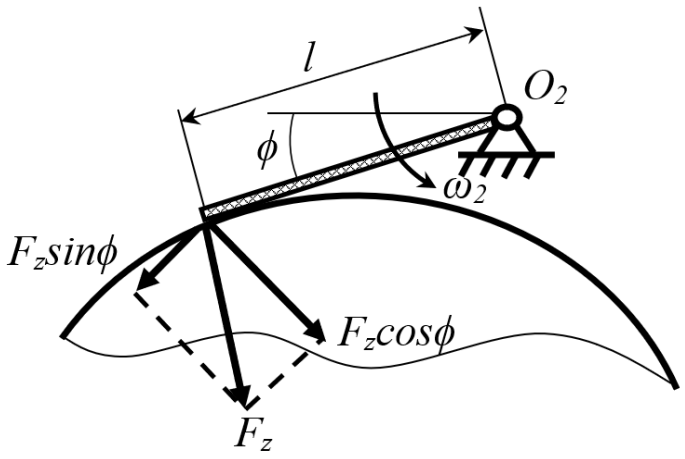

Fig. 2.5. Schematic diagram for determining the effect of the elastic blade on the ribs of the mesh drum

During the interaction process, according to [72; pp. 1–15], two types of deformation occur in the elastic blade, namely elastic deformation and deformation caused by changes in velocity. Therefore, in elastic deformation, the potential energy is expressed as follows (Fig. 2.6).

$$П = \frac{F_z \Delta x}{2}, \qquad (2.11)$$

Here, F_z is the impact (elastic) force, N; Δx is the deformation value of the elastic blade, m.

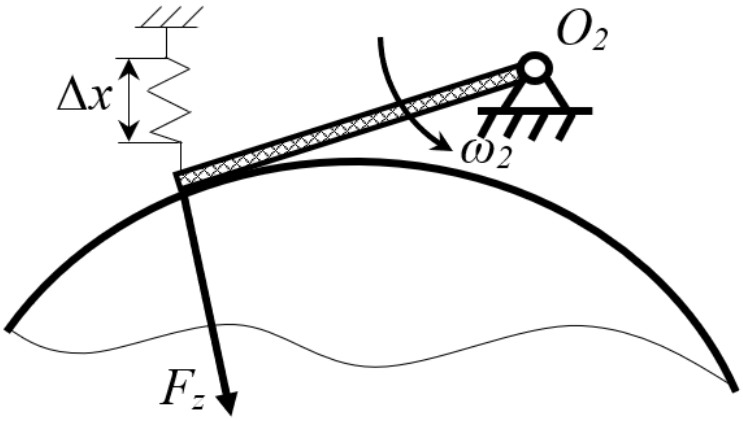

Fig. 2.6. Schematic illustrating the deformation of the elastic blade

On the other hand, as a result of the interaction and the induced motion of the screened material, it acquires kinetic energy, namely

$$W = \frac{m_{s.m} v_2^2}{2}, \qquad (2.12)$$

Here, $m_{s.m}$ is the mass of a particle of the screened material, kg; v_2 is the linear velocity of the elastic blade, m/s.

According to [73; p. 12], the linear velocity of the elastic blade is expressed as follows

$$v_2 = \omega_2 l, \qquad (2.13)$$

Here, ω_2 is the angular velocity of the shaft with elastic blades, rad/s.

Using the equality of potential energy and kinetic energy, the impact force is expressed as follows

$$F_z = \frac{m_{s.m} \omega_2^2 l^2}{\Delta x}. \qquad (2.14)$$

If it is taken into account that the elastic blade acts on the mesh drum at the impact point, then equation (2.14) takes the following form

$$F_z = \frac{4 m_{s.m} \omega_2^2 l^2}{9 \Delta x}. \qquad (2.15)$$

To determine the variation range of the impact force exerted by the elastic blade on the mesh drum, the numerical solution of expression (2.15) is carried out using Microsoft Office Excel software at the following parameter values: $m_{s.m}$ = (0,001…0,005) kg, ω = (3…5) rad/s, l = 0,25 m, Δx = (0,002…0,004) m

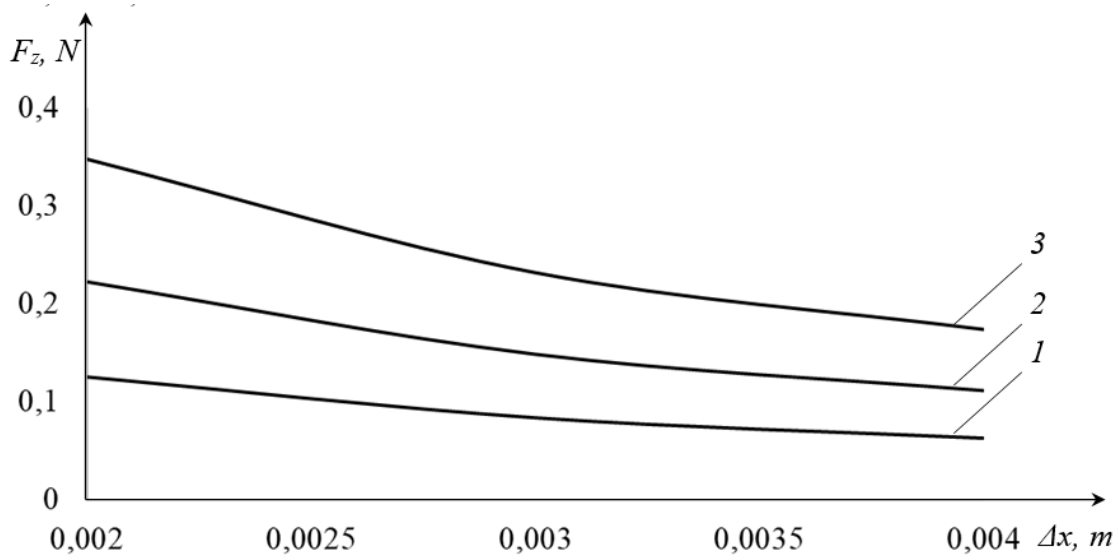

***1*- ω=3 rad/s; *2*- ω=4 rad/s; *3*- ω=5 rad/s.**

Fig. 2.7. Graph of the dependence of the impact force exerted by the elastic blade on the mesh drum on the deformation value of the elastic blade

2.4. Determination of the axial velocity of the screened material in a rotating mesh drum

The main purpose of studying the screening process of bulk materials is to determine the dependence of the kinematic and structural parameters of screening machines on the physical and mechanical properties of the screened material.

In our studies, we consider the axial motion of the screened bulk material along the rotation axis of the drum. As is known, the mesh drum is installed at an inclination relative to the horizontal plane and performs rotational motion about its own axis. According to the computational scheme shown in Fig. 2.8 *a*, the motion is analyzed in a two-dimensional *XOY* coordinate system.

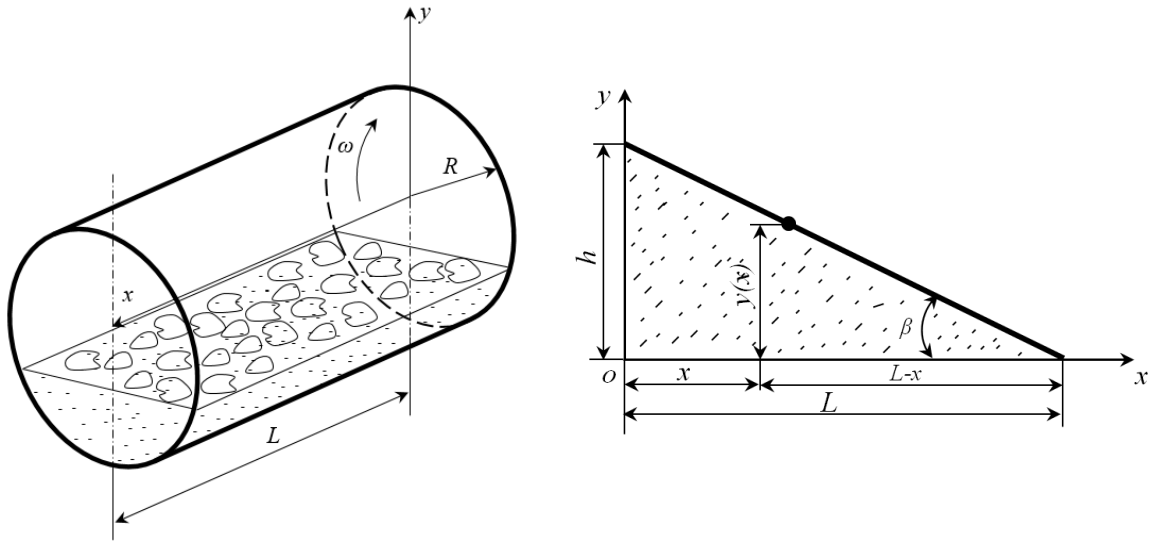

a- constructive, *b-technological*

Fig. 2.8. Computational scheme

Let the mesh drum rotate about its axis with angular velocity ω; then the angular velocity of the screened bulk material moving together with the drum can be expressed as follows [1]

$$\omega' = k\omega, \qquad (2.16)$$

Here, k is the coefficient accounting for the slipping of the bulk material relative to the drum.

If the effects of the elastic blades acting on the mesh drum are taken into account, then the screened bulk material also acquires an additional angular velocity ω_0. Thus, the combined angular velocity of the screened bulk material together with the drum is rewritten as follows

$$\omega' = k\omega + \omega_0. \qquad (2.17)$$

Denoting the axial velocity of the bulk material inside the drum as v_x, and according to Newton's second law, the equation of motion is written as follows:

$$m\frac{dv_x}{dt} = F_m + F_r, \qquad (2.18)$$

here, m is the mass of the bulk material, kg; F_m is the force moving the bulk material along the length of the drum, N; F_r is the resisting force to motion, N.

The forces acting on the screened bulk material are expressed as follows

$$F_m = -gradU\,, \qquad (2.19)$$

$$F_r = m\omega' v\,, \qquad (2.20)$$

Here, U is the value of the potential energy of the screened material at an arbitrary point *"x"* along the length L of the mesh drum, J.

According to the computational scheme shown in Fig. 2.8b, the potential energy at an arbitrary point *"x"* is expressed as follows

$$U(x) = mgy(x)\,, \qquad (2.21)$$

here, g is the acceleration due to gravity, m/s^2; $y(x)$ is the function describing the height of the screened material at an arbitrary point *"x"*, m.

According to Fig. 2.8 *b*, the function describing the height of the screened material at an arbitrary point *"x"* is expressed as follows:

$$y(x) = \frac{h(L-x)}{L}\,, \qquad (2.22)$$

here, h and L are parameters characterizing the bulk material, m.

If it is taken into account that $tg(\beta) = \frac{h}{L}$ and equation (2.22) is considered, then expression (2.21) takes the following form

$$U(x) = mg(L-x)tg(\beta)\,. \qquad (2.23)$$

Taking expression (2.23) into account, expression (2.19) is rewritten as follows

$$F_m = mgtg(\beta)\vec{i}\,, \qquad (2.24)$$

here, $\vec{i}$ is the unit vector along the OX axis.

Taking expressions (2.20) and (2.24) into account, expression (2.18) is rearranged, and the following is obtained:

$$m\frac{dv_x}{dt} = -m\omega' v_x + mgtg(\beta)\,. \qquad (2.25)$$

Dividing both sides of expression (2.25) by m, we obtain the following

$$\frac{dv_x}{dt} = -\omega' v_x + gtg(\beta). \qquad (2.26)$$

We seek the solution of equation (2.26) in the following form

$$v_x = c(t)e^{-\omega' t}. \qquad (2.27)$$

Here, the unknown function c(t) must satisfy the following differential equation, namely

$$c'(t) = gtg(\beta)e^{\omega' t}. \qquad (2.28)$$

The solution of equation (2.28) has the following form

$$c(t) = \frac{g}{\omega'} tg(\beta)e^{\omega' t} + C_0. \qquad (2.29)$$

Substituting expression (2.29) into expression (2.27), we obtain the following

$$v_x = \frac{g}{\omega'} tg(\beta) + C_0 e^{-\omega' t}. \qquad (2.30)$$

To determine the constant of integration in expression (2.29), the following initial conditions are introduced

$$t = 0;\ v_x = 0. \qquad (2.31)$$

Taking expression (2.30) into account, expression (2.29) is evaluated as follows

$$C_0 = -\frac{g}{\omega'} tg(\beta). \qquad (2.32)$$

Taking expression (2.32) into account, expression (2.30) is rewritten as follows

$$v_x = \frac{g}{\omega'} tg(\beta)(1 - e^{-\omega' t}). \qquad (2.33)$$

If it is taken into account that the mesh drum is inclined at an angle α relative to the horizontal plane, then the axial velocity of the screened bulk material along the drum axis can be expressed as follows:

$$v_x = \frac{g}{\omega'} tg(\beta)cos(\alpha)(1 - e^{-\omega' t}). \qquad (2.34)$$

Here, taking expression (2.17) into account, expression (2.34) takes the following form

$$v_x = \frac{g}{(k\omega + \omega_0)} tg(\beta)cos(\alpha)(1 - e^{-(k\omega+\omega_0)t}). \qquad (2.35)$$

If, taking into account that

$$v_0 = \frac{g}{(k\omega + \omega_0)} tg(\beta)cos(\alpha), \qquad (2.36)$$

the discharge time of the unscreened bulk material from the drum can be expressed as follows

$$t(L) = \frac{(k\omega + \omega_0)L}{gtg(\beta)cos(\alpha)}. \qquad (2.37)$$

To determine the laws governing the variation of axial velocity of the screened bulk material in the mesh drum and its discharge time, the numerical solution of equations (2.35) and (2.37) was carried out using Microsoft Office Excel software at the following parameter values: e = 2,7; k = 0,8; g = 9,81 m/s^2; β = 30°; α = 5°…25°; ω = (2…3) rad/s; L = (3…11) m.

The graphs constructed based on the numerical solution of expression (2.35) are presented in Fig. 2.9. The curves in these graphs show that the velocity of the screened bulk material along the drum axis stabilizes after approximately 2 seconds, increases slightly within small intervals, and reaches a steady value after 7 seconds. For example, when the drum angular velocity is ω = 2 rad/s, within the first 2 seconds the velocity increases from 0 m/s to 3,27 m/s, in the interval of 2…7 seconds it increases from 3,27 m/s to 3,41 m/s, and after 7 seconds it reaches a stable velocity of 3,41 m/s (Fig. 2.9).

The graphs constructed based on the numerical solution of expression (2.37) are shown in Fig. 2.10. The curves in these graphs show that the discharge time of the screened bulk material from the drum increases linearly as the drum length increases. At the same time, an increase in drum angular velocity and inclination angle also leads to an increase in the discharge time

of the screened bulk material from the drum. For example, when the drum angular velocity is ω = 2 rad/s and the drum length increases from 3 m to 11 m, the discharge time of the screened bulk material varies in the range of 0,88…3,22 s; when the drum angular velocity is ω = 2,5 rad/s and the drum length increases from 3 m to 11 m, the discharge time varies in the range of 1,1…4,03 s; and when the drum angular velocity is ω = 3 rad/s and the drum length increases from 3 m to 11 m, the discharge time varies in the range of 1,3…4,8 s.

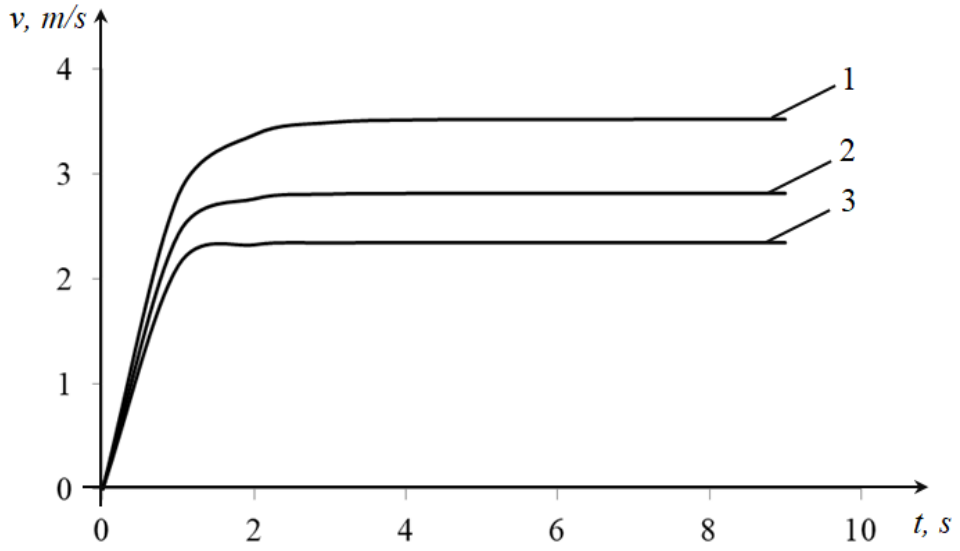

1-ω=2 rad/s; 2-ω=2,5 rad/s; 3-ω=3 rad/s

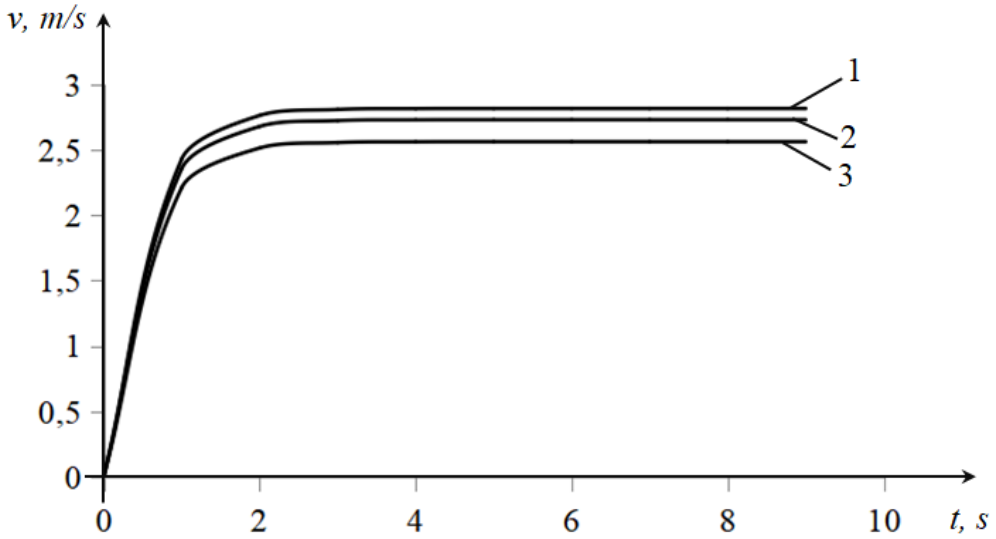

1-α=5º; 2-α=15º; 3-α=25º

Fig. 2.9. Graph of the time dependence of the axial velocity of the bulk material in the drum

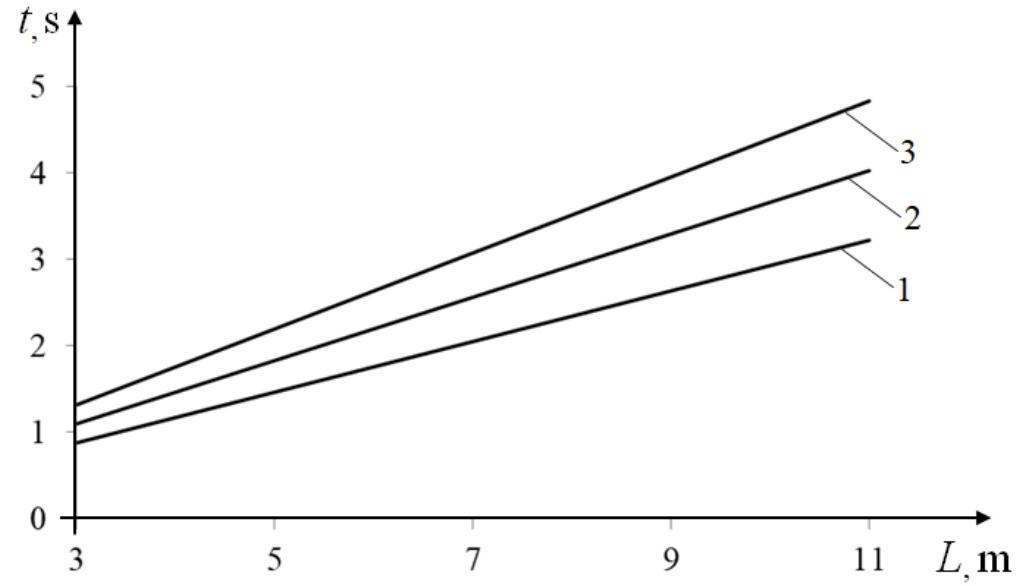

1-ω=2 rad/s; 2-ω=2,5 rad/s; 3-ω=3 rad/s

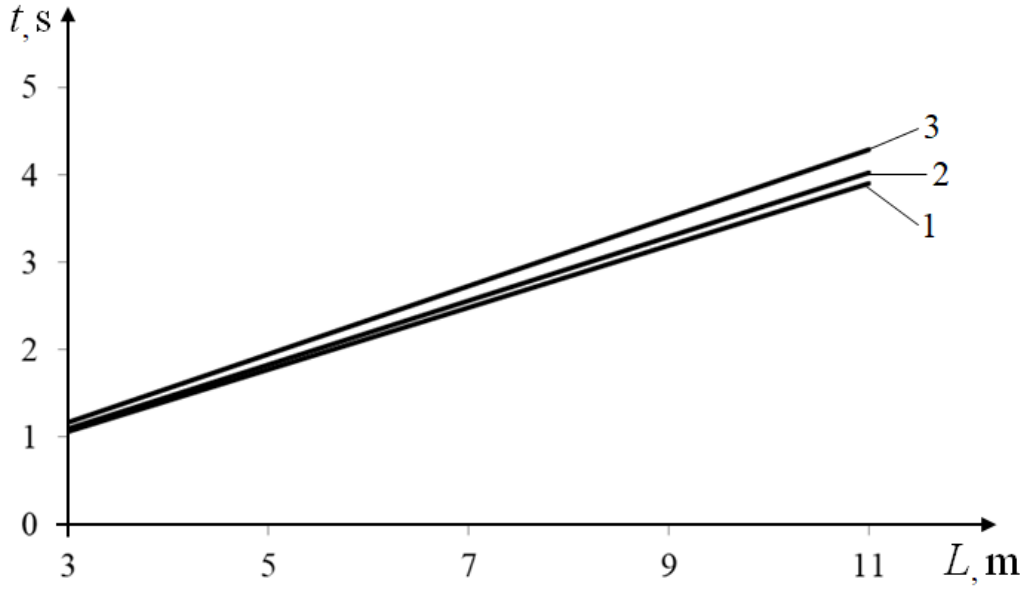

1-α=5°; 2-α=15°; 3-α=25°

Fig. 2.10. Graph of the dependence of the discharge time of the bulk material on the drum length

In conclusion, it can be stated that in mesh drums used for screening bulk materials, the velocity of the screened material and its discharge time are considered important parameters. This is because these parameters form the basis for determining the productivity of the machine as well as its structural and kinematic parameters.

2.5. Dynamic analysis of the mesh drum of the screening device

The main working elements of the bulk material screening device are the mesh drum and the shaft with elastic blades. In this study, the effects of the elastic blades are considered as a resistance force, and the mesh drum is analyzed dynamically. Figure 2.11 shows the computational scheme of the mesh drum.

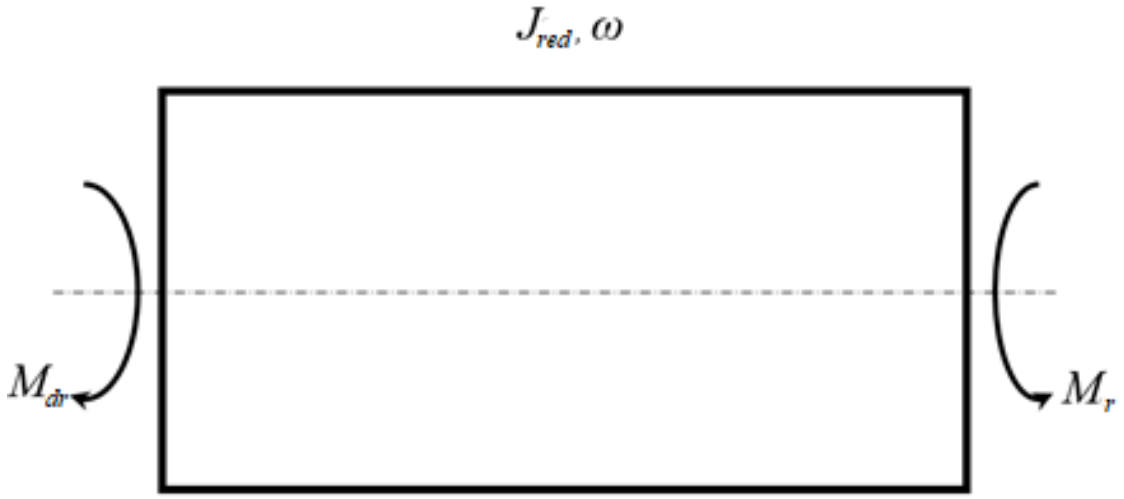

Fig. 2.11. Computational scheme of the mesh drum

For the computational scheme shown in Fig. 2.11, according to [78; p. 60], the mathematical model is formulated as follows

$$\begin{cases} \dfrac{\dot{M}_{dr}}{2 f_c M_c} + \dfrac{M_{dr} S_c}{2 M_c} - 1 + \dfrac{\dot{\varphi}}{i\omega_0} = 0 \\ J_{red}\ddot{\varphi} - i\eta M_{dr} + M_r = 0 \end{cases}, \qquad (2.38)$$

here, M_{dr} is the driving torque of the electric motor and M_c is its critical value, N·m; ω is the angular velocity of the mesh drum, rad/s; ε is the angular acceleration of the mesh drum, rad/s²; ω_0 is the ideal angular velocity, rad/s; S_c is the critical slip; J_{red} is the reduced moment of inertia, kg·m²; M_r is the moment of resistance forces, N·m; f_c is the system frequency, Hz; i is the transmission ratio; η is the efficiency coefficient of the transmission.

To specify the moments of technological resistance forces, the forces acting on the mesh drum are considered separately. First of all, based on the

function of the screening device, the moment of resistance force from the screened material is formed, which is expressed as follows

$$M_{s.m} = G_{s.m}\left(R_d - h_{s.m}\right) + M_0 \sin nt, \qquad (2.39)$$

Here, $G_{s.m}$ is the weight force exerted by the screened material, N; R_d is the radius of the mesh drum, m; $h_{s.m}$ is the thickness of the layer of screened material, m; M_0 is the amplitude of the resistance force moment coming from the screened material, N·m; n is the frequency of variation of the resistance force moment, Hz

Next, the moments of the frictional resistance forces are expressed as follows

$$M_i = \left(G_{s.m} + G_d + G_{sh}\right) R_{sh} \mu, \qquad (2.40)$$

Here, G_d is the weight force of the mesh drum, N; G_{sh} is the weight force of the drum shaft, N; R_{sh} is the radius of the drum shaft, m; μ is the coefficient of friction between the mesh drum and the screened material.

The moment of the resistance force exerted by the elastic blade is expressed as follows

$$M_e = zG_{e.b}R_d \mu_1 \sin z\omega_2 t, \qquad (2.41)$$

here, $G_{e.b}$ is the weight force of the elastic blade, N; z is the number of elastic blades acting simultaneously; μ_1 is the coefficient of friction between the mesh drum and the elastic blade; ω_2 is the angular velocity of the shaft with elastic blades, rad/s; t is time, s.

Thus, taking expressions (2.39), (2.40), and (2.41) into account, the total moment of resistance forces is given as follows

$$M_r = G_{s.m}\left(R_d - h_{s.m}\right) + M_0 \sin nt + \left(G_{s.m} + G_d + G_{sh}\right) R_{sh}\mu + zG_{e.b}R_d \mu_1 \sin z\omega_2 t$$
. (2.42)

Taking the above into account, oscillograms for equation (2.42) were constructed using Microsoft Excel. The following parameter values were adopted: $G_{s.m}$= (1000…1500) kg; R_d = 0,5 m; $h_{s.m}$ = 0,1 m; M_0= 5,5 N·m; G_d =

500 kg; G_{sh} = 80 kg; R_{sh} = 0,05 m; μ_1 = 0,4; μ = 0,7; z = 2, 4, 6 pcs; $G_{e.b}$ = 1 kg; ω_2 = 3,5 rad/s; n = 4 rad/s.

If equation (2.42) is taken into account, then the second equation of the system (2.38) can be written as follows

$$J_{red}\ddot{\varphi} - i\eta M_{dr} + G_{s.m}\left(R_d - h_{s.m}\right) + \left(G_{s.m} + G_d + G_{sh}\right)R_{sh}\mu + \\ + M_0 \sin nt + zG_{e.b}R_d\mu_1 \sin z\omega_2 t = 0 \quad .$$

(2.43)

Taking the first derivative of the differential equation (2.43) with respect to time, we obtain the following:

$$J_{red}\dddot{\varphi} - i\eta \dot{M}_{dr} + M_0 n\cos nt + zG_{e.b}R_d\mu_1\omega_2 \cos z\omega_2 t = 0 .$$

(2.44)

From the differential equations (2.43) and (2.44), we determine M_{dr} and $\dot{M}_{dr}$ as follows

$$M_{dr} = \frac{J_{red}\ddot{\varphi} + G_{s.m}\left(R_d - h_{s.m}\right) + \left(G_{s.m} + G_d + G_{sh}\right)R_{sh}\mu}{i\eta} + \\ + \frac{M_0 \sin nt + zG_{e.b}R_d\mu_1 \sin z\omega_2 t}{i\eta} \quad ,$$

(2.45)

hamda

$$\dot{M}_{dr} = \frac{J_{red}\dddot{\varphi} + M_0 n\cos nt + zG_{e.b}R_d\mu_1\omega_2 \cos z\omega_2 t}{i\eta} . \qquad (2.46)$$

Taking expressions (2.45) and (2.46) into account, the first equation of the system of equations (2.38) is rewritten, and the following is obtained

$$\frac{J_{red}\dddot{\varphi}}{2f_c M_c i\eta} + \frac{J_{red}\ddot{\varphi}S_k}{2M_c i\eta} + \frac{\dot{\varphi}}{i\omega_0} = 1 - \frac{M_0 n\cos nt}{2f_c M_c i\eta} - \\ - \frac{zG_{e.b}R_d\mu_1\omega_2 \cos z\omega_2 t}{2f_c M_c i\eta} - \frac{G_{s.m}\left(R_d - h_{s.m}\right) + \left(G_{s.m} + G_d + G_{sh}\right)R_{sh}\mu}{2M_k i\eta} - \\ - \frac{M_0 \sin nt}{2M_c i\eta} - \frac{zG_{e.b}R_d\mu_1 \sin z\omega_2 t}{2M_c i\eta} \quad .$$

(2.47)

If it is taken into account that $\ddot{\omega} = \dddot{\varphi}$, $\dot{\omega} = \ddot{\varphi}$, and $\omega = \dot{\varphi}$, then expression (2.47) is rewritten as follows:

$$\frac{J_{red}\ddot{\omega}}{2 f_c M_c i\eta} + \frac{J_{red}\dot{\omega} S_c}{2 M_c i\eta} + \frac{\omega}{i\omega_0} = 1 - \frac{M_0 n \cos nt}{2 f_c M_c i\eta} - \frac{z G_{e.b} R_d \mu_1 \omega_2 \cos z\omega_2 t}{2 f_c M_c i\eta} -$$
$$- \frac{G_{s.m}\left(R_d - h_{s.m}\right) + \left(G_{s.m} + G_d + G_{sh}\right) R_{sh}\mu}{2 M_c i\eta} - \frac{M_0 \sin nt}{2 M_c i\eta} - \frac{z G_{e.b} R_d \mu_1 \sin z\omega_2 t}{2 M_c i\eta}$$

. (2.48)

To simplify the solution of equation (2.11), the following notations are introduced:

$$A = \frac{J_{red}}{2 f_c M_c i\eta}; \qquad B = \frac{J_{red} S_c}{2 M_c i\eta}; \qquad C = \frac{1}{i\omega_0}; \qquad D = \frac{M_0 n}{2 f_c M_c i\eta};$$

$$E = \frac{z G_{e.b} R_d \mu_1 \omega_2}{2 f_c M_c i\eta}; \qquad F = \frac{G_{s.m}\left(R_d - h_{s.m}\right) + \left(G_{s.m} + G_d + G_{sh}\right) R_{sh}\mu}{2 M_c i\eta};$$

$$K = \frac{M_0}{2 M_c i\eta}; \; L = \frac{z G_{e.b} R_d \mu_1}{2 M_c i\eta}.$$

Taking the above notations into account, expression (2.48) is written as follows

$$A\ddot{\omega} + B\dot{\omega} + C\omega = 1 - D\cos nt - E\cos z\omega_2 t - F - K\sin nt - L\sin z\omega_2 t.$$

(2.49)

Before obtaining the solution of differential equation (2.49), we first consider the characteristics of the induction motor in the drive system of the bulk material screening device. The parameters of the AIR 132S6 induction motor are given in [79; pp. 65–66].:

rated power of the electric motor – N=5,5 kW;

rated rotation frequency of the electric motor rotor – n=955 r/min;

ratio of the starting torque of the electric motor to its rated torque

$$\frac{M_{st}}{M_{rat}} = 2,4,$$

ratio of the maximum (critical) torque of the electric motor to its rated torque

$$\lambda = \frac{M_{\max}}{M_{rat}} = 2,4,$$

ratio of the minimum torque of the electric motor to its rated torque

$$\frac{M_{\min}}{M_{rat}} = 1,8,$$

flywheel (moment of inertia) of the electric motor rotor – GD^2=0,24 $\text{N}\cdot\text{m}^2$;

frequency of the electrical power supply – f_c=50 Hz;

number of pole pairs – p=3.

The main parameters and coefficients of the electric motor are determined in the following order:

rotational frequency of the system

$$\omega_c = 2\pi f_c = 2 \cdot 3,14 \cdot 50 = 314 \text{ rad/s},$$

rated angular velocity of the electric motor rotor

$$\omega_{rat} = \frac{\pi n}{30} = \frac{3,14 \cdot 955}{30} = 99,95 \text{ rad/s},$$

angular velocity of the electric motor rotor under ideal no-load conditions

$$\omega_0 = \frac{2\pi f_c}{p} = \frac{3,14 \cdot 50}{3} = 104,6 \text{ rad/s},$$

moment of inertia of the electric motor rotor

$$J_p = \frac{GD^2}{4g} = \frac{0,24}{4 \cdot 9,81} = 0,06116 \text{ kg} \cdot \text{m}^2,$$

rated torque of the electric motor

$$M_{rat} = \frac{9550N}{n} = \frac{9550 \cdot 5,5}{955} = 55 \text{ N} \cdot \text{m};$$

critical torque of the electric motor

$$M_c = \lambda M_{rat} = 2,4 \cdot 55 = 132 \text{ N} \cdot \text{m};$$

rated value of slip

$$S_n = \frac{\omega_0 - \omega_n}{\omega_0} = \frac{104,6 - 99,95}{104,6} = 0,044;$$

critical value of slip

$$S_k = \lambda S_n \left(1 + \sqrt{1 - \frac{1}{\lambda^2}}\right) = 2,4 \cdot 0,044 \cdot \left(1 + \sqrt{1 - \frac{1}{2,4^2}}\right) = 0,202.$$

Based on the above calculations and analysis of the literature, the numerical solution of differential equation (2.49) was carried out using the MAPLE 21 software under the following parameter values: J_{red} = 14,76 kg·m^2; f_c = 50 Hz; M_c = 132 N·m; i = 30; η = 0,9; S_c = 0,25; ω_0 = 104,6 rad/s; M_0 = 5,5 N·m; z = 2, 4, 6 pcs; $G_{e.b}$ = 1 kg; $Gs.m$ = (1000…1500) kg; G_d = 500 kg; G_{sh} = 80 kg; R_d = 0,5 m; $h_{s.m}$ = 0,1 m; R_{sh} = 0,05 m; μ_1 = 0,4; μ = 0,7; ω_2 = 3,5 rad/s; n = 4 rad/s.

Based on the numerical solution of expression (2.49), the laws of variation of the angular velocity of the mesh drum were constructed (Fig. 2.12).

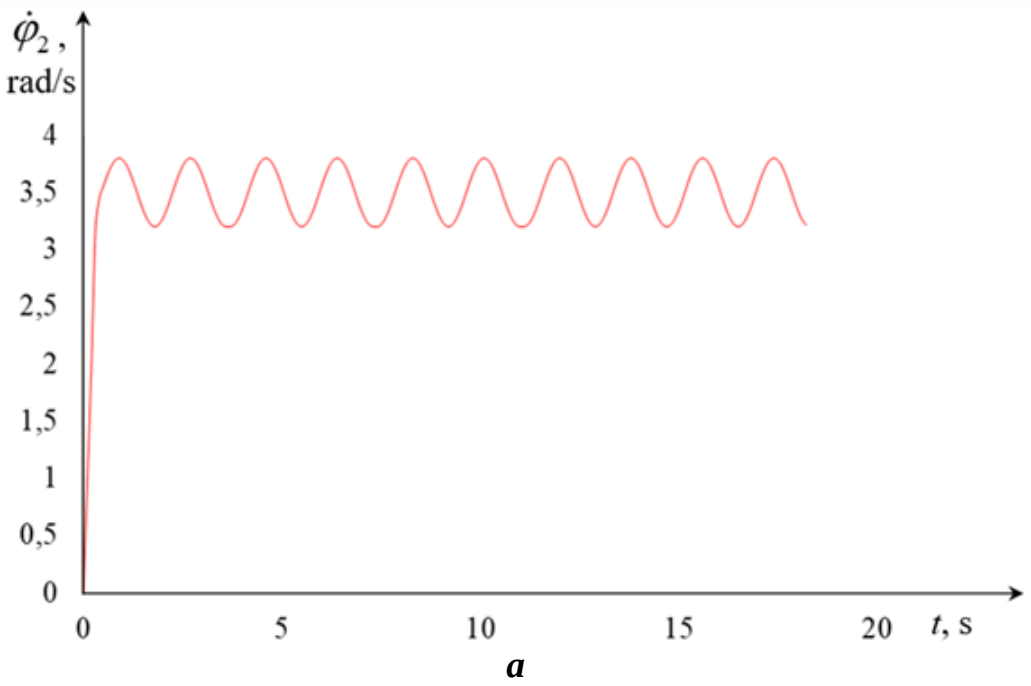

a

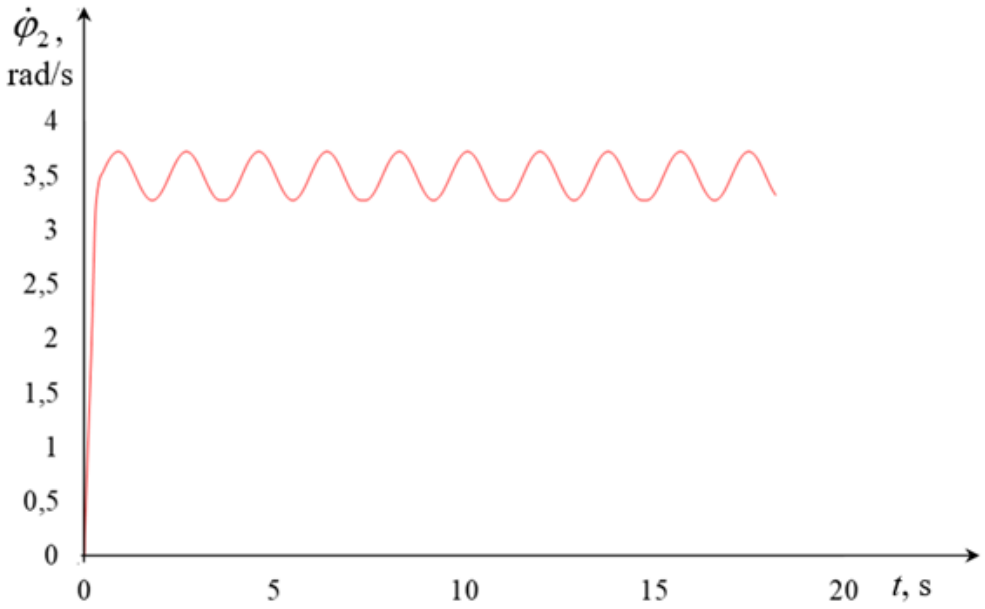

b

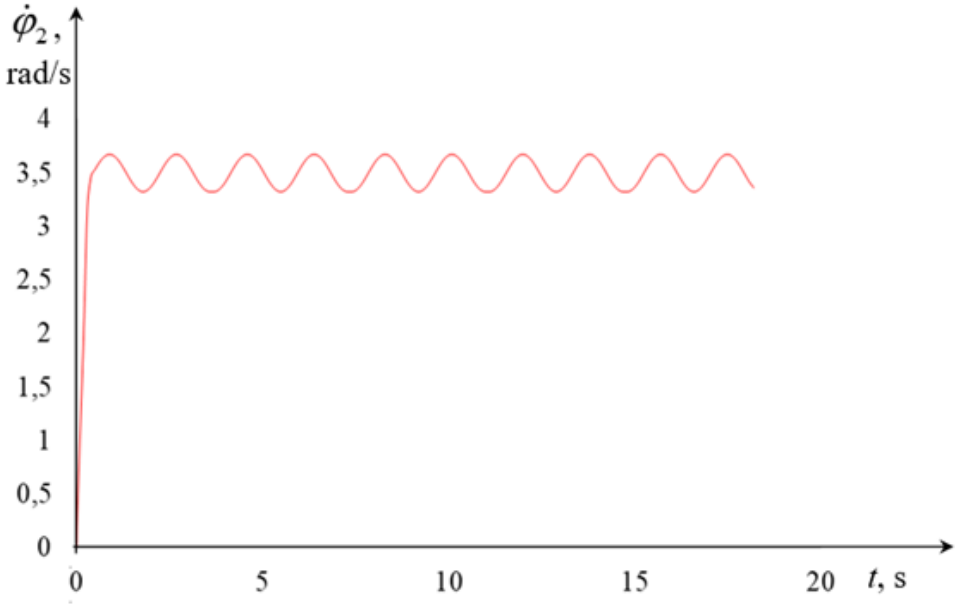

c

a- $G_{s.m.}$=1000 kg; b- $G_{s.m.}$=1250 kg; c- $G_{s.m.}$=1500 kg

Fig. 2.12. Law of variation of the angular velocity of the mesh drum

From these laws it can be seen that with an increase in the resistance moment, the oscillation frequency of the angular velocity of the mesh drum remains unchanged. However, a decrease in the oscillation amplitude is observed. Analysis of the laws presented in Fig. 2.13 shows that with an increase in the mass of the screened material in the mesh drum, the oscillation amplitude of the angular velocity decreases according to a nonlinear law. For example, when the angular velocity of the elastic blade is 5 rad/s, the mass of

the screened material is 1000 kg, and the angular velocity of the mesh drum is 3,5 rad/s, its oscillation amplitude is 0,6 rad/s, as can be seen from Fig. 2.13. At the same time, when the mass of the screened material is 1250 kg and 1500 kg, and the angular velocity of the elastic blade is 5 rad/s, the average value of the angular velocity of the mesh drum remains constant, i.e., 3,5 rad/s, while its oscillation amplitude becomes 0,45 rad/s and 0,35 rad/s, respectively (Fig. 2.13).

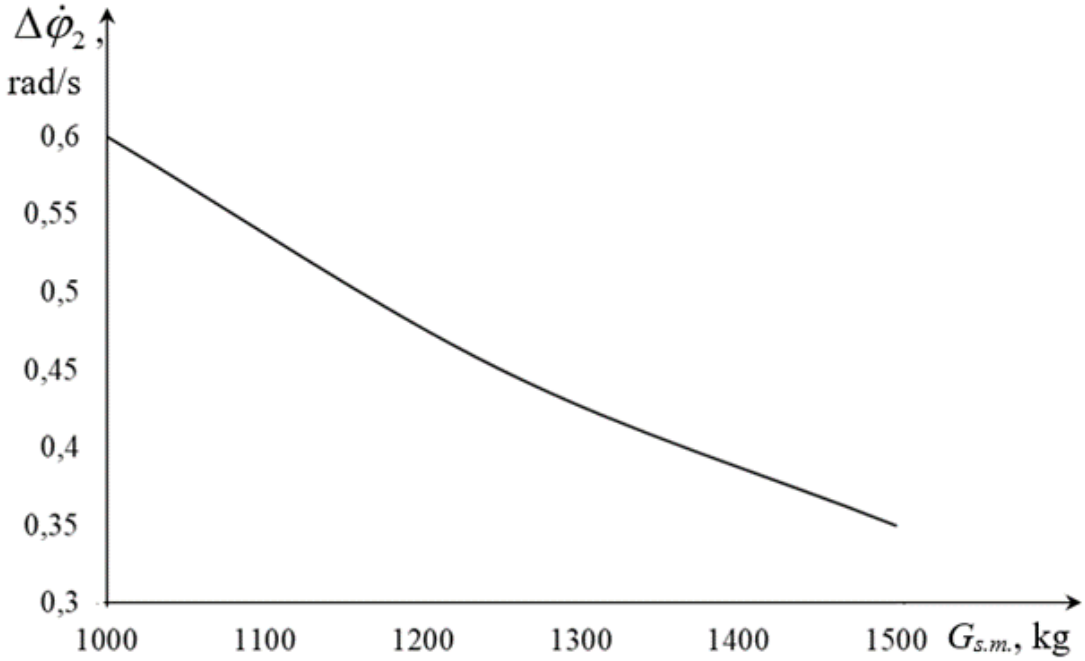

Fig. 2.13. Graph of the variation of the oscillation amplitude of the angular velocity of the mesh drum depending on the mass of the screened material

It should be emphasized that with an increase in the angular velocity of the shaft with elastic blades, the average value of the angular velocity of the mesh drum remains constant, while its amplitude decreases (Fig. 2.14).

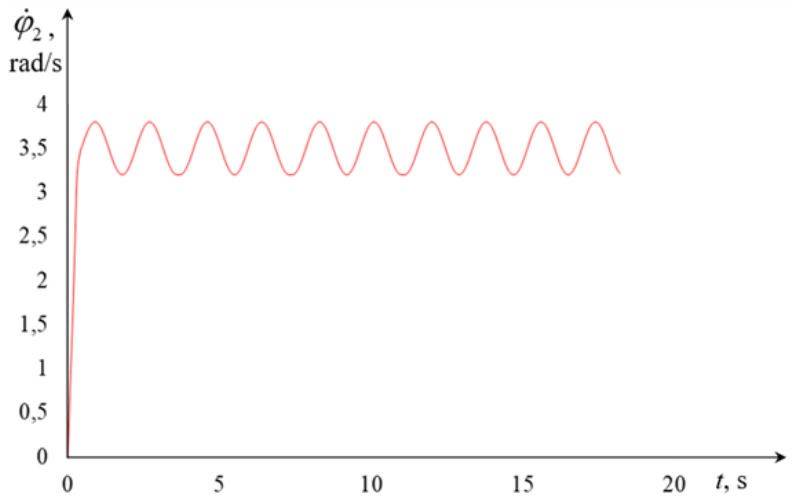

a

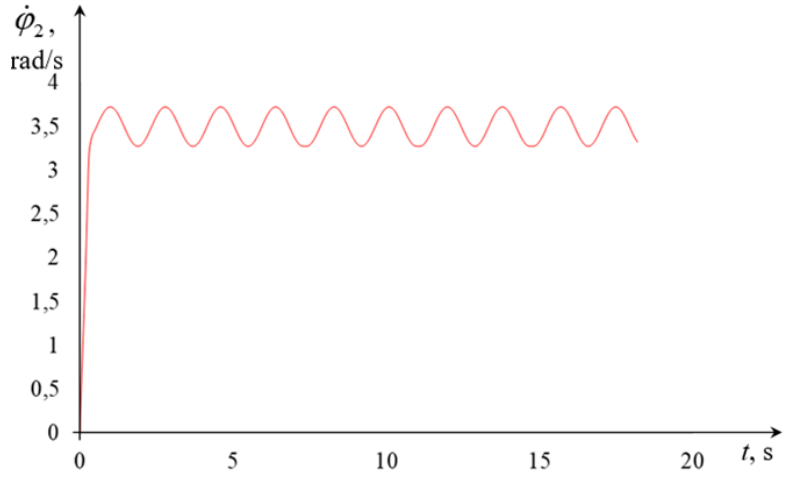

b

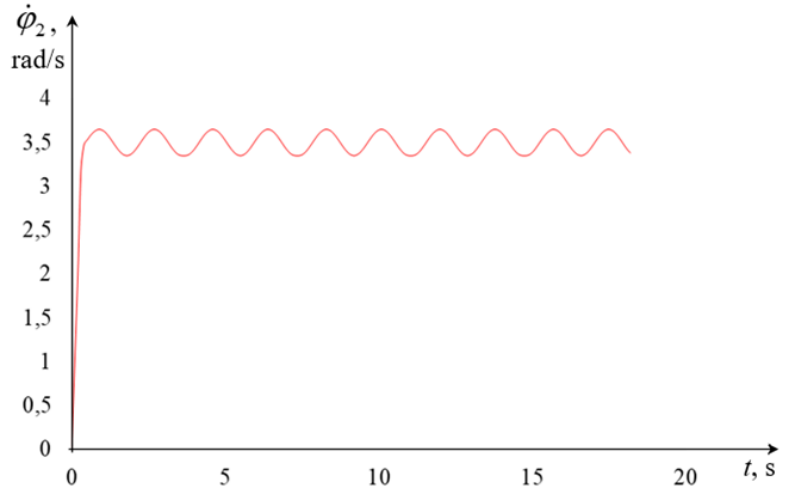

c

a- $\dot{\varphi}_3 = 3rad/s$; ***b***- $\dot{\varphi}_3 = 4rad/s$; ***c***- $\dot{\varphi}_3 = 5rad/s$

Fig. 2.14. Law of variation of the angular velocity of the mesh drum

The analysis of the laws presented in Fig. 2.14 shows that with an increase in the angular velocity of the mesh drum, the oscillation amplitude of the angular velocity decreases according to a nonlinear law. For example, when the angular velocity of the elastic blade is 4 rad/s, the mass of the screened material is 1250 kg, and the angular velocity of the mesh drum is 3,5 rad/s, its oscillation amplitude is 0,65 rad/s. When the angular velocity of the elastic blade is 5 rad/s and 6 rad/s, the average value of the angular velocity of the mesh drum remains constant, i.e., 3,5 rad/s, while its oscillation amplitude becomes 0,45 rad/s and 0,3 rad/s, respectively (Fig. 2.15).

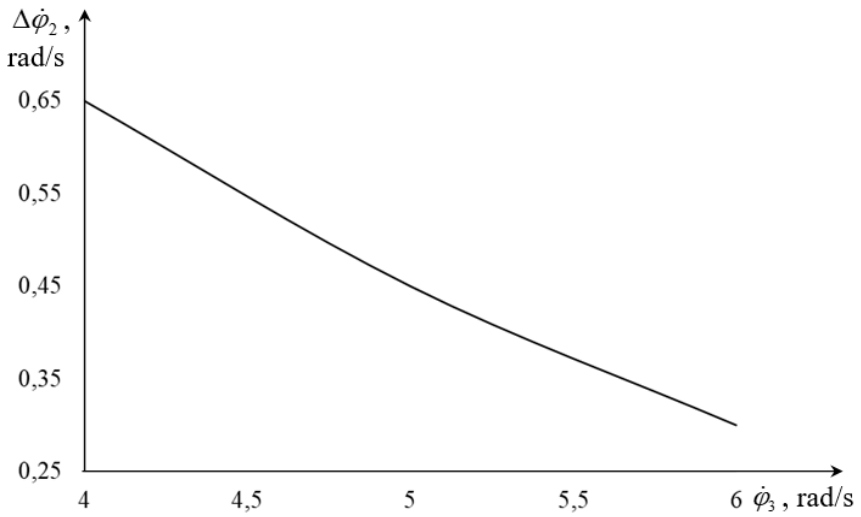

Fig. 2.15. Graph of the variation of the oscillation amplitude of the angular velocity of the mesh drum depending on the angular velocity of the shaft with elastic blades

Conclusions of Chapter II

1. Based on the analysis of literature sources, an improved design of a bulk material screening device equipped with a mesh drum and a shaft with elastic blades was developed.

2. Theoretical studies showed that the impact point of the blade is located at a distance equal to 2/3 of its length from the axis of rotation.

3. A graph of the dependence of the impact force exerted by the elastic blade on the mesh drum on the deformation value of the elastic blade was

constructed, and it was found that with an increase in impact force, the deformation of the elastic blade decreases according to a nonlinear law.

4. It was established that the velocity of the screened material and its discharge time are important parameters in mesh drum screening systems, since these parameters form the basis for determining productivity as well as structural and kinematic parameters of the drum.

5. Since the main working elements of the developed bulk material screening device are the mesh drum and the shaft with elastic blades, the effects of the elastic blades were considered as a resistance force in the theoretical study, and a dynamic analysis of the mesh drum was carried out. Based on the dynamic analysis, the laws of variation of the angular velocity of the mesh drum were obtained.

CHAPTER III. RESULTS OF EXPERIMENTAL INVESTIGATIONS OF THE DRUM SCREENING DEVICE

3.1. Aim and objectives of the experimental research

Based on the results of the conducted theoretical studies, an experimental stand of the bulk material screening device was developed as the objective of the experimental investigations (Fig. 3.1).

Fig. 3.1. Experimental stand of the bulk material screening device

In order to study the influence of the device parameters on the screening quality of bulk materials and its energy performance, the following tasks were planned:

– to investigate the effect of the rotation frequency of the shaft with elastic blades and the stiffness of the elastic blades on the force applied to the mesh drum;

– to study the laws of variation of the torque on the shaft of the mesh drum;

– to optimize the parameters of the bulk material screening device using the method of mathematical design of experiments.

3.2. Methodology of conducting the experimental research

Fig. 3.2 shows the electro-tensometric scheme of the bulk material screening device.

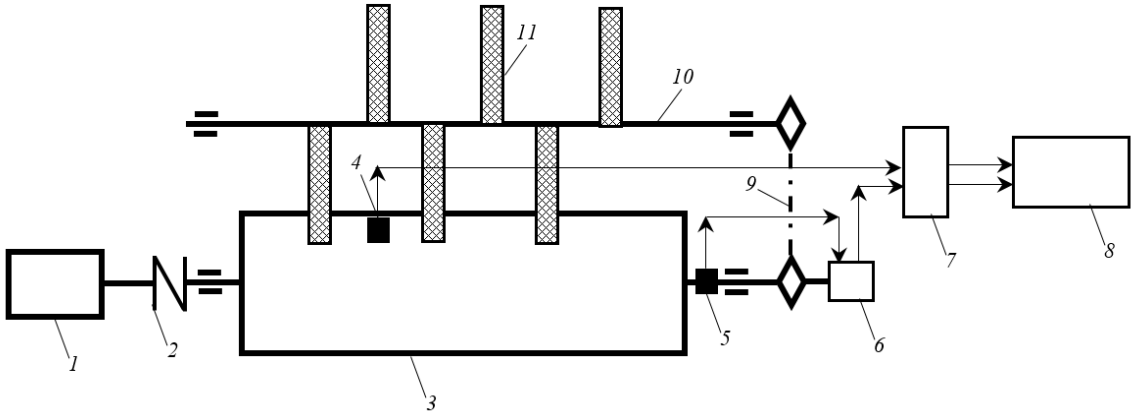

1 – electric motor, 2 – coupling, 3 – mesh drum, 4 – S-shaped strain gauge sensor, 5 – strain gauge sensor, 6 – slip ring (current collector), 7 – data processing unit, 8 – computer, 9 – chain transmission, 10 – shaft with elastic blades, 11 – elastic blade.

Fig. 3.2. Electro-tensometric scheme of the bulk material screening device

For measuring the force exerted by the elastic blade on the mesh drum, the drum was removed from the device. Instead, an S-shaped strain gauge sensor was installed. In this case, the S-shaped sensor was arranged in such a way that a single elastic blade acted on it. In the experiments, three different rotation frequencys of the shaft with elastic blades and three different stiffness values of the elastic blades were selected. The rotation frequency of the shaft was varied by changing the sprockets, while the stiffness of the elastic blades was adjusted by replacing the blades.

To determine the impact force of the elastic blade, a YZC-516C strain gauge sensor with a maximum load capacity of 100 kg was used. Figure 3.3 shows the YZC-516C sensor, its calibration process, and its mounted position on the experimental stand.

a

b

Fig. 3.3. YZC-516C strain gauge sensor (a), its calibration process (b)

To study the variation of torque on the mesh drum shaft, the rotation frequency of the drum was selected in the range of 20 r/min to 30 r/min, the inclination angle of the drum relative to the horizontal plane from 5° to 20°,

the productivity from 1,2 t/h to 2,0 t/h, and the stiffness of the elastic blades from 200 N/m to 400 N/m.

In this case, the rotation frequency was adjusted using an inverter (Fig. 3.4) by changing the frequency of the electric motor.

Figure 3.4. Inverter

For measuring the torque on the mesh drum shaft, BUVNF1000-3NA strain gauge sensors were used. The strain gauges were bonded to the cleaned surface of the shaft at an angle of 45° relative to its axis using a bridge configuration. The scheme of bonding the strain gauges to the shaft is shown in Fig. 3.5.

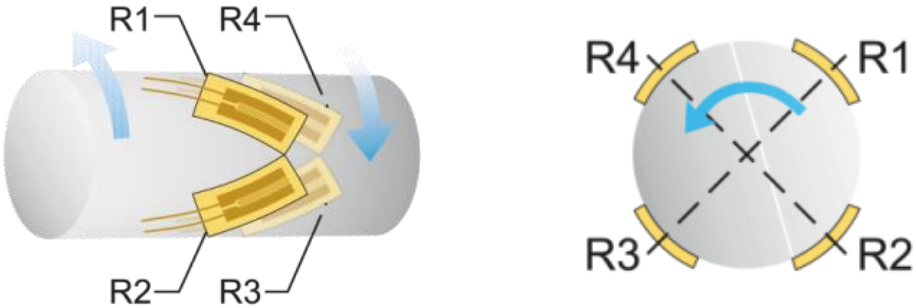

Fig. 3.5. Scheme of bonding strain gauges to the shaft

The process of measuring the torque on the mesh drum shaft is carried out in the following order. When motion is transmitted from the electric motor to the reducer and then to the mesh drum shaft, the strain gauges bonded to its surface detect the deformation of the shaft and convert it into an electrical signal. This signal is transmitted via a slip ring (Fig. 3.6) to the *Arduino UNO* (Fig. 3.7) microcontroller for data processing. The device processes the signals and transmits them to a computer, where the received data are converted into graphical form.

Fig. 3.6. Slip ring

Fig. 3.7. Arduino UNO microcontroller

In order to verify the correct installation of the strain gauges and to check their data transmission capability, the mesh drum was operated under

no-load conditions, and the variation of numerical values on the computer screen was observed. In this case, the arrival of data and the proper operation of the strain gauges were confirmed.

In order to improve the accuracy of the obtained results, the experiments were repeated three times under identical operating conditions. At the beginning and at the end of the experiment, the mesh drum shaft was calibrated in a static state. For this purpose, a special lever with a length of 0.5 m was prepared; one end of the lever was rigidly fixed to the output part of the mesh drum shaft. A special hook for hanging loads was installed at the other end of the lever. During calibration, loads were gradually applied to the lever in equal increments from 2 kg to 20 kg (Fig. 3.8), and based on the obtained data, the calibration graph was constructed (Fig. 3.9).

Fig. 3.8. Calibration process of the torque on the mesh drum shaft

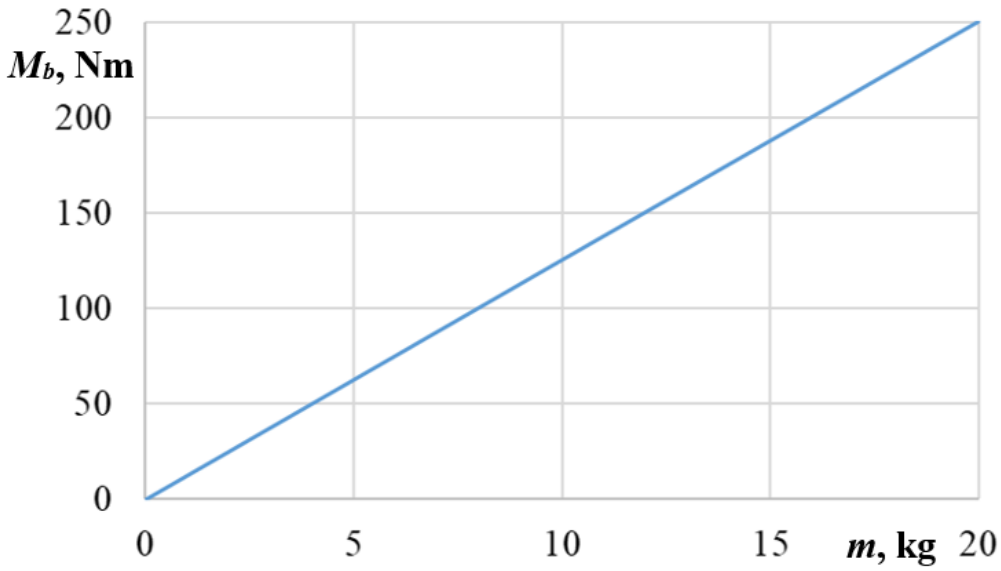

Fig. 3.9. Calibration graph of the torque on the mesh drum shaft

3.3. Results of studying the influence of the rotation frequency of the shaft with elastic blades and the stiffness of the elastic blades on the force applied to the mesh drum

In the conducted experimental investigations, the variation laws of the force exerted on the mesh drum by the elastic blade were obtained in the form of oscillograms (Figs. 3.10–3.12). Based on these laws, it can be stated that the force applied to the mesh drum by the elastic blade increases with the increase in both the stiffness of the elastic blade and its rotation frequency.

It is known that an increase in the stiffness of the elastic blade leads to greater resistance to deformation. In other words, it responds more quickly and more strongly to external influence. As a result, when any impact occurs, the magnitude of the impact force increases.

An increase in the rotation frequency of the elastic blade also leads to an increase in its linear velocity, which in turn increases momentum. The response time of the system to external influence decreases, resulting in a further increase in the impact force.

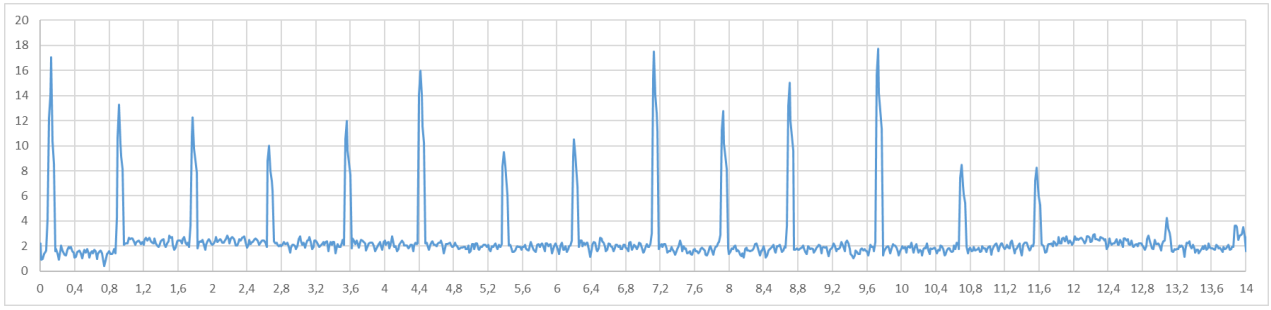

a

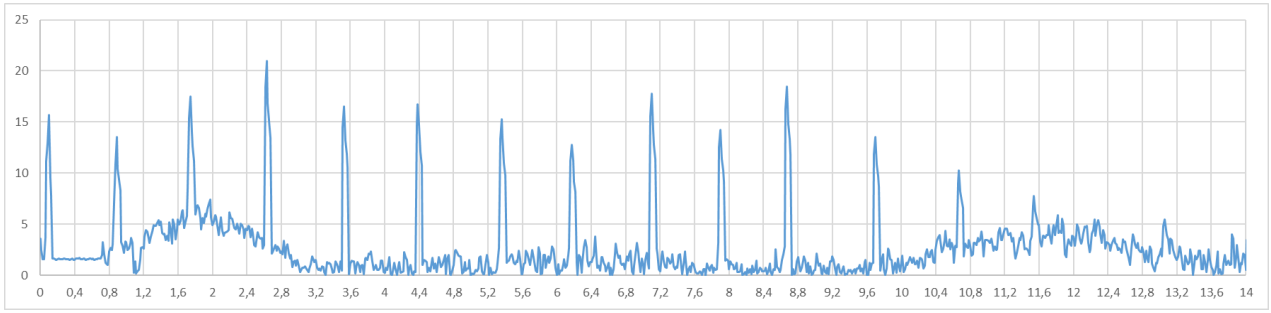

b

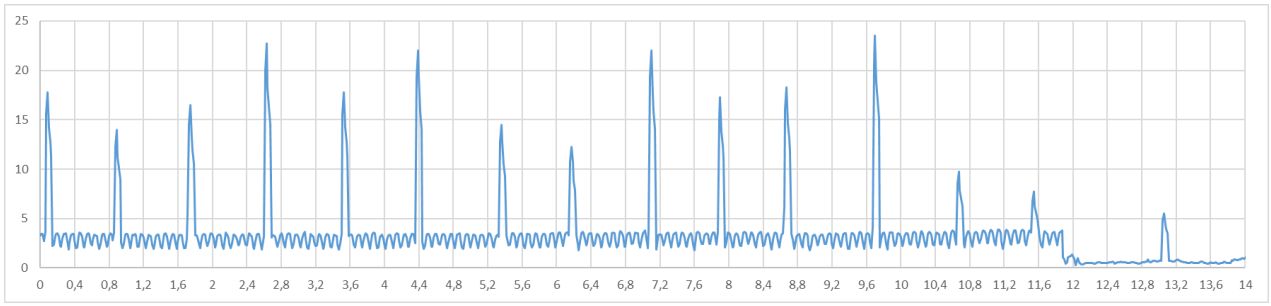

c

Fig. 3.10. Variation law of impact force at a rotation frequency of the elastic blade of 50 r/min and stiffness coefficients of 200 N/m *(a)*, 300 N/m *(b)*, and 400 N/m *(c)*

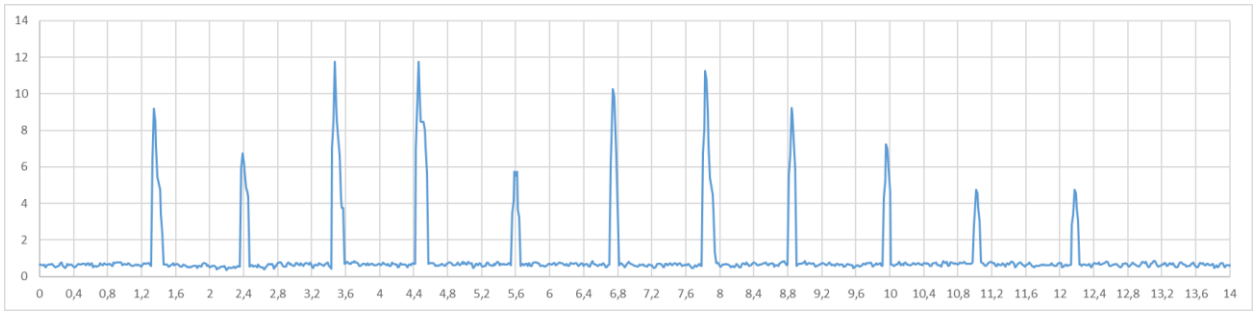

a

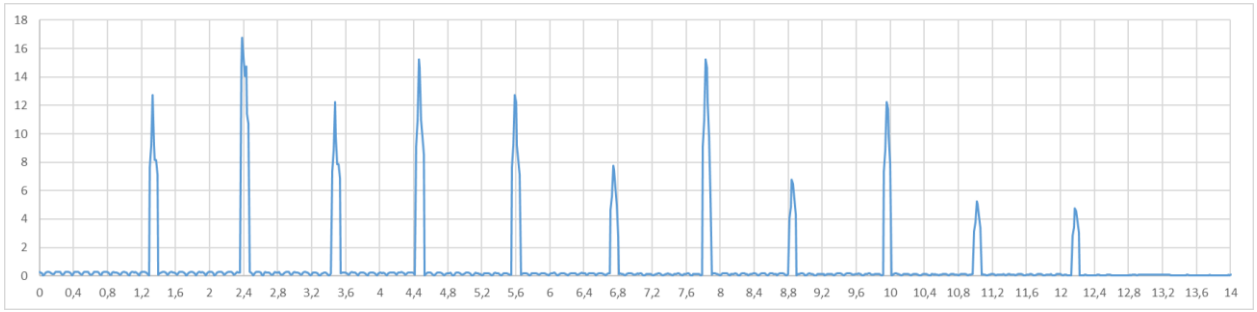

b

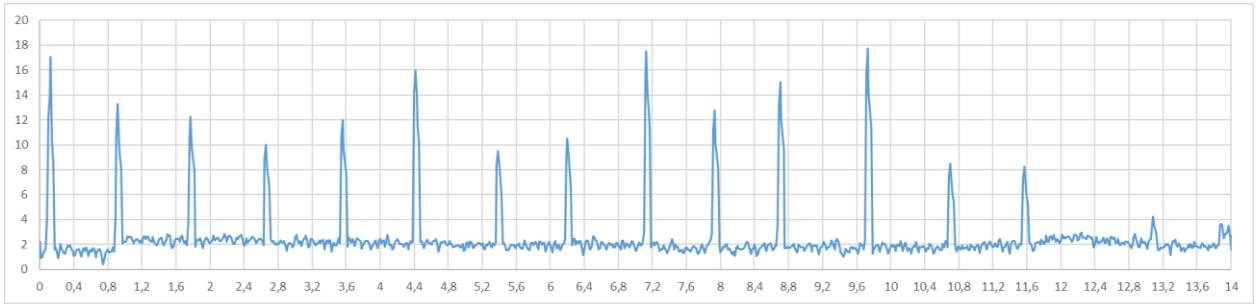

c

Fig. 3.11. Variation law of impact force at a rotation frequency of the elastic blade of 40 r/min and stiffness coefficients of 200 N/m *(a)*, 300 N/m *(b)*, and 400 N/m *(c)*

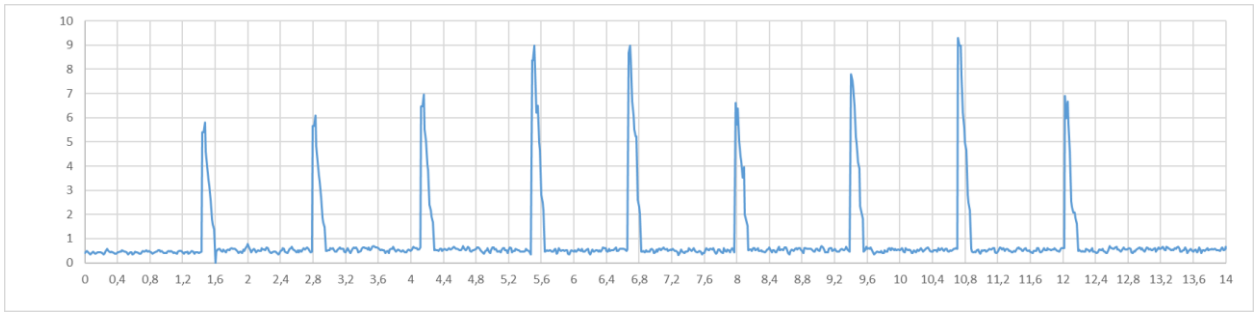

a

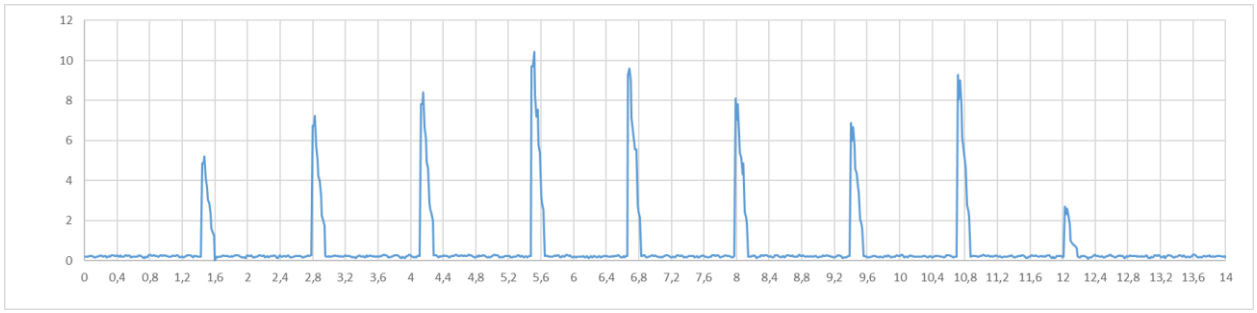

b

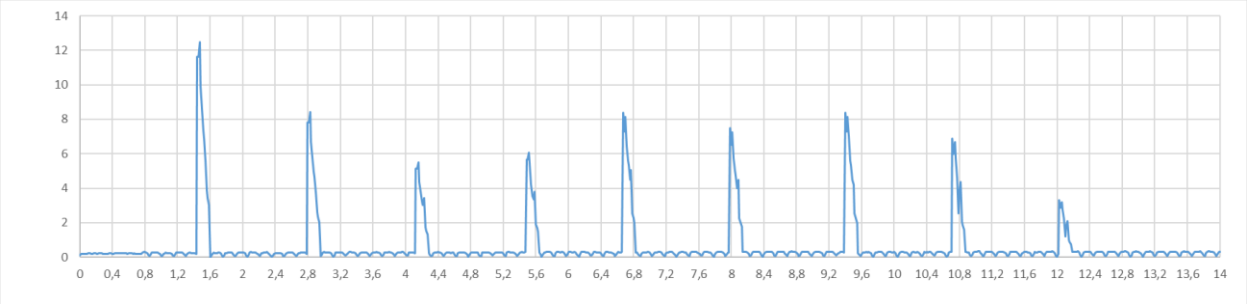

c

Fig. 3.12. Variation law of impact force at a rotation frequency of the elastic blade of 30 r/min and stiffness coefficients of 200 N/m *(a)*, 300 N/m *(b)*, and 400 N/m *(c)*

From Fig. 3.10a, it can be seen that when the rotation frequency of the elastic blade is 50 r/min and the stiffness coefficient is 200 N/m, the average value of the force applied to the mesh drum is 13,63 N, the maximum value is 17,75 N, and the minimum value is 9,73 N. When the stiffness coefficient of the elastic blade is 300 N/m and 400 N/m, the average value of the force applied to the mesh drum is 15,75 N and 16,86 N, the maximum value is 21,0 N and 23,56 N, and the minimum value is 10,75 N and 11,86 N, respectively (Figs. 3.10b and 3.10c).

From Fig. 3.11a, it can be seen that when the rotation frequency of the elastic blade is 40 r/min and the stiffness coefficient is 200 N/m, the average value of the force applied to the mesh drum is 11,87 N, the maximum value is 16,77 N, and the minimum value is 7,0 N. When the stiffness coefficient of the elastic blade is 300 N/m and 400 N/m, the average value of the force applied to the mesh drum is 10,9 N and 8,7 N, the maximum value is 13,77 N and 9,82 N, and the minimum value is 8,06 N and 6,84 N, respectively (Figs. 3.11b and 3.11c).

From Fig. 3.12a, it can be seen that when the rotation frequency of the elastic blade is 30 r/min and the stiffness coefficient is 200 N/m, the average value of the force applied to the mesh drum is 10,6 N, the maximum value is 12,47 N, and the minimum value is 8,74 N. When the stiffness coefficient of the elastic blade is 300 N/m and 400 N/m, the average value of the force applied to the mesh drum is 9,81 N and 7,42 N, the maximum value is 10,04

N and 8,04 N, and the minimum value is 7,31 N and 6,74 N, respectively (Figs. 3.12b and 3.12c).

Based on the analysis of the oscillograms presented in Figs. 3.10–3.12, graphs of parameter dependencies were constructed (Figs. 3.13 and 3.14). From Fig. 3.13, it can be seen that with an increase in the stiffness coefficient of the elastic blade, the impact force exerted on the mesh drum increases according to a nonlinear law.

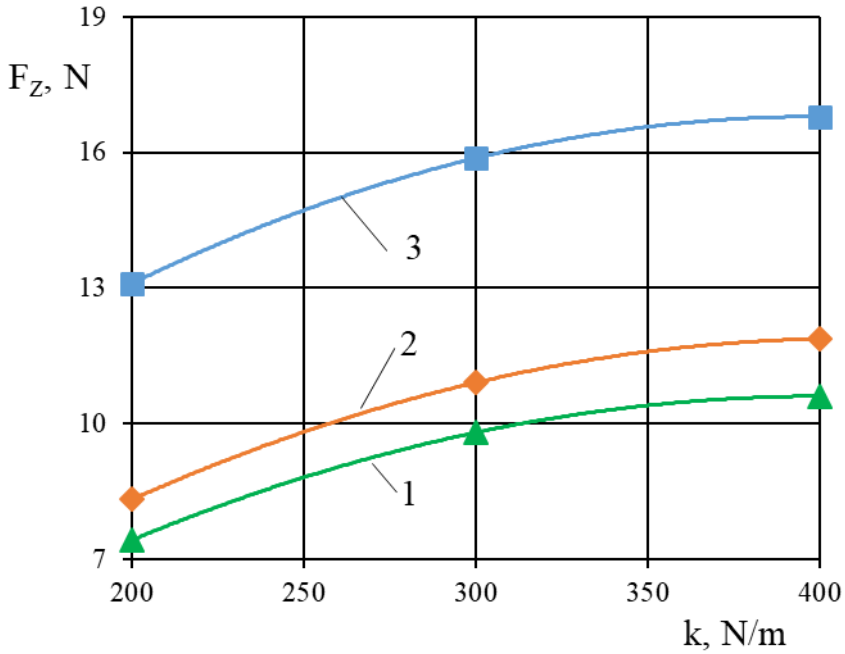

1, 2, and 3 – correspond to the rotation frequencys of the elastic blade of 30 r/min, 40 r/min, and 50 r/min, respectively

Fig. 3.13. Graph of the dependence of the impact force exerted on the mesh drum on the stiffness coefficient of the elastic blade

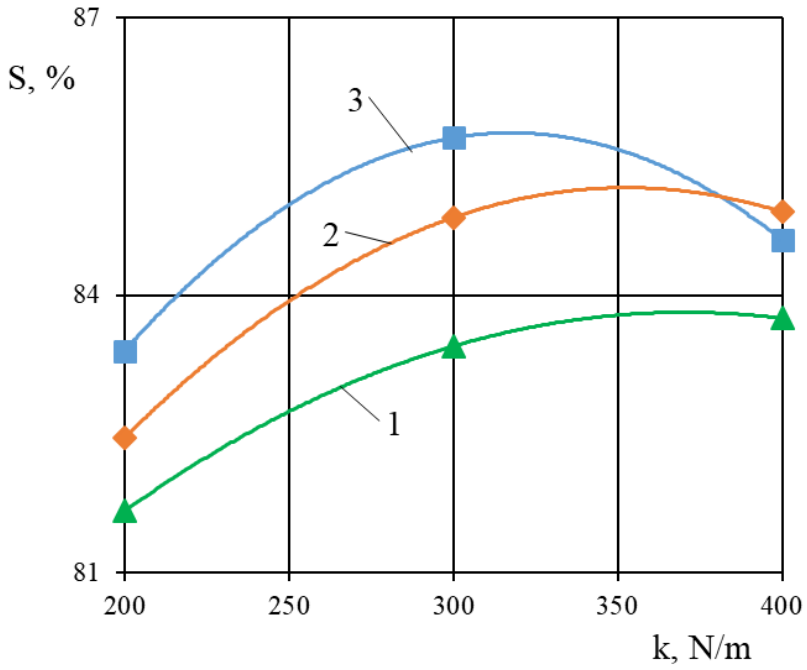

1, 2, and 3 – correspond to the rotation frequency of the elastic blade of 30 r/min, 40 r/min, and 50 r/min, respectively

Fig. 3.14. Graph of the dependence of the degree of screening on the stiffness coefficient of the elastic blade

From Fig. 3.14, it can be seen that as the stiffness coefficient of the elastic blade increases, the degree of screening increases according to a nonlinear law when the rotation frequency of the shaft with elastic blades is 30 r/min and 40 r/min. However, when the rotation frequency of the shaft with elastic blades is 50 r/min, it first increases and then decreases. As the stiffness coefficient of the elastic blade increases, the degree of screening of bulk materials changes differently depending on the rotation frequency; these variations are explained by the change in impact force. This is because, as the impact force increases excessively, the vibration of the mesh drum also increases, and the material inside the drum does not have sufficient time to be screened and passes through without being screened due to its axial velocity.

3.4. Determination of the torque on the mesh drum shaft

In the experimental investigations, in order to determine the laws of variation of the torque on the mesh drum shaft, the value of the resistance force moment was taken as 125 N·m, 150 N·m, and 175 N·m, the rotation frequency of the mesh drum shaft as 20 r/min, 25 r/min, and 30 r/min, the

rotation frequency of the shaft with elastic blades as 30 r/min, 40 r/min, and 50 r/min, and the stiffness coefficient of the elastic blades as 200 N/m, 300 N/m, and 400 N/m. In this case, the inclination angle of the mesh drum was kept constant at 10 degrees.

In the conducted experimental studies, the measured results were obtained in numerical form, and in order to study the laws of variation of the torque on the mesh drum shaft, oscillograms were constructed using Microsoft Excel software (Figs. 3.15–3.19). Based on the literature, it can be stated that for rotating working organs and mechanisms of machines, it is sufficient to study the values of the investigated parameters over at least 6 cycles of operating mode [81, p. 97].

Figures 3.15–3.17 present the laws of variation of the torque on the mesh drum shaft depending on the rotation frequency.

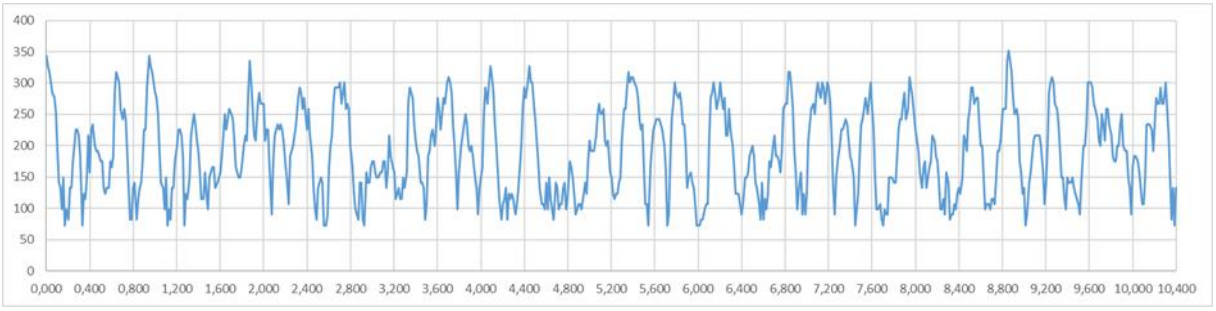

a

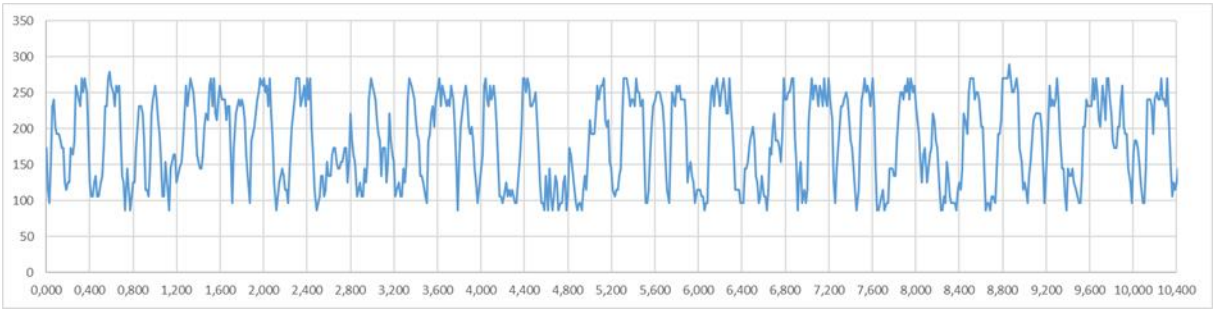

b

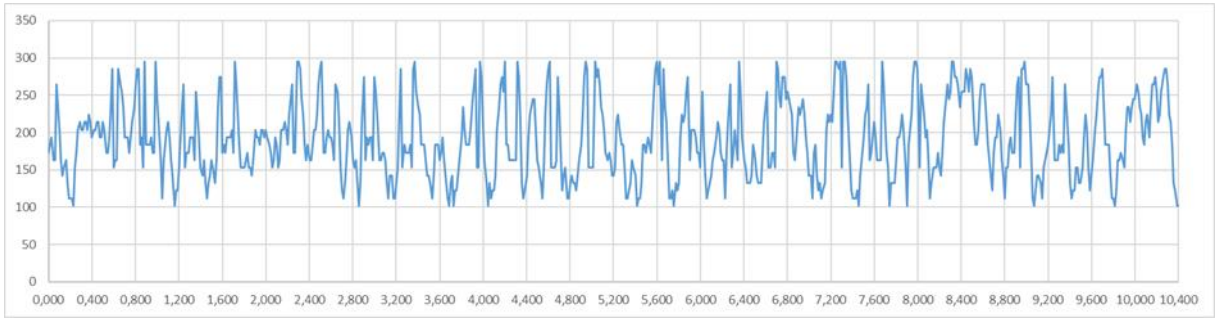

c

***a*-n_2=20 r/min; *b*-n_2=25 r/min; *c*-n_2=30 r/min**

Fig. 3.15. Law of variation of the torque on the mesh drum shaft depending on the rotation frequency (resistance moment 175 N·m)

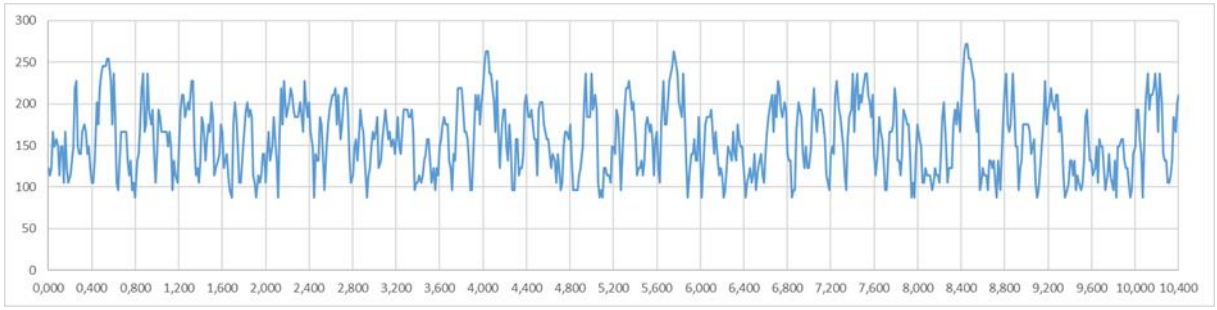

a

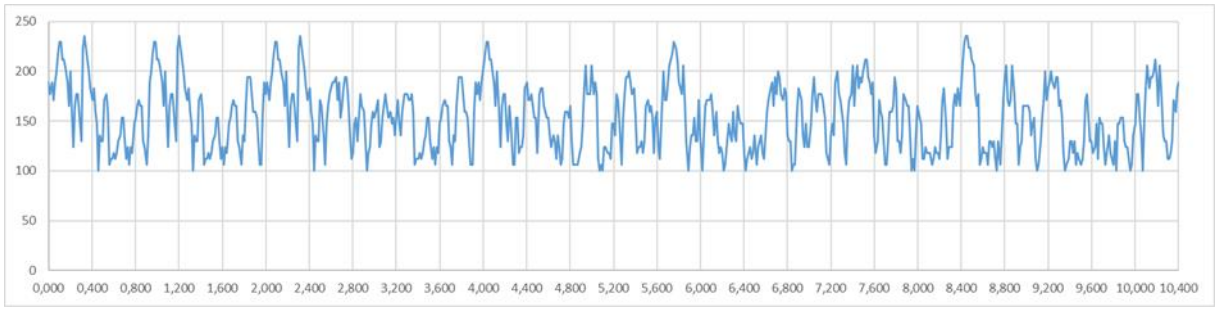

b

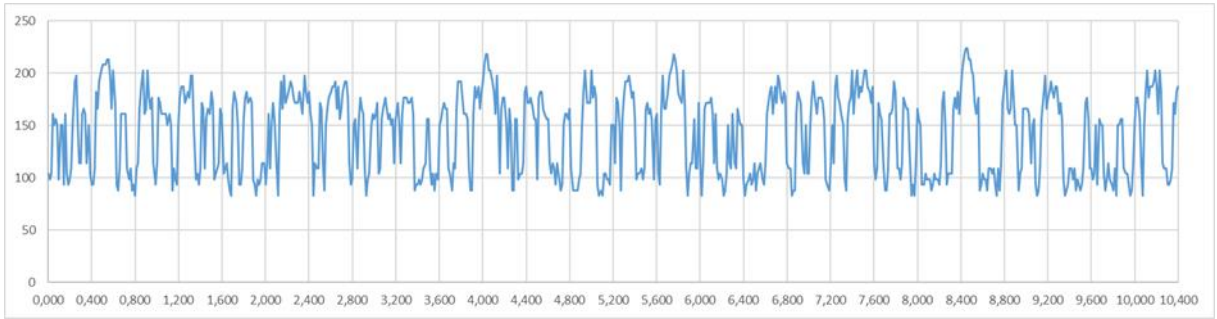

c

a-n_2=20 r/min; b-n_2=25 r/min; c-n_2=30 r/min

Fig. 3.16. Law of variation of the torque on the mesh drum shaft depending on the rotation frequency (resistance moment 150 N·m)

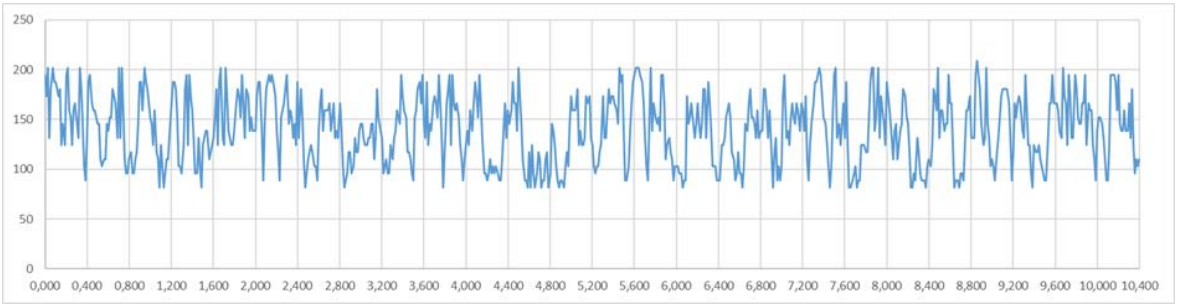

a

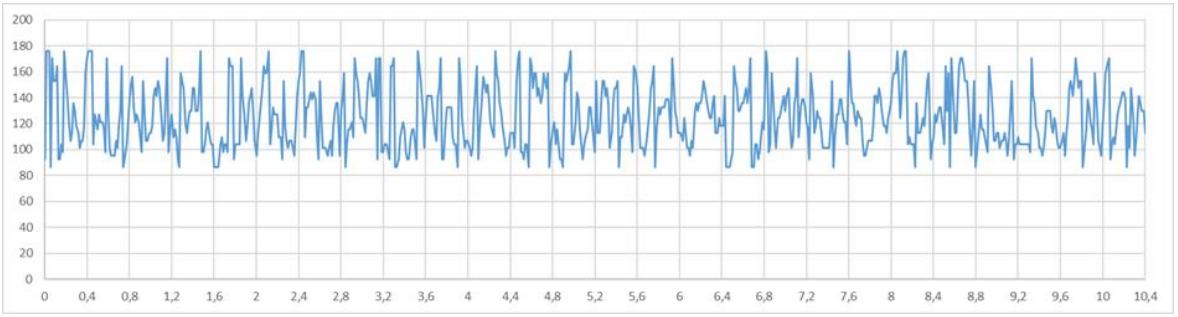

b

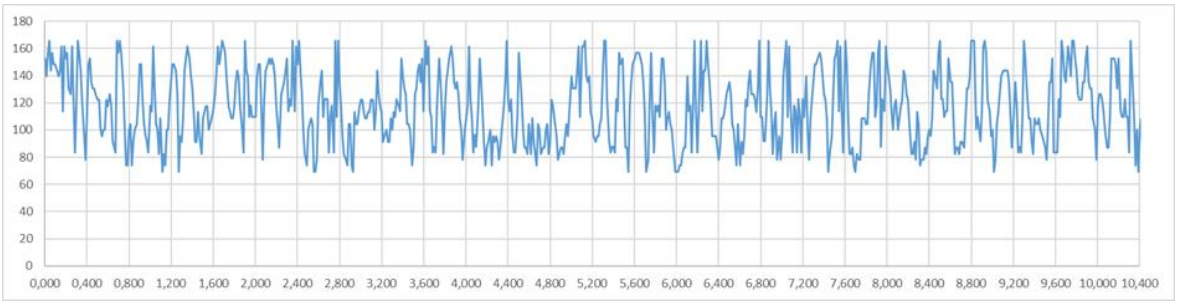

c

***a*-n_2=20 r/min; *b*-n_2=25 r/min; *s*-n_2=30 r/min**

Fig. 3.17. Law of variation of the torque on the mesh drum shaft depending on the rotation frequency (resistance moment 125 N·m)

Fig. 3.15 presents the laws of variation of the torque under the condition that the resistance moment is 175 N·m and the rotation frequency of the mesh drum shaft is 20 r/min (Fig. 3.15a), 25 r/min (Fig. 3.15b), and 30 r/min (Fig. 3.15c).

Fig. 3.16 presents the laws of variation of the torque under the condition that the resistance moment is 150 N·m and the rotation frequency of the mesh drum shaft is 20 r/min (Fig. 3.16a), 25 r/min (Fig. 3.16b), and 30 r/min (Fig. 3.16c).

Fig. 3.17 presents the laws of variation of the torque under the condition that the resistance moment is 125 N·m and the rotation frequency of the mesh drum shaft is 20 r/min (Fig. 3.17a), 25 r/min (Fig. 3.17b), and 30 r/min (Fig. 3.17c).

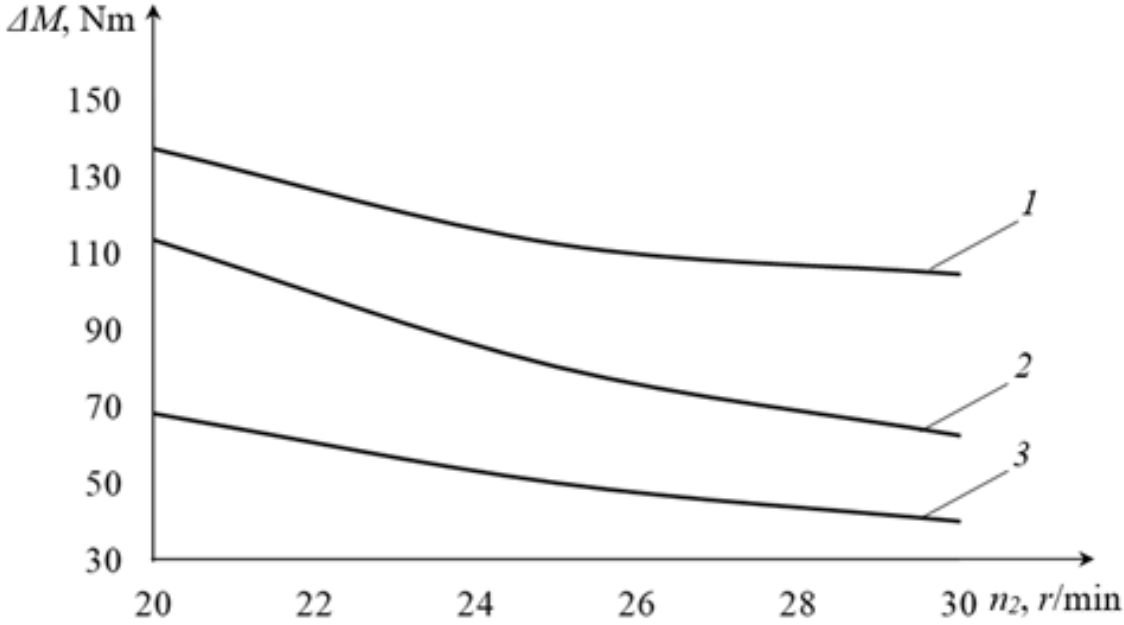

***1*-*M*=175 N·m; *2*-*M*=150 N·m; *3*-*M*=125 N·m**

Fig. 3.18. Graph of the dependence of the oscillation amplitude of the torque on the mesh drum shaft on the rotation frequency

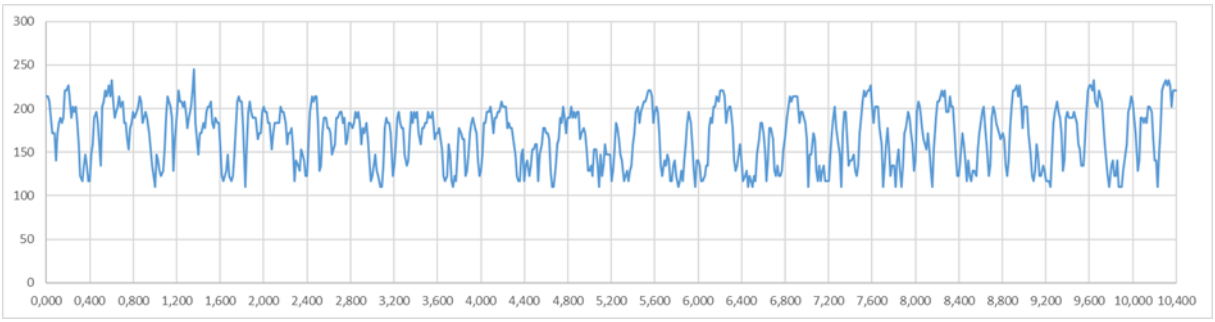

a

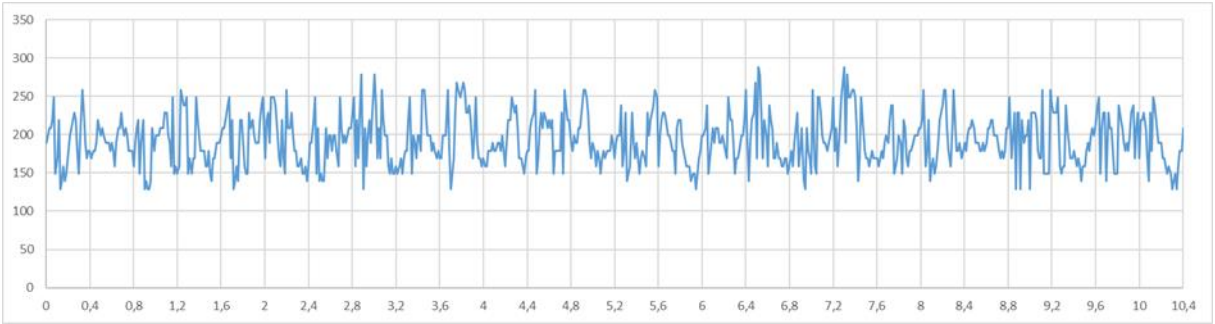

b

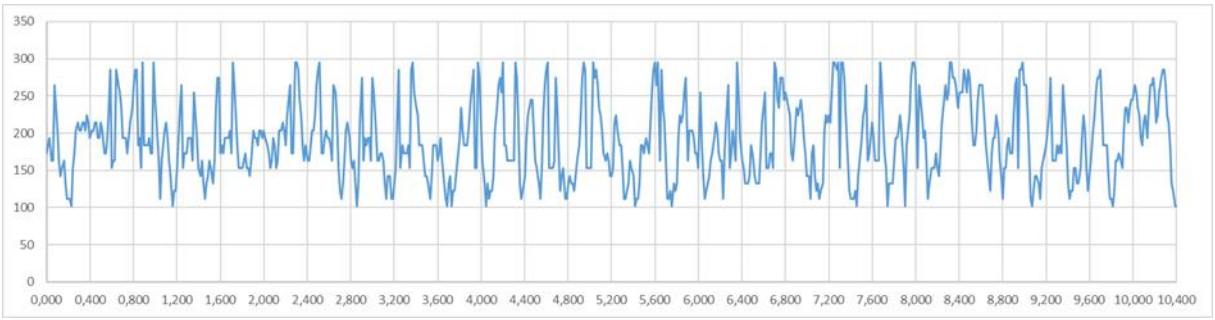

c

a-n_3=30 r/min; b-n_3=40 r/min; c-n_3=50 r/min

Fig. 3.19. Law of variation of the torque on the mesh drum shaft depending on the rotation frequency of the shaft with elastic blades (resistance moment 175 N·m)

The analysis of the above laws shows that with an increase in the rotation frequency, the oscillation frequency of the torque on the mesh drum shaft also increases. Based on the analysis of the variation laws presented in Figs. 3.15–3.17, a graph of the dependence of the oscillation amplitude of the torque on the mesh drum shaft on the rotation frequency was constructed (Fig. 3.18). From this relationship graph, it can be seen that as the rotation frequency increases, the oscillation amplitude of the torque on the mesh drum shaft decreases according to a nonlinear law. For example, when the rotation frequency increases from 20 r/min to 30 r/min and the resistance moment is 175 N·m, the oscillation amplitude of the torque on the mesh drum shaft decreases from 137,4 N·m to 104,7 N·m; when the resistance moment is 150 N·m, it decreases from 113,65 N·m to 62,64 N·m; and when the resistance moment is 125 N·m, it decreases from 68,4 N·m to 40,3 N·m.

Fig. 3.19 presents the law of variation of the torque on the mesh drum shaft depending on the rotation frequency of the shaft with elastic blades. According to it, it can be seen that as the rotation frequency of the shaft with elastic blades increases, the oscillation frequency of the torque on the mesh drum shaft decreases. This is explained by the fact that an increase in the rotation frequency of the elastic blade reduces the period of interaction of the elastic blades attached to it with the mesh drum.

Based on the analysis of the laws presented in Fig. 3.19, a graph of the dependence of the torque on the mesh drum shaft on the rotation frequency of the shaft with elastic blades was constructed (Fig. 3.20).

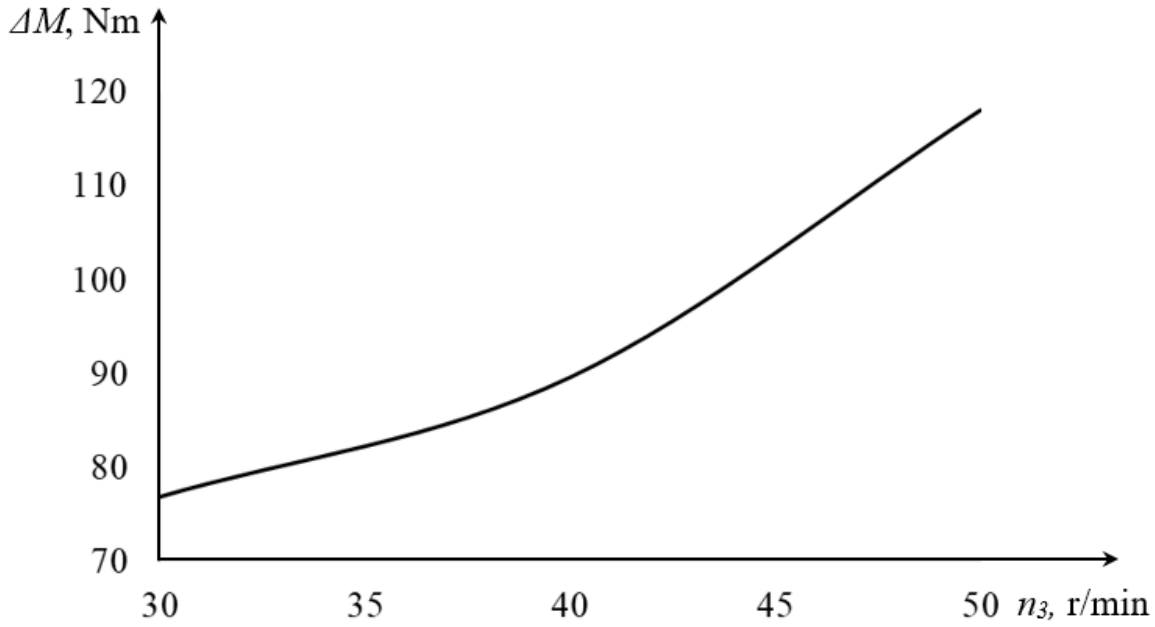

Fig. 3.20. Graph of the dependence of the torque on the mesh drum shaft on the rotation frequency of the shaft with elastic blades

From Fig. 3.20, it can be seen that as the rotation frequency of the shaft with elastic blades increases, the oscillation amplitude of the torque on the mesh drum shaft increases according to a nonlinear law. In this case, when the rotation frequency of the shaft with elastic blades increases from 30 r/min to 50 r/min and the resistance moment is 175 N·m, the oscillation amplitude of the torque on the mesh drum shaft increases from 76,84 N·m to 118,06 N·m.

Fig. 3.21 presents the laws of variation of the torque on the mesh drum shaft depending on the stiffness coefficient of the elastic blade. From these laws, it can be seen that with an increase in the stiffness coefficient of the elastic blade, the oscillation frequency of the torque on the mesh drum shaft decreases. This may have a positive effect on intensifying the screening process of bulk materials. This assumption will be substantiated in further studies on the optimization of the parameters of the screening device.

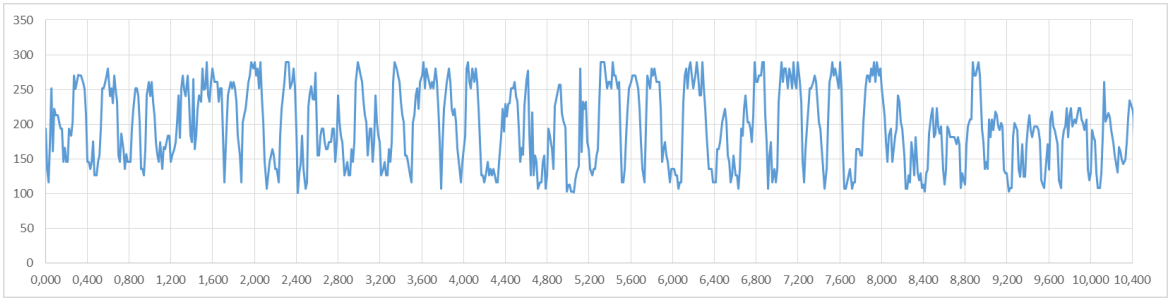

a

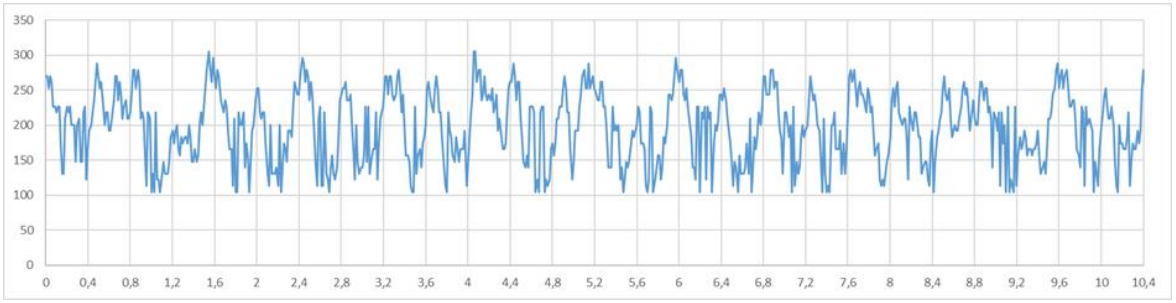

b

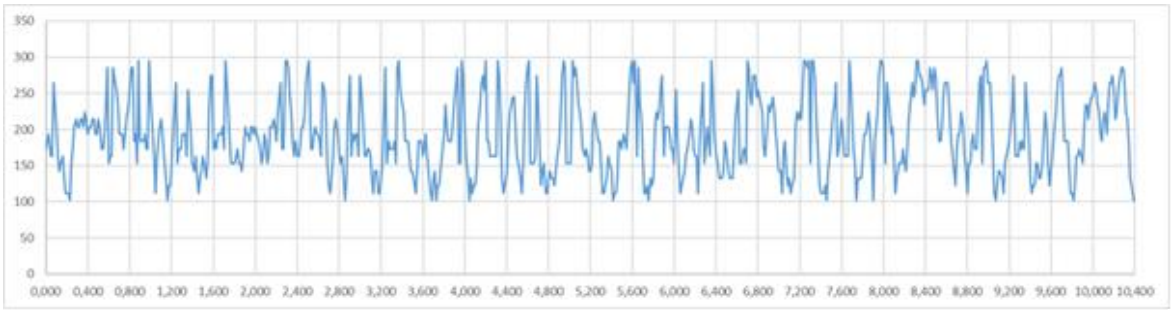

c

***a*-*k*=200 N/m; *b*- *k*=300 N/m; c- *k*=400 N/m**

Fig. 3.21. Law of variation of the torque on the mesh drum shaft depending on the stiffness coefficient of the elastic blade (resistance moment 175 N·m)

Based on the analysis of the laws presented in Fig. 3.21, a graph of the dependence of the torque on the mesh drum shaft on the stiffness coefficient of the elastic blade was constructed (Fig. 3.22).

From Fig. 3.22, it can be seen that as the value of the stiffness coefficient of the elastic blade increases, the oscillation amplitude of the torque on the mesh drum shaft also increases according to a nonlinear law. In this case, when the resistance moment is 175 N·m and the stiffness coefficient of the elastic blade is 200 N/m, the oscillation amplitude of the torque on the mesh drum shaft is 92,41 N·m; when the stiffness coefficient is 300 N/m, the

oscillation amplitude of the torque on the mesh drum shaft is 114,8 N·m; and when the stiffness coefficient is 400 N/m, the oscillation amplitude of the torque on the mesh drum shaft is 118,6 N·m.

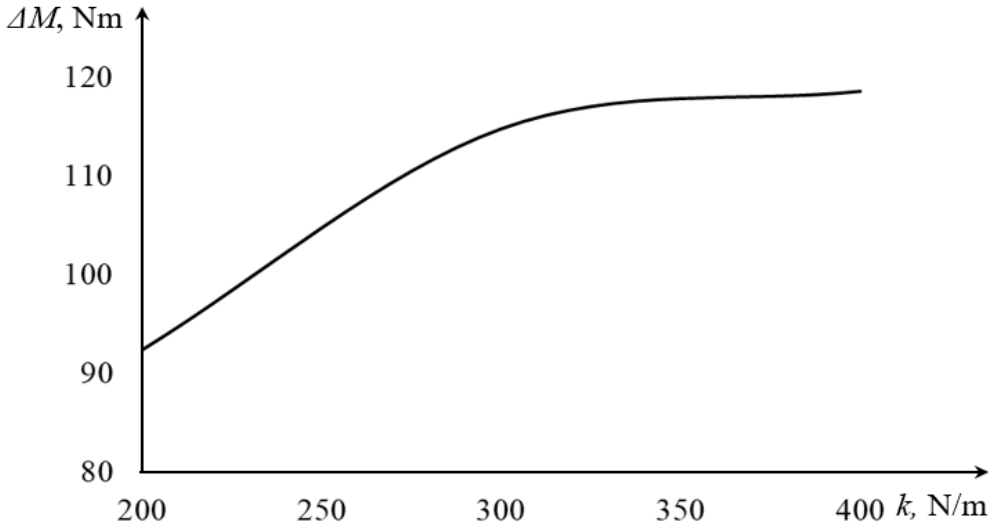

Fig. 3.22. Graph of the dependence of the torque on the mesh drum shaft on the stiffness coefficient of the elastic blade

The results obtained from the experimental investigations indicate that it is appropriate to determine the optimal operating parameters of the bulk material screening device by conducting multi-factor experiments using the method of experimental design in order to evaluate their influence on the operating mode and efficiency of the device. Therefore, the subsequent research will be focused on carrying out multi-factor experimental studies.

3.5. Optimization of the parameters of the drum screening device based on multi-factor experimental design

In order to increase the reliability of the results obtained from theoretical and experimental studies carried out to justify the parameters of the drum screening device, the method of mathematical design of experiments for multi-factor experiments was applied [81, 82, 83]. In this case, it was assumed that the influence of factors on the evaluation criteria is sufficiently described by a second-order polynomial, and the experiments were carried out according to the Hartley-5 (N_5) design.

Soil was selected as the bulk material in the experiments. Based on the

results of theoretical studies and single-factor experiments, the following parameters were chosen as influencing factors of the screening process: the rotation frequency of the mesh drum, the inclination angle, the rotation frequency of the shaft with elastic blades, the stiffness coefficient of the elastic blades, and productivity. The degree of screening of soil was selected as the output parameter. The input factors were denoted as follows: X_1 – rotation frequency of the mesh drum, X_2 – inclination angle of the mesh drum, X_3 – rotation frequency of the shaft with elastic blades, X_4 – stiffness coefficient of the elastic blade, X_5 – productivity. Table 3.1 presents the designations, variation ranges, and levels of the input factors.

In order to reduce the influence of uncontrolled factors on the evaluation criteria, the sequence of experiments was determined using a random number table.

The experimental data were processed using the "PLANEXP" software developed at the experimental testing department of the Research Institute of Mechanization of Agriculture. In this case, the Cochran criterion was used to evaluate the homogeneity of variance, the Student criterion to assess the significance of regression coefficients, and the Fisher criterion to evaluate the adequacy of the regression models.

Table 3.1. Designation, variation ranges, and levels of input factors

Factors and their measurement units	Symbol designation	Variation range	Levels		
			lower (–1)	basic (0)	upper (+1)
Rotation frequency of the mesh drum, r/min	X_1	5	20	25	30
Inclination angle of the mesh drum, degrees	X_2	5	5	10	15
Rotation frequency of the shaft with elastic blades, r/min	X_3	10	30	40	50
Stiffness coefficient of the elastic blade, N/m	X_4	100	200	300	400
Productivity, t/h	X_5	0,3	1,2	1,5	1,8

The experimental results were processed in the established order, and the following regression equations expressing the adequacy of the evaluation criteria were obtained:

- degree of screening, %:

$$Y_1 = 83{,}130 + 1{,}740X_1 - 4{,}244X_2 + 3{,}230X_3 - 1{,}691X_4 - 1{,}917X_5 -$$

$$-1{,}917X_1^2 - 1{,}904X_1X_2 - 4{,}139X_1X_3 + 0{,}381X_1X_4 - 6{,}266X_1X_5 -$$

$$-3{,}477X_2^2 - 2{,}973X_2X_3 + 0{,}793X_2X_4 - 1{,}118X_2X_5 - 2{,}055X_3^2 +$$

$$+1{,}239X_3X_4 - 3{,}281X_3X_5 - 1{,}135X_4^2 + 0{,}720X_4X_5 + 0{,}7118X_5^2.$$

(3.1)

The analysis of the obtained regression equation (3.1) and the graphical relationships constructed based on it (Fig. 3.23) shows that all factors have a significant influence on the evaluation criteria.

From Figs. 3.23a and 3.23c, it can be seen that with an increase in the rotation frequency of the mesh drum and the shaft with elastic blades, the degree of soil screening increases according to a nonlinear law. However, it can also be observed that as productivity increases, the degree of soil screening decreases.

From Figs. 3.23b and 3.23d, it can be seen that with an increase in the inclination angle of the mesh drum and the stiffness coefficient of the elastic blade, the degree of soil screening decreases according to a nonlinear law. In these cases as well, an increase in productivity leads to a decrease in the degree of soil screening.

The regression equation (3.1) was solved under the condition of maximizing the criterion Y_1, i.e., the degree of soil screening, and the following values of the factors ensuring the fulfillment of this condition were obtained (Table 3.2).

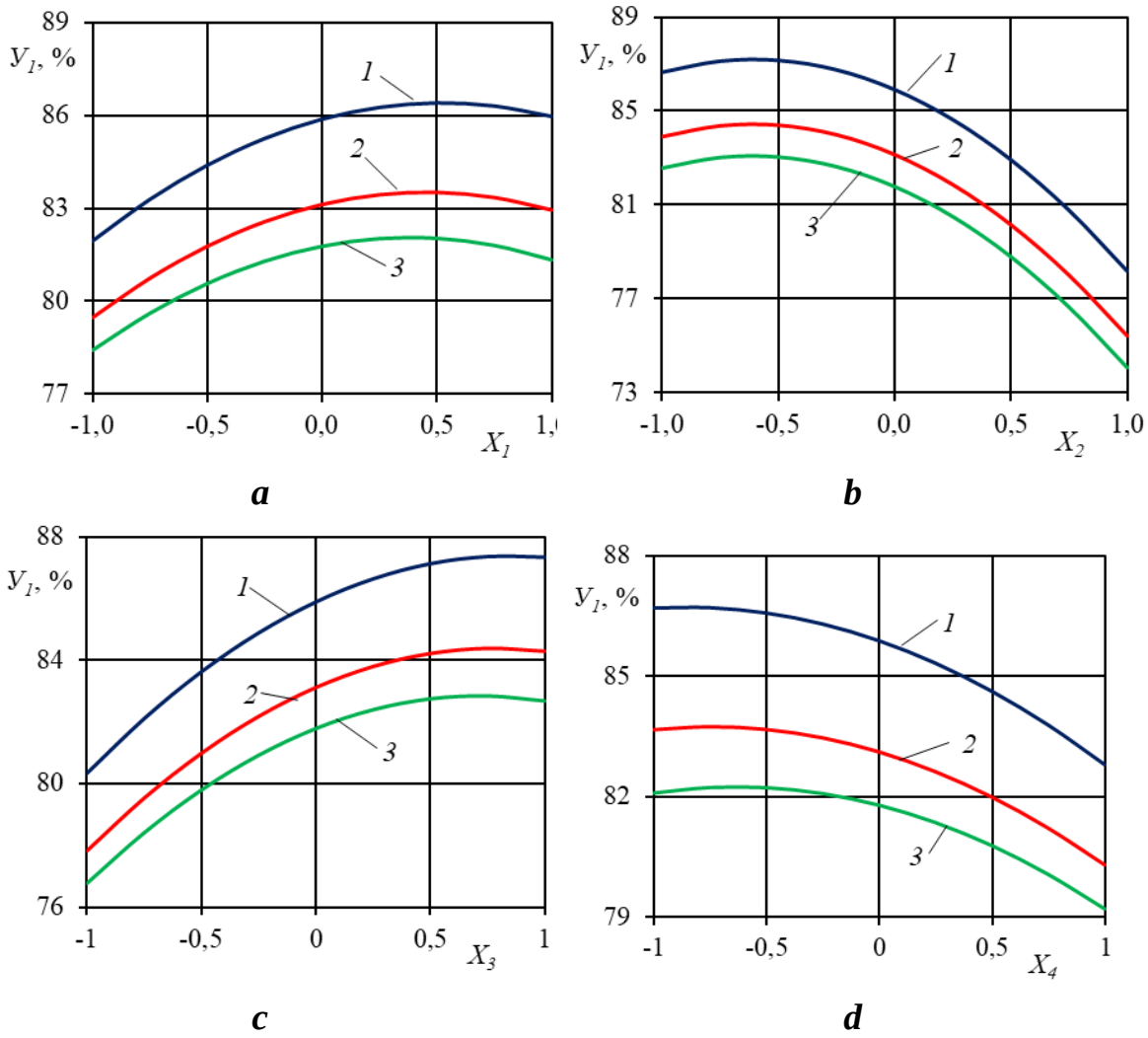

1-X_5=-1; 2-X_5=0; 3-X_5=1

Fig. 3.23. Variation of the degree of screening depending on factors X_1, X_2, X_3 and X_4

Table 3.2. Optimal values of the bulk material screening device parameters

X_5		X_1		X_2		X_3		X_4	
cod.	real.	cod.	real.	cod.	real.	cod.	real.	cod.	real.
1	1,8	0,1697	25,8487	0,34	11,72	0,2847	30,66	0,6522	265,22
0	1,5	0,5018	27,5091	0,21	11,03	0,5515	35,33	0,6609	266,09
-1	1,2	0,9996	29,9979	0,64	13,22	0,8536	40,95	0,8641	386,41

To ensure the required operating quality of the bulk material screening device with low energy consumption at a productivity of (1,2 … 1,8) t/h, the

following optimal parameter ranges were determined: the rotation frequency of the mesh drum should be (25,84 … 29,9) r/min, the inclination angle (11°43' … 13°13'), the rotation frequency of the shaft with elastic blades (30,6 … 40,95) r/min, and the stiffness coefficient of the elastic blades (265 … 386) N/m.

At these parameter values, the degree of soil screening was (80,76 … 82,26) %, and the torque on the mesh drum shaft was (165,9 … 177,39) N·m.

Conclusions of Chapter III

1. It was established that with an increase in the stiffness coefficient of the elastic blade, the degree of screening of bulk materials changes differently depending on the rotation frequency. These variations are related to the change in impact force. It was found that when the impact force increases excessively, the vibration of the mesh drum also increases, and the material inside the drum does not have sufficient time to be screened and remains unscreened due to its axial velocity.

2. It was determined that in order for the proposed bulk material screening device to ensure the required screening quality at a productivity of (1,2 … 1,8) t/h with low energy consumption, the rotation frequency of the mesh drum should be (25,84 … 29,9) r/min, the inclination angle (11°43' … 13°13'), the rotation frequency of the shaft with elastic blades (30,6 … 40,95) r/min, and the stiffness coefficient of the elastic blades (265 … 386) N/m.

3. It was found that the screening efficiency of the bulk material screening device is (80,76 … 82,26) %, and the torque on the mesh drum shaft is (165,9 … 177,39) N·m.

CHAPTER IV. IMPLEMENTATION OF RESEARCH RESULTS AND CALCULATION OF ECONOMIC EFFICIENCY

4.1. Research results of the proposed drum screening device under industrial conditions

Based on the results of the conducted studies, an experimental prototype of the drum screening device equipped with a shaft with elastic blades was manufactured at “TEKNIK INNOVATSION” LLC located in the Altiariq district of Fergana region (Fig. 4.1).

Fig. 4.1. Experimental prototype of the soil screening device

The experimental studies on the implementation of the proposed drum screening device were carried out at “Ko‘shan” LLC in Chortoq district of Namangan region and at “WHITEBRICK” LLC in Kokand city of Fergana region (Fig. 4.2) (Appendices 3, 4).

During the experimental trials, the soil screening device was

implemented in a brick production enterprise, and the productivity was set to 70 t/h. In the tests, the rotation frequency of the mesh drum was selected as 30 r/min, the inclination angle as 12 degrees, the rotation frequency of the shaft with elastic blades as 40 r/min, and the stiffness coefficient of the elastic blades as 300 N/m.

During the tests, the proposed soil screening device operated without interruptions and performed its assigned functions with high quality. Due to the impact forces applied to the mesh drum by the elastic blades, the screening efficiency increased from 78% to 82%.

Fig. 4.2. Process of implementation of the soil screening device

4.2. Economic efficiency of the practical implementation of the drum screening device

The expected economic effect from the application of the developed soil screening device is achieved due to the increase in operational efficiency compared to the soil screening equipment currently used in brick production enterprises.

The economic efficiency of new machines and mechanisms is determined by evaluating the magnitude of the economic effect calculated for the new variant in comparison with the base one. To assess the consumption of fuel and energy resources, energy efficiency indicators and specific energy intensity of technologies and machines are used [84].

The economic efficiency of the proposed soil screening device was calculated in accordance with [84].

The economic efficiency of certain types of new equipment that do not affect product processing quality, sales volume, price, or device performance is expressed through cost reduction, and the expected annual economic effect is determined by the following expression

$$E = \left(R_E - R_P\right) \cdot K, \qquad (4.1)$$

where E is the annual economic efficiency of the soil screening device, in UZS; R_E and R_P are the total costs of the existing and proposed devices, respectively, in UZS; K is the annual operating load, in days.

The calculation of economic efficiency was carried out by comparing the existing soil screening device with the proposed soil screening device equipped with a shaft with elastic blades in terms of electricity consumption during soil screening. In this case, both devices were operated under identical conditions.

The test results showed that the existing soil screening device processed 60 tons of soil per hour and consumed 4,8 kW of electrical energy, while the proposed device equipped with a shaft with elastic blades processed 70 tons of soil per hour and consumed 5 kW of electrical energy. In this case, an increase in productivity of the proposed device by 1,16% was achieved. In addition, an improvement in the soil screening degree was also obtained.

Average daily operating time of the device: A = 12 h.

Productivity of the existing soil screening device: B_E = 60 t/h.

Productivity of the proposed soil screening device with elastic blades: B_P = 70 t/h.

Electricity price (for legal entities): H = 1000 UZS (as of 01.05.2025).

Electricity consumption of the existing soil screening device: S_E = 4,8 kW·h.

Electricity consumption of the proposed soil screening device: S_P = 5 kW·h.

Thus, the electricity cost for the existing and proposed devices is determined as follows:

$$R_E = A \cdot B_E \cdot H \cdot S_E = 12 \cdot 60 \cdot 1000 \cdot 4{,}8 = 3456000 \text{ UZS};$$

$$R_P = A \cdot B_P \cdot H \cdot S_P = 12 \cdot 70 \cdot 1000 \cdot 5 = 4200000 \text{ UZS}.$$

In the proposed soil screening device, the annual savings obtained due to the reduction in electricity consumption were determined according to (4.1) as follows

$$E = (4200000 - 3456000) \cdot 180 = 133920000 \text{ UZS}$$

Thus, due to the 1,16% increase in productivity of the proposed soil screening device equipped with a shaft with elastic blades, the annual economic efficiency of a single unit amounts to 133 920 000 UZS.

Conclusions of Chapter IV

1. It was achieved that the proposed soil screening device equipped with a shaft with elastic blades operates without interruptions and performs its assigned functions with high quality. Due to the impact forces applied to the mesh drum by the elastic blades, the screening efficiency increased from 78% to 82%.

2. When the soil screening device equipped with a shaft with elastic blades is used, an increase in productivity of 1,16% was achieved, and the annual economic efficiency of a single unit amounts to 133 920 000 UZS.

GENERAL CONCLUSIONS

1. It was established that in the screening of bulk materials, the geometric dimensions of drums, rotation frequency, inclination angle relative to the horizontal plane, type of motion, and friction angles are of great importance. Therefore, by taking these parameters into account in design and calculations, it is possible to develop energy- and resource-saving constructions.

2. Based on the analysis of literature sources, an improved design of a bulk material screening device equipped with a mesh drum and a shaft with elastic blades was developed.

3. Theoretical studies showed that the impact point of the blade is located at a distance equal to 2/3 of its length from the axis of rotation.

4. It was established that the velocity of the screened material and its discharge time are important parameters in mesh drum screening systems, as they form the basis for determining productivity as well as structural and kinematic parameters of the drum.

5. Since the main working elements of the developed screening device are the mesh drum and the shaft with elastic blades, the influence of elastic blades was considered as a resistance force in the theoretical studies, and dynamic analysis of the mesh drum was carried out. Based on this analysis, laws of variation of the angular velocity of the mesh drum were obtained.

6. It was found that with an increase in the stiffness coefficient of the elastic blade, the degree of screening of bulk materials changes differently depending on the rotation frequency. These changes are related to the variation of impact force. It was confirmed that excessive impact force increases drum vibration, causing the material inside the drum not to be screened properly due to axial velocity.

7. It was determined that in order for the proposed screening device to ensure the required quality at a productivity of (1,2 … 1,8) t/h with low

energy consumption, the mesh drum rotation frequency should be (25,84 … 29,9) r/min, inclination angle 11°43' … 13°13', rotation frequency of the shaft with elastic blades (30,6 … 40,95) r/min, and stiffness coefficient of elastic blades (265 … 386) N/m.

8. It was achieved that the proposed soil screening device equipped with a shaft with elastic blades operates without interruptions and ensures high-quality performance of its functions. Due to the impact forces applied to the mesh drum by elastic blades, the screening efficiency increased from 78% to 82%.

9. When the soil screening device equipped with a shaft with elastic blades was used, a 1,16% increase in productivity was achieved, and the annual economic efficiency of a single unit amounted to 133 920 000 UZS.

LIST OF REFERENCES

1. Коноплин, А. Н. (2008). *Совершенствование процесса центробежной сепарации сыпучих материалов* [Автореф. дис. ... канд. техн. наук: 05.20.01]. Воронеж.

2. Стрикунов, Н. И., Беляев, В. И., & Тарасов, Б. Т. (2007). *Очистка зерна и семян. Машины и технологии*. Изд-во АГАУ.

3. Горячкин, В. П. (1965). *Собрание сочинений* (Т. 1, с. 244–253). Колос.

4. Дринча, В. М. (2006). *Исследование сепарации семян и разработка машинных технологий их подготовки*. НПО «МОДЭК».

5. Гончаров, Е. С. (1986). *Механико-технологическое обоснование и разработка универсальных виброцентробежных зерновых сепараторов* [Автореф. дис. ... д-ра техн. наук]. Москва.

6. Гортинский, В. В., Демский, А. Б., & Борискин, М. А. (1980). *Процессы сепарирования на зерноперерабатывающих предприятиях*. Колос.

7. Зильбернагель, А. В. (2005). *Интенсификация процесса сепарации зерна на плоских решетах с продолговатыми отверстиями, расположенными под углом* [Автореф. дис. ... канд. техн. наук]. Новосибирск.

8. Кожуховский, И. Е. (1974). *Зерноочистительные машины*. Машиностроение.

9. Тарасов, Б. Т., Стрикунов, Н. И., & Леканов, С. В. (2009). Процесс сепарации на подсевном решете с пластинчатым барабаном центробежно-решетного сепаратора с вертикальной осью вращения. *Сибирский вестник сельскохозяйственной науки*, *(7)*, 69–77.

10. Тарасов, Б. Т. (1970). *Исследование процесса сепарации зерна по длине вертикальными цилиндрическими решетами при ориентации зерен в активном слое* [Дис. ... канд. техн. наук]. Барнаул.

11. Папин, Б. Д. (1989). Методология детерминированно-статистического моделирования процессов сепарации. В *Электротехнологические методы и установки в с.-х. пр-ве* (с. 5–21). Челябинск.

12. Леканов, С. В. (2006). *Обоснование параметров цилиндрического подсевного решета с внутренним пластинчатым барабаном центробежно-решетного сепаратора с вертикальной осью вращения* [Автореф. дис. ... канд. техн. наук]. Барнаул.

13. Куринная, Н. О. (2009). *Повышение эффективности сепарации зерна круговыми колебаниями решет в режиме самоочистки отверстий от застрявших частиц* [Автореф. дис. ... канд. техн. наук]. Челябинск.

14. Ксифилинов, Х. А. (1954). О кинематическом режиме работы плоского решета. *Сельхозмашина, (10),* 17–21.

15. Akase, A., & Tsuchiya, M. (1989). Studies on the vertical rotating screen separator of brown rice. 1. On the screening performance and its affecting factors. *Japan. Soc. Agr. Mach, 51*(1), 89–96.

16. Harris, C., & Crede, Ch. (1976). *Shock and vibration handbook*. McGraw-Hill.

17. Зверков, Р. А. (2007). *Интенсификация технологического процесса сепарации зерна на зерноочистительной машине с цилиндрическими качающимися решетами* [Автореф. дис. ... канд. техн. наук]. Новосибирск.

18. Слепов, А. П. (1984). *Исследование процесса разделения зерновой смеси центрофугованием в сочетании с потоком воздуха (пневмоцентрифугование)* [Автореф. дис. ... канд. техн. наук]. Волгоград.

19. Хижников, А. А. (2011). *Интенсификация процесса очистки зерна на цилиндрическом подсевном решете* [Дисс. ... канд. техн. наук: 05.20.01]. Барнаул.

20. Тарасевич, С. В. (2006). *Обоснование параметров сепаратора с вибрационно-качающейся решетной поверхностью для зерновых материалов* [Дисс. ... канд. техн. наук: 05.20.01]. Барнаул.

21. Летошнев, М. Н. (1955). *Сельскохозяйственные машины*. Наука.

22. Гладков, Н. Г. (1961). *Зерноочистительные машины*. Наука.

23. Авдеев, Н. Е., & Странадко, Г. Г. (2001). Стабилизация режимов центробежных сепараторов. *Вестник Российский академии с/х наук*, *(4)*, 70–81.

24. Беляев, В. И., Стрикунов, Н. И., Тарасов, Б. Т., & Леканов, С. В. (2006). Результаты исследования влияния основных параметров подсевного решета на эффективность работы центробежно-решетного сепаратора. *Вестник Алтайского государственного аграрного университета*, *(2)*, 49–54.

25. Зверков, Р. А. (2007). *Интенсификация технологического процесса сепарации зерна на зерноочистительной машине с цилиндрическими качающимися решетами* [Автореф. дис. ... канд. техн. наук]. Новосибирск.

26. Иванов, Н. И., Торопов, В. Р., & Сухопаров, А. А. (2013). Оценка процесса сепарации зерна в цилиндрическом колосовом решете с винтовым распределителем. *Вестник Алтайского государственного аграрного университета*, *6*(104), 88–91.

27. Леканов, С. В., Стрикунов, Н. И., & Черкашин, С. А. (2014). К вопросу классификации способов предварительной подготовки зернового материала центробежно-решѐтных сепараторов с вертикальной осью вращения. *Вестник Алтайского государственного аграрного университета*, *4*(114), 142–148.

28. Сухопаров, А. А. (2014). *Параметры и режимы работы цилиндрического решета с винтовым распределителем для*

предварительной очистки зерна [Автореф. дис. ... канд. техн. наук]. Новосибирск.

29. Ткачев, В. В. (2011). Условие очистки отверстий решет семяочистительных машин. *Вестник Красноярского государственного аграрного университета*, *(5)*, 128–131.

30. Хижников, А. А., & Стрикунов, Н. И. (2010). Повышение эффективности очистки зерна на подсевном решете центробежно-решѐтного сепаратора. *Вестник Алтайского государственного аграрного университета*, *4*(66), 72–76.

31. Черняков, А. В., Коваль, В. С., & Сухов, А. В. (2009). Экспериментальное исследование работы двух цилиндрических качающихся решѐт с продолговатыми отверстиями, расположенными под углом к плоскости их движения. *Омский научный вестник*, *2*(80), 152–154.

32. Якимов, А. В. (2016). *Повышение эффективности функционирования сепаратора зернового материала путём совершенствования технологического процесса и параметров цилиндрических решёт* [Дисс. ... канд. техн. наук: 05.20.01]. Киров.

33. Турбин, Б. Г., Лурье, А. Б., Григорьев, С. М., и др. (1967). *Сельскохозяйственные машины*. Машиностроение.

34. Григорьев, С. М., Киреев, М. В., & Муллаянов, Р. Г. (1959). Графоаналитическое исследование движения точки по внутренней поверхности вращающегося цилиндра. *Механизация и электрификация сельского хозяйства*, *(76)*, 30–48.

35. Ding, Y. L., Forster, R., Seville, J. P. K., & Parker, D. J. (2002). Segregation of granular flow in the transverse plane of a rolling mode rotating drum. *International Journal of Multiphase Flow, 28*, 635–663.

36. Zhao, Y., Zhang, L., Song, C., Li, W., Qin, H., & Wang, Q. (2023). Numerical simulations of particle motions at continuous rotation

frequency changes in horizontal rotating drums. *Processes, 11*, 47. https://doi.org/10.3390/pr11010047

37. Свердлик, Г. И. (1999). *Развитие научных основ создания барабанных сыпучесредных агрегатов горнодобывающих предприятий* [Автореф. дисс. докт. техн. наук]. Владикавказ.

38. Тарасов, В. П. (2002). *Технологическое оборудование зерноперерабатывающих предприятий: учеб. пособие*. Изд-во АлтГТУ.

39. Федоренко, И. Я., & Пирожков, Д. Н. (2006). *Вибрируемый зернистый слой в сельскохозяйственной технологии: монография*. Изд-во АГАУ.

40. Климок, А. И. (1981). *Исследование процесса сепарации на решѐтах с профилированной поверхностью* [Автореф. дис. ... канд. техн. наук: 05.20.01]. Новосибирск.

41. Климок, А. И. (1979). Технологические основы организации процессов послеуборочной обработки зерна. *Научн. техн. бюл. СибНИИ мех. и электриф. С. х-ва, (5)*, 3–9.

42. Лапшин, И. П., Архипов, А. С., & Лопан, А. А. (1997). *Решето* (Патент Рос. Федерация № 2071843, МПК B07B 1/04, B07B 1/46).

43. Лапшин, И. П., Архипов, А. С., & Лопан, А. А. (2001). *Решето* (Патент Рос. Федерация № 2161541, МПК B07B 1/04).

44. Жолобов, Н. В. (2006). *Технология и технические средства очистки зерна на решѐтах: Учебное пособие*. Вятская ГСХА.

45. Федоренко, И. Я. (2008). Перемещение частицы по поперечно вибрирующей шероховатой плоскости. В *Машиннотехнологическое, энергетическое и сервисное обслуживание сельскохозпроизводителей Сибири: матер. Междунар. науч.-практич. конф.* (с. 548–554). Россельхозакадемия; Сибирское отделение; ГНУ СибИМЭ.

46. Тищенко, Л. Н., Ольшанский, В. П., & Ольшанский, С. В. (2009). О гидродинамической модели движения зерновой смеси по наклонному плоскому решету. *Пол. НТУ, 3*(25), 205–213.

47. Злочевский, В. Л., Баранов, А. В., & Тарасевич, С. В. (2005). Моделирование движения зернового материала на сепараторах со сложным движением рабочих органов. В *Матер. 11-й Междунар. научн.-практ. конф. «Природные и интеллектуальные ресурсы Сибири (СИБРЕСУРС-11-2005)»* (с. 139–141). ТГУ.

48. Злочевский, В. Л., & Тарасевич, С. В. (2005). Исследование процесса сепарирования зернового материала на решетной поверхности со сложным движением. В *Матер. 8-ой Научн.-практ. конф. с Междунар. участием «Современные проблемы техники и технологии пищевых производств»* (с. 39–43). Алт.ГТУ.

49. Беляев, В. И., Стрикунов, Н. И., & Леканов, С. В. (2006). Результаты исследования влияния основных параметров подсевного решета на эффективность работы центробежно-решетного сепаратора. *Вестник АГАУ*, *2*(22), 49–54.

50. Волынкин, В. В. (2007). *Повышение эффективности процесса отделения крупных примесей из зернового вороха скальператором* [Автореф. дис. ... канд. техн. наук: 05.20.01]. Челябинск.

51. Зверков, Р. А. (2007). *Интенсификация технологического процесса сепарации зерна на зерноочистительной машине с цилиндрическими качающимися решетами* [Автореф. дис. ... канд. техн. наук: 05.20.01]. Новосибирск.

52. Зильбернагель, А. В. (2005). *Интенсификация процесса сепарации зерна на плоских решетах с продолговатыми отверстиями, расположенными под углом* [Автореф. дис. ... канд. техн. наук: 05.20.01]. Новосибирск.

53. Коноплин, А. Н. (2008). *Совершенствование процесса центробежной сепарации сыпучих материалов* [Автореф. дис. ... канд. техн. наук: 05.20.01]. Воронеж.

54. Куринная, Н. О. (2009). *Повышение эффективности сепарации зерна круговыми колебаниями решет в режиме самоочистки отверстий от застрявших частиц* [Автореф. дис. ... канд. техн. наук: 05.20.01]. Челябинск.

55. Патрин, В. А., Патрин, А. В., & Крум, В. А. (2009). Графический метод выбора режимов работы вертикальных цилиндрических виброрешет. *Вестник ТГСХА*, *3*(10), 138–140.

56. Патрин, В. А., Патрин, А. В., & Крум, В. А. (2009). Определение оптимальных режимов работы вертикальных цилиндрических виброрешет графическим способом. *Механизация и электрификация сельского хозяйства*, *(8)*, 11–12.

57. Белов, М. И., & Романенко, В. Н. (2008). Математическая модель сепарации зерна на решете очистки. *Механизация и электрификация сельского хозяйства*, *(5)*, 10–13.

58. Белов, М. И., Романенко, В. Н., & Славкин, В. И. (2008). Математическая модель движения частицы по решету очистки. *Тракторы и сельськохозяйственные машины*, *(8)*, 33–36.

59. Лапшин, И. П., & Косилов, Н. И. (2002). *Расчёт и конструирование зерноочистительных машин*. ГИПП «Зауралье».

60. Повышение эффективности процесса решётного сепарирования сыпучих продуктов. (n.d.). *CyberLeninka*. https://cyberleninka.ru/article/n/povyshenie-effektivnosti-protsessa-reshyotnogo-separirovaniya-sypuchih-produktov

61. Летошнев, М. Н. (1955). *Сельскохозяйственные машины*. М; Л.

62. Киршин, В. Н. (1991). *Повышение технологической эффективности быстроходного цилиндрического решета на очистке*

семян льна совершенствованием конструкции и контролем качества очистки [Автореф. дисс. канд. техн. наук]. Ленинград.

63. Фоминых, А. В., Чумаков, В. Г., Шевцов, И. В., & Косовских, А. М. (2010). Методика расчета процесса просеивания проходов частиц в круглых отверстия решет. *Аграрный вестник Урала*, *7*(73), 80–81.

64. Фоминых, А. В. (2006). Расчет просеиваемости решетных сепараторов. *Механизация и электрификация сельского хозяйства*, *(7)*, 35–36.

65. Блехман, И. И. (1984). *Вибрационная механика*. Физматлит.

66. Лопан, А. А., Фоминых, А. В., & Чумаков, В. Г. (1995). Методика расчета траектории движения частиц в свободного затопленной струе. В *Через опыт – в науку: сборник науч. трудов* (с. 25). ИПП «Зауралье».

67. Лопарев, Д. В., Мекшун, Ю. Н., Лопарева, С. Г., & Овчинников, Д. Н. (2018). Применение конвейера в качестве сепарирующего устройства машин для предварительной очистки зернового вороха. В *Методы механики в решении инженерных задач: материалы II Всероссийской науч.-практ. конф.* (с. 28–32). Курганстkой ГСХА.

68. Фоминых, А. В., Мекшун, Ю. Н., Лопарев, А. В., & Ковшова, Н. А. (2019). Теоретические исследования движения зерна по решету, совершающему колебания в своей плоскости. *Вестник Курганской ГСХА*, *(3)*, 72–74.

69. Фоминых, А. В., & Чумаков, В. Г. (2010). Алгоритм расчета процесса сепарации на решетах устройствах. *Аграрный вестник Урала*, *7*(73), 77–79.

70. Кульбачный, О. И., Гродзенская, Л. С., Желиговский, А. В., и др. (1970). *Теория механизмов и машин. Проектирование*. Высшая школа.

71. Усмонхўжаев, Х. Х. (1981). *Механизм ва машиналар назарияси*. Ўқитувчи.

72. Кочетков, А. В., & Федотов, П. В. (2013). Некоторые вопросы теории удара. *Интернет-журнал «НАУКОВЕДЕНИЕ», (5),* 1–15.

73. Трофимова, Т. И. (2006). *Курс физики: учеб. пособие для вузов*. «Академия».

74. Коноплин, А. Н. (2008). *Совершенствование процесса центробежной сепарации сыпучих материалов* [Автореф. дис. ... канд. техн. наук: 05.20.01]. Воронеж.

75. Стрикунов, Н. И., Беляев, В. И., & Тарасов, Б. Т. (2007). *Очистка зерна и семян. Машины и технологии*. Изд-во АГАУ.

76. Гладков, Н. Г. (1961). *Зерноочистительные машины*. Наука.

77. Ding, Y. L., Forster, R., Seville, J. P., & Parker, D. J. (2002). Segregation of granular flow in the transverse plane of a rolling mode rotating drum. *International Journal of Multiphase Flow, 28,* 635–663.

78. Xakimov, M. M. (2024). *Ko‘chma don quritish mashinasi konstruksiyasini takomillashtirish hamda uning kinematik va dinamik tahlili* [Tex. fan. bo‘yicha fals. dokt. diss.]. Namangan.

79. Джураев, А., Мухитдинов, С. С., Самарходжаев, Х. Х., & Мирхамидов, Д. Х. (1990). *Ротационные механизмы технологических машин с переменными передаточными отношениями*. Мехнат.

80. Комилов, С. Р. (2022). *Ўқлараро масофаси ўзгарувчан занжирли узатма конструкцияси ва ҳисоблаш усулини ишлаб чиқиш* [Тех. фан. бўйича фалс. докт. дисс.]. Наманган.

81. Доспехов, Б. А. (1979). *Методика полевого опыта*. Колос.

82. Аугамбаев, М., Иванов, А. З., & Терехов, Ю. И. (1993). *Основы планирования научно-исследовательского эксперимента*. Укитувчи.

83. Джонсон, Н., & Лион, Ф. (1990). *Статистика и планирование эксперемента в технике и науке. Методы обработки данных* / Пер. с английского. Мир.

84. *Экономическая эффективность стандартизации. ГОСТ 20779-81. Методы определения. Основные положения*. (1982). Издательство стандартов.

85. Зулпиев, С. М., Давидбаев, Б. Н., Турдалиев, В. М., & Рузалиев, Х. Ш. (2025). *Устройство для сортировки сыпучего материала* (Патент Кырг. Рес. №448, заявка № 20250014.1).

86. Turdaliev, V. M., Davidboev, B. N., & Ruzaliev, X. Sh. (2025). Panjarali barabanga ta’sir etuvchi elastik parrakning zarb markazini aniqlash. *Mexanika va texnologiya ilmiy jurnali*, *(2).*

87. Turdaliyev, V. M., Davidboyev, B. N., & Ruzaliyev, X. Sh. (2025). Sochiluvchan materiallarni barabanli saralash qurilmasini ishlab chiqish va parametrlarini asoslash. *FarPI ilmiy-texnika jurnali, 29*(4-maxsus son), 21–25.

88. Turdaliyev, V. M., Davidboyev, B. N., & Ruzaliyev, X. Sh. (2025). Determination of the axial velocity of the material being sorted in a rotating perforated drum. *American Journal of Mechanics and Applications*, 81–86.

89. Ruzaliyev, X. Sh. (2025). Elastik parrak tomonidan panjarali baraban qovurg‘asiga beriladigan zarb kuchini tadqiqi. B *Ishlab chiqarish korxonalarida innovatsion, resurstejamkor texnika va texnologiyalarni joriy etish hamda atrof-muhitni muhofaza qilishning dolzarb muammolari va yechimlari mavzusidagi II Xalqaro ilmiy anjumani materiallar to‘plami I* (b. 67–70). Farg‘ona.

90. Turdaliyev, V. M., Davidboyev, B. N., & Ruzaliyev, X. Sh. (2025). Sochiluvchan materiallarni saralash qurilmasining yangi konstruksiyasini ishlab chiqish. B *Transport va yo‘l muhandisligi istiqbollari*

va muammolari mavzusidagi respublika ilmiy va ilmiy-texnik konferentsiya materiallari to‘plami II (b. 230–233). Namangan.

91. Turdaliyev, V. M., Davidboyev, B. N., & Ruzaliyev, X. Sh. (2025). Panjarali barabanga ta’sir etuvchi elastik parrakning zarb markazini aniqlash. B *Transport va yo‘l muhandisligi istiqbollari va muammolari mavzusidagi respublika ilmiy va ilmiy-texnik konferentsiya materiallari to‘plami II* (b. 508–511). Namangan.

92. Turdaliyev, V. M., Davidboyev, B. N., & Ruzaliyev, X. Sh. (2025). Determining the exit time of bulk material from the perforated drum. B *E-Global Congress Hosted online from Dubai, U. A. E., E-Conference* (b. 15–17). Dubay.

93. Ruzaliev, Kh. Sh. (2025). Theoretical study of the design of a device for sorting bulk materials and the impact force of an elastic blade. B *International scientific and practical conference topical issues of modern science and their innovative solutions* (b. 218–220). Farg‘ona.

94. Давидбоев, Б. Н., & Рузалиев, Х. Ш. (2025). Разработка и экперементальные исследование эффективной конструкции устройства для сортировки сыпучего материаллов. В *Актуальные проблемы инновационных технологий, интеграция образования и производства в Ферганской долине: энергосберегающие и инновационные решения. Сборник научных работ международной научно-технической конференции* (Ч. 2, с. 114–117). Фергана.

95. Davidboyev, B. N., Turdaliyev, V. M., & Ruzaliyev, X. Sh. (2026). Ko‘p omilli tajribalar o‘tkazish asosida barabanli saralash qurilmasining parametrlarini maqbullashtirish. B *Ishlab chiqarish va sanoatda transport tizimlarining innovatsion istiqbollari: avtomatlashtirish, raqamli transformatsiya va ekologik samaradorlik mavzusidagi respublika miqyosidagi ilmiy va ilmiy-texnikaviy anjumani materiallar to‘plami* (2-qism, b. 247–250). Farg‘ona.

96. Djuraev, A., Davidbaev, B. N., & Jumaev, A. S. (2022). *Improvement of the design of the belt conveyor and scientific basis for calculation of parameters*. Global Book Publishing Services.

97. Davidboev, B., Mirzakhanov, Y., Makhmudov, I., & Davidboeva, N. (2020). Research of lateral assembly of the belt in flat-belt transmissions and transport mechanisms. *International Journal of Scientific and Technology Research*, *9*(1), 3666–3669.

98. Djurayev, A., Davidbayev, B. N., & Jurayev, N. N. (2022). *Scientific basis of the design and parameter calculation of the construction and parameters of a double-inlet and wavy surface resource controller screw conveyor for spillable materials*. Global Book Publishing Services.

99. Zh, D. A., Davidbaev, B. N., & Davidbaeva, N. B. (2020). Determination Of OscilationAnpelitude Of Cotton Particle at Interaction with. PlateShpokAbsocter Of The Separator. *International Journal Of Abvanced Research in Science, Engieering and Technology, 7*(9), 14977–14981.

100. Zh, D. A., Davidbaev, B. N., & Davidbaeva, N. B. (2020). Substantiation Parameters ofReflektor With Rubbers Shock Absorber Of Cotton Separator. *Solid State Technology*, *63*(6), 1718–1726.

101. Давидбаев, Б. Н., & Джураев, А. Д. (2025). Разработка и исследование эффективной конструкции цепной передачи. *Механика и технология, 6*(4), 9–12.

102. Djuraevich, D. A., Nizomitdinovich, D. B., & Bakhtiyerdjanovna, D. N. (2020). Substantiation Parameters Of Reflector With Rubber Shock Absorber Of Cotton Separator. *Solid State Technology*, *63*(6), 1718–1726.

103. Davidbaev, B. N., Dzhuraev, A. Z., Mirzakhonov, Y. U., & Davidbaeva, N. B. (2021). Production testing of the effective structure of the centering tensioning devices. *Scientific and Technical Journal of the Fergana Polytechnic Institute*, *(3)*.

104. Джўраев, А., Давидбоев, Б., & Мамахонов, А. (2014). *Қайишқоқ элементли ва таранглаш қурилмали занжирли механизмларни кинематик ва динамик таҳлили: Монография*. Наврўз.

105. Turdaliev, Voxidjon Maxsudovich, Davidboev, Baxtiyordjan Nizamitdinovich, & Ruzaliev, Xojiakbar Shermaxammad o‘g‘li. (2025). Panjarali barabanga ta’sir etuvchi elastik parrakning zarb markazini aniqlash. *Механика и технология, 6*(2), 23–26.

106. Davidboyev, B. N., Turdaliyev, V. M., & Ruzaliyev, X. S. (2026, March). Ko‘p omilli tajribalar o‘tkazish asosida barabanli saralash qurilmasining parametrlarini maqbullashtirish. В *International Online Multidisciplinary Conference* (pp. 247–250).

107. Давидбаев, Б. Н., Жураев, А. Ж., & Давидбаева, Н. Б. (2024). *Разработка и расчет шарнирно-рычажных механихмов*. ALPHA BRAND.

108. Davidboyev, B. N., & Davidbayeva, N. B. (2017). *Ko‘tarish tashish mashinalari*. Navro‘z.

109. Muradov, O. J., Djurayev, A., Davidbayev, B. N., & Davidbayeva, N. B. (2025). *Improvement of the design of the scientific basis for calculation of working bodies of the separation and cleaning zone of the flow line for processing raw cotton*. Global Book Publishing Services.

110. Давидбаев, Б. Н., Жураев, А. Ж., & Давидбаева, Н. Б. (2022). *Разработка и расчет шарнирно-рычажных муфт карданных механизмов*. LAP LAMBERT Academic Publishing.

111. Джураев, А. Ж., Давидбаев, Б. Н., Жаляев, А. А., & Мирзахонов, Ю. У. (n.d.). *Плоскоременная передача с натяжным роликом* (Патент Уз. Рес. UZ IAP 4228).

112. Джураев, А. Д., Давидбаев, Б. Н., Зулпиев, С. М., & Давидбаева, Н. Б. (2013). *Структурный кинематический и динамический анализ рычажно-шарнирных муфт с упругими элементами карданного механизма*. Фаргона.

113. Джураев, А., Давидбаев, Б., & Зулпиев, С. (2009). Структурный анализ рычажно-шарнирной муфты. *Ж. «ФерПИ илмий техника журнали»*, 30.

114. Давидбоев, Б. Н. (1989). *Кутариш-ташишмашиналари*. Укитувчи.

115. Джураев, А. Ж., Давидбаев, Б. Н., Мирзахонов, Ю. У., & Давидбаева, Н. Б. (n.d.). *Шарнирно–рычажная муфта* (Авторское свидетельство КР № 116).

116. Джураев, А., Давидбаев, Б., & Давидбаева, Н. (2020). Анализ процесса выпадения частиц хлопка в зоне взаимодействия с амортизирующем отражателям сепаратора. *Научно-технический журнал Ферганского политехнического института*, 144–147.

117. Джураев, А. Д., Давидбаев, Б. Н., Алимов, О., & Давидбаева, Н. Б. (2020). *Сепаратор для волокнистых материаллов* (Патент Узбекистан IAP 6300).

118. Джураев, А. Ж., Давидбаев, Б. Н., Жаляев, А. А., Мелемедов, Р. Ю., & др. (2023). *Натяжной ролик плоскоремённой передачи*. Патент.

119. Джураев, А., Давидбаев, Б., & Давидбаева, Н. (2020). Влияние взаимодействие летучки с амортизирующей пластин. Сепаратора на качественные показателей хлопка-сырца. *Збірник наукових праць*.

120. Джураев, А. Д., Давидбаев, Б. Н., & Давидбаева, Н. Б. (2019). Разработка эффективной конструкции и результаты испытаний сепаратора хлопка-сырца. *Фергане,* 4.

121. Джураев, А. Д., Давидбаев, Б. Н., & Давидбаева, Н. Б. (2019). Обоснование параметров амартизирующий пластины резиновой подушке сепаратора хлопка-сырца. *Наманганский инженерно-технологически институт, Научно-технический журнал*.

122. Джураев, А. Ж., & Мирзаханов, Ю. У. (2021). Совершенствование конструкций и обоснование параметров

центрирующего натяжного устройства транспортёра. *Central Asian Journal of Theoretical and Applied Science, 2*(11), 237–247.

123. Давидбаев, Б. Н., & Мирзаханов, Ю. У. (2007). О плоскоременных передачах с центрирующими натяжными устройствами. *Наука и новые технологии*, 139–142.

124. Давидбаев, Б. Н., Давидбаева, Н. Б., & Октамов, Н. М. (2026). Разработка и исследование новой конструкции цепной передачи. *International Online Multidisciplinary Conference*, 250–253.

125. Амирбек, К. Г., & Беделбаев, А. (2025). Известия Национальной академии наук Кыргызской Республики. *Известия, 1*(S1), 336–341.

126. Давидбаев, Б. Н., Джураев, А., & Давидбаева, Н. Б. (2024). Разработка эффективной конструкции хлопкового сепаратор для хлопка-сырца. *Механика и технология, 5*(Спецвыпуск 3), 172–176.

127. Davidbaev, B. N., & Davidbaeva, N. B. (2022). Improvement of the design of the cotton separator SS-15A. *Innovative Technologica: Methodical Research Journal, 3*(11), 64–69.

128. Зулпиев, С. М., Давидбаев, Б. Н., & Давидбаева, Н. Б. (2022). О движение летучки хлопка-сырца по поверхности перфорированной сетки сепаратора СС-15А. *Известия Национальной академии наук Кыргызской Республики*, 173–178.

129. Мирзаханов, Ю. У., Сиддиков, М. З. Ў., & Уришев, Д. И. Ў. (2022). Исследование бокового схода ремня в плоскоременных передачах и транспортирующих механизмах. *Oriental Renaissance: Innovative, Educational, Natural and Social Sciences, 2*.

130. Джураев, А., Давидбаев, Б. Н., & Давидбаева, Н. Б. (2021). Определение передаточной функции рычажно-шарнирной муфты с учетом упругих элементов в шарнирах механизма. *Механика и технология, 2*(3), 9–15.

131. Давидбаев, Бахтиёрджон, Джураев, Анвар, & Давидбаева, Наргизахон. (2020). Исследование взаимодействия частицы хлопка–сырца с амортизирующей пластин сепаратора. *Збірник наукових праць ΛΌГОΣ*, 82–86.

132. Anvar, D., Kuliev, T. M., & Davidbayev, B. (2020). Designing and methods of calculating parameters of a fibrous material cleaner from large litter. *International Journal of Advanced Science and Technology*, *29*(8 Special Issue).

133. Джураев, А. Д., Алимов, О. Н., Давидбаев, Б. Н., & Давидбаева, Н. Б. (2020). *Сепаратор для волокнистых материалов* (US Patent IAP 06,300).

134. Джураев, А., Давидбаев, Б. Н., Зулпиев, С., & Давидбаева, Н. Б. (2011). Влияние угла расхождения валов рычажно-шарнирной муфты на характер движения системы. *Известия ВУЗов Кыргызстан*, 70–72.

135. Джураев, А., Давидбаев, Б. Н., Зулпиев, С., & Давидбаева, Н. Б. (2011). Гармонический анализ крутящего момента на ведомом валу рычажно-шарнирной муфты. *Известия ВУЗов Кыргызстан*, 18–21.

136. Джураев, А. Д., Давидбаев, Б. Н., & Зулпиев, С. М. (2009). Структурный синтез рычажно-шарнирной муфты. *Наука и новые технологии*, 50–52.

137. Абдуллаев, М. М., Давидбаев, Б. Н., & Орипов, Э. О. (1992). *Устройство для транспортировки и распределения волокнистого материала*.

138. Усманходжаев, Х. Х., Рахматкариев, Ш. У., Давидбаев, Б. Н., & др. (1980). *Способ джинирования хлопка-сырца и устройство для его осуществления*.

139. Usmankhodzhaev, K. K., Rakhmatkariev, S. U., Davidbaev, B. N., & Dzhuraev, A. (1975). Study of a machine unit with a mechanism of an operating spindle of a gin. *Doklady Akademii nauk UzSSR*.

140. Usmankhodzhaev, K. K., Rakhmatkariev, S. U., & Davidbaev, B. N. (1974). Exeperimental determination of the discharge of air from perforated tubes and the attraction strength of volatile acids of cotton seeds. *Doklady Akademii nauk UzSSR*.

141. Токоева, А. Т. (n.d.). Известия Национальной академии наук Кыргызской Республики. *Известия*, 123–126.

DEVELOPMENT OF THE DESIGN AND SUBSTANTIATION OF THE PARAMETERS OF A DRUM SCREENING DEVICE

MONOGRAPH

ABOUT THE MONOGRAPH

This monograph presents the results of research devoted to the development of a bulk material screening device equipped with a shaft with elastic blades. Theoretical investigations are used to substantiate the optimal operating modes and parameters of the drum screening device.

Experimental and industrial test results are also presented to evaluate screening efficiency and the performance of the developed design. The publication is intended for researchers, specialists, and doctoral students working in the field of bulk material processing and screening equipment.

AUTHORS DETAILS

Baxtiyordjan N. Davidbayev
Candidate of Technical Sciences, Professor, Department of Applied Mechanics, Fergana State Technical University, Fergana, 150100, Uzbekistan

Vokhidjon M. Turdaliyev
Doctor of Technical Sciences, Professor, Dean of the Faculty of Transport, Namangan State Technical University, Namangan, 160100, Uzbekistan

Khojiakbar Sh. Ruzaliyev
Independent PhD Researcher, Namangan State Technical University, Namangan, 160100, Uzbekistan

Recommended for publication by the Scientific Council of Fergana State Technical University under Resolution No. 9 dated May 2, 2026.

DOI: https://doi.org/10.37547/gbps-46

ISBN: 978-1-957653-67-9

FERGANA - 2026